NORTH-WEST UNIVERSITY
YUNIBESITI YA BOKONE-BOPHIRIMA
NOORDWES-UNIVERSITEIT
MAFIKENG CAMPUS

SPECTROSCOPIC ANALYSIS OF HISTORICAL DOCUMENTS

K. DZINAVATONGA

20770227

Thesis submitted for the degree of Doctor of Philosophy in Physics at the Mafikeng Campus of the North West University.

SUPERVISORS : **PROF. T.R. MEDUPE**

: **DR. L. PRINSLOO**

DATE OF SUBMISSION : **MAY 2015**

DECLARATION

I, KAITANO DZINAVATONGA (student number: 20770227), hereby declare that this research is my original work. Unless specifically stated, all the references listed have been consulted. The work of this dissertation is a record that has been done by me and has not been previously accepted for any higher degree or professional qualification at any other educational institution.

Signed…….

MR. K. DZINAVATONGA

Date ……

This dissertation has been submitted with my approval as a university supervisor and would certify that the requirements for the applicable Doctor of Philosophy in Physics degree rules and regulations have been fulfilled.

Signed……..

PROF .T.R. MEDUPE

Date…….

Signed……..

DR. L. PRINSLOO

Date……..

Abstract

The aim of this was work to assess the degradation risk and suggest conservation methods of certain historical documents. All the documents studied were obtained from the National Library of South Africa except one that was obtained from a private library at the city of Timbuktu, Mali. Five methods were used to carry out the assessment, namely Abbey pH pen test, X-Ray Flourescence (XRF), Mössbauer spectroscopy, Fourier Transform Infrared Spectrometer (FTIR) and Polarised Light Microscopy (PLM). The Abbey pH pen method was used to check the pH level of all the samples. It was found that all the samples except two were acidic. These are the *Het Leven* and *South Africa (Barrow)* samples. The sample from the Timbuktu manuscripts was found to be extremely acidic with a pH level of below 5.0. It is recommended that all the acidic samples be de-acidified using the Bookkeeper process in order to retard the process of degradation due to hydrolysis.

Energy dispersive X-ray fluorescence technique was used to study the elemental composition of the above mentioned samples. In all the samples six elements namely Fe, Cu, Mn, Ca, K and S were detected. It was found that older documents had higher concentrations of Ca and hence have a considerable alkaline buffer than recent documents. It was also observed that the levels of Ca dropped significantly in the samples dating between 1800 and 1890 coinciding with the period during which paper making technology changed. The concentrations of K and S also decreased around 1890. Iron remained considerably high and was detected in all the samples. Copper and manganese were found to be at very low concentrations compared to Fe. This research confirmed that Fe has the potential to impact negatively on paper permanency unless de-acidification is undertaken because of relative abundance of Fe compared to Cu.

The valence state of iron in five of the samples studied was determined using the Mössbauer spectroscopy. This is the first time paper is studied in this way. This technique was time consuming because of the trace quantities of Fe in the samples. Spectrum collection lasted for several days making the method unsuitable for analysing many of samples normally found in libraries and archives. It was found that all the samples had Fe^{3+}. Only one sample namely, the *Wildsport of Africa* sample

showed the presence of both Fe^{2+}(21%) and Fe^{3+}(79%). The detection Fe^{2+} in the *Wildsport of Africa* sample showed that oxidative degradation is also occurring in this document. It was recommended that the use of radical scavengers or chelation of transition metals in paper be used to slow down oxidative degradation of the historical documents.

The nature of the fibres that make up the samples studied was determined using FTIR. The results showed that all the samples were made of cellulose. The Courier sample was also found to have both lignin and hemicellulose. The Total Crystallinity Index (TCI) of each of the samples was also calculated in order to determine the susceptibility of cellulose to degradation agents. This index is the ratio of the integrals of the FTIR band at 1372 cm^{-1} to that at 2900 cm^{-1}. The integrals were taken over the ranges 1390 – 1339 cm^{-1} and 2959 – 2830 cm^{-1} for the bands at 1372 cm^{-1} and 2900 cm^{-1} respectively. The Lateral Order Index (LOI) was also calculated using the ratio of the integrals of the absorption bands at 1420 cm^{-1} to that at 898 cm^{-1}. These bands are known to be sensitive to the relative amounts of crystalline versus amorphous structure in the cellulose. It was also observed that all the samples had clay but none of the samples had gypsum as a filler material. Traces of calcium carbonate were found in four of the samples studied. Kaolin was also found in all the samples except two. Only one sample showed the presence of gelatine.

The optical properties of the sample fibres were investigated using PLM. Birefringence measurements showed that only one sample was made from linters fibers, seven from hemp and four from rammie fibres. It was also observed that the morphology and birefringence of the fibres were not affected by ageing.

This research work showed for the first ever that Mössbauer spectroscopy can be used to determine the valence state of trace amounts of iron in paper. A direct implication of the result of this study is that MS analysis of any sample on paper substrate will also contain information about the valence state of the iron in the substrate. This is particularly important in the MS analysis of inks on historical documents. If the analysis of the ink is done *in situ*, that is without removing the ink from the paper, it is necessary to separate the MS spectrum of the paper form that of the ink.

Acknowledgements

I am very grateful to my supervisor Prof T.R. Medupe for the academic guidance and moral support. I really appreciate the hours you spent going through my work. I am also grateful to Dr. Linda Prinsloo for the immense contribution and constructive suggestions that helped to shape direction of this work. I also wish to thank members of the Physics Department for their understanding and sacrifices during the most trying times and for securing the equipment used to analyse some of the samples.

Many thanks to the National Library of South Africa for supplying most of the samples used and the Abbey pen test kit. To iThemba laboratories in Cape Town, I want to express my gratitude for granting me access to their Mössbauer spectrometer. Special thanks to Prof Krish Baruth-Ram for his patience in showing me the intricacies of the Mössbauer spectrometer. I also wish to thank Prof Isabirye and Prof Ebenso in the Chemistry Department North West University (Mafikeng Campus) for access to the XRF and FTIR instruments and the OPUS software.

Finally, I would like to express my sincere gratitude to my family for the sacrifices, moral, emotional and financial support that they gave me. It was through their prayers and selflessness that I managed to complete this work. To Tafadzwa Marara, I say thank you for the stimulating discussions, support and time spent in perfecting this document.

Dedications

To my beloved brother Clever Magadza who untimely passed on.

Table of Contents

List of Figures

List of Tables

Abbreviations

ATR	Attenuated Total Reflection
DRIFT	Diffuse Reflectance Infrared Fourier Transform
ED	Energy Dispersed
EDXRF	Energy Dispersed X-Ray Fluorescence
ESI-MS	Electro Spray Ionisation – Mass Spectroscopy
FTIR	Fourier Transform Infrared
LOI	Lateral Order Index
HMF	Hyperfine Magnetic Fields
HS	Hyperfine Splitting
IRE	Internal Reflection Element
IS	Isomer Shift
MHS	Magnetic Hyperfine Splitting
MS	Mössbauer Spectroscopy
NLSA	National Library of South Africa
PIXE	Particle Induced X-ray Emission
PLM	Polarised Light Microscopy
TCI	Total Crystallinity Index
XRF	X-Ray Fluorescence
VOC	Volatile Organic Compounds
WD	Wavelength Dispersed
CSN	Chain Scission Number
SFCU	Scission Fraction of Cellulose Unit
LODP	Levelling Off Degree of Polymerisation
DP	Degree of Polymerisation

CHAPTER 1: INTRODUCTION

1.1 Background

Historical documents of intrinsic value are often destroyed by a variety of paper/cellulose degradation agents. These range from the environmental conditions to the constituent material that makes up such documents. The rate at which a historical document degrade with time depend on the sizing (process of imparting to paper some degree of resistance to the absorption or penetration of liquids), fillers, the included transition metals as well as the cellulose fibre morphology and accessibility. The processes by which historical documents degrade with time are well documented [1-4]. The degradation mechanisms as well as potential intervention techniques have been well studied [3]. A particular degradation process often produce specific byproducts notably carbonyl and carboxyl functional groups that can give an indication of the underlying chemical process.

An analysis of the history of paper production shows that there was a marked change in the paper making process around 1850 AD. This was mainly due to the shift from using potassium aluminium sulphate (alum) to aluminium sulphate (paper maker's alum) as the sizing agent [5]. It has been observed that such a change in sizing agent was associated with increasing acidity of the paper produced [6]. Transition metals like iron (Fe), copper (Cu) and manganese (Mn) play a significant role in influencing the oxidative degradation of cellulose through their catalytic action. The presence of such transition metal ion species, though in trace quantities, is potentially detrimental to the oxidative stability of paper. It therefore means the detection of these ion species in historical documents is of importance from a document conservation point of view.

Metal ions can be hydrolysed and displace hydrogen during reaction with water as shown in the following equation [1];

$$M^{z+} + zH_2O \rightarrow M(OH)_z + zH^+ \qquad (1.1)$$

where *M* is the transition metal and *z* is an integer representing the oxidation state. The hydrogen (zH^+) ions can then induce hydrolysis and cross linking reactions in

secondary reactions. The metal hydroxides ($M(OH)_z$) can also be transformed to oxides with further hydrogen ion formation [4]. This means that metal oxides and metal hydroxides can catalyse cellulose hydrolysis in the absence of free oxygen. The degradation of cellulose is more pronounced for metals that are more easily hydrolysed, in the order Fe^{3+}, Fe^{2+}, Cu^{2+} and Mn^{2+} [5]. Hydrolytic degradation is more dominant in an acidic paper than in alkaline paper.

Acidity in paper can be neutralized by using aqueous solutions of calcium or magnesium hydrogen carbonates [3] through the so called Bookkeeper's process. This process effectively raises the pH range of paper to between 7 and 9, transforming it to archival quality. It has, however, been observed that the catalytic activity of copper increases steadily in the pH interval of 7-9 [4]. It is therefore plausible to conclude that the higher pH macromolecular environment may decrease the activity of Fe-containing paper samples but not in paper samples containing Cu. Cu therefore remains a threat to paper stability even after de-acidification process. It is therefore important that the elemental content of archival material be ascertained in order to prepare for a comprehensive preservation intervention.

As the pH level of paper increases to the alkaline region, the catalytic activity of trace quantities of transition metals in paper also increases as demonstrated by the production of oxidising species in Fenton-like reactions in the pH interval 5.5–9 [3]. This means that oxidative degradation of paper becomes dominant in alkaline paper after de-acidification. Iron, in particular, is found in both historic and contemporary paper. It enters the paper matrix either through water during the paper making process, via the normal wear and tear within the paper making machinery or as contaminants in additives [5]. X-ray fluorescence (XRF) [6] and Particle Induced X-ray Emission (PIXE) analysis have been used to determine the elemental presence and their relative concentrations in iron-gall inks [7]. These two methods, however, do not give any information about the valence state of the detected elements. It is therefore important to determine the valence state of the Fe ions in the sampled documents as this will give an indication of their oxidative degradation risk. From a document conservation perspective, iron is very important in that it is relatively abundant in paper and is one of the transition metals present in cellulosic paper that is very active as an oxidising catalyst. The degradation potential of iron or any other transition metal is due to its ability to generate free radicals.

Knowledge of the compounds used to manufacture the paper and ink, their acidity, and their degradation products allows us to try to describe the degradation mechanisms and consequently to avoid them [8]. Information about compounds found in the composition of degraded inks, as well as the influence of oxidation in cellulose when using different de-acidifying solutions [9] such as calcium hydroxide, calcium bicarbonate, or magnesium bicarbonate—can be very useful when studying the degradation of paper or manuscripts [10].

Historical documents are, in many cases, unique and valuable. Specific methodologies must be applied in order to minimize the amount of sample to be used and, consequently, to avoid any damage to manuscripts. Infrared spectroscopy has been successfully applied to the analysis of papers and inks [11-13]. Different methodologies and accessories can be used depending on the size of sample, level of destruction, and information required. Two different methods can be used with a Fourier Transform Infrared (FTIR) instrument: diffuse reflection and microscopy. The microscope can be used either in transmission mode with a diamond cell or with an attenuated total reflectance (ATR) objective. Depending on the type of sample, FTIR can be applied to achieve the following aims:

- to identify sizing material in paper samples for example gelatine, starch kaolin, gypsum etc
- to identify the paper sample matrix constituent make-up, for example, cellulose, hemicellulose, lignin etc.
- to determine the differing degree of cellulose oxidation
- to identify compounds in inks
- to determine the molecular organisation of the cellulose in the samples by determining the crystallinity index of cellulose

Raman spectroscopy can also be used as a complementary method to FTIR for the determination of size and fillers in document samples. X-Ray Flourescence (XRF) is the ideal technique in determining the elemental content of the samples since it is non-destructive and requires no sample preparation. The method of determining the valence state of the transition metals present in these historical documents will depend on the metals that would have been detected. Section 2.6 shows the detailed discussion of all the methods used.

1.2 Problem Statement

Over long periods of time, human history and cultural heritage have been recorded on paper. This medium of storage of our most valuable history is not permanent and is susceptible to chemical, physical and biological processes that severely attack the cellulose that forms the matrix of the paper.

Libraries, archives and museums are the custodians of a wealth of human history in the form of documents and important works of art. These institutions had often in the past, until recently, relied on visual inspection to determine the preservation status of documents. The use of scientific examination in order to shed light on the past was fostered when major museums began to build laboratories for that purpose on their premises [14]. The National Library of South Africa (NLSA) from which most of the samples were obtained for this study does not have such laboratory facilities capable of scientifically examining their collection. They however have a document preservation unit that comprises a de-acidification plant and a bindery unit. The document preservation unit has the capability to determine the acidity of documents by means of the Abbey test pen. This pen is used to test the books before and after the de-acidification process in order to evaluate the effectiveness of the process.

Documents can however also deteriorate via catalytic oxidation even after neutralization of acidity. Such a process can only be determined by spectroscopic examination of the document's constituent materials. The detection of deterioration by-products will assist in determining other chemical processes occurring on the document concerned. This will assist in assessing the deterioration risk of the documents in the National Library of South Africa. It is therefore not possible to recommend a comprehensive conservative action for such documents unless their constituent material composition is determined. The NLSA cannot do such an assessment on its own because of lack of technical know-how and lack of appropriate equipment. This work therefore seeks to determine the material composition of the document samples under study. Knowledge of the transition metals ions and their valence states present in the sampled historical documents is also essential. X-ray fluorescence (XRF) spectrometry can be used to determine the elemental composition of the documents under investigation. It is a well established technique for elemental analysis at micro and trace levels. The method has been

used before to study the elemental composition of iron-gall inks. This method provides a quick non-destructive analysis and has sensitivities at the level of parts per million. It gives information about the elemental composition without the need for any pre-treatment. The technique is independent of the chemical state of the element and it does not give information about the chemical bonds of the detected elements. A number of spectroscopic techniques have been used to determine the valence state of iron in a variety of samples [15,16]. In particular, Mössbauer Spectroscopy (MS) has been used to determine the valence states of Fe in iron-gall inks of 16th century manuscripts [16]. However, in all the literature surveyed no MS measurements have been done yet to determine the valence state of trace quantities of iron within the paper samples. This thesis aims to address this problem by applying MS technique on paper samples. Mössbauer spectrum is normally described using three parameters, namely; the isomers shift (δ), electric quadrupole splitting (ΔE) and hyperfine splitting (HS). The description of these parameters and the standard experimental set up for MS measurements are treated in depth elsewhere [17-19]. The isomer shift and quadruple splitting can be used to effectively determine the valence state of iron.

1.3 Research Aim and Objectives

The aim of this research was to assess the risk of degradation of specific documents, the majority of which were from the National Library of South Africa with the ultimate goal of providing recommendations on possible remedial and preventative actions. This will be achieved through a comprehensive spectroscopic and microscopic analysis of the selected documents. The analysis involved the determination of both the organic and inorganic composition of the selected documents. In particular the extent to which the composition of the paper itself affects its stability was investigated. In order to achieve this, the following objectives have been identified;

a) Determination of the elemental composition of the documents.
b) Determination of the valence state of the most abundant transition metal in paper.

c) Evaluation of the degree of acidity/alkalinity in the studied samples.
d) Identification of the sizing material, fillers and any other organic inclusions in the paper.
e) Evaluation of the optical properties of the fibres of the paper samples.
f) Determination of the relationship between the change in the sizing material used in paper production and the elemental content of the paper produced, particularly the concentrations of transition metals.

1.4 Outline of the Thesis

The structure of this thesis is as detailed below

Chapter 1: Introduction

This Chapter consists of the Background of the problem, problem statement and research aims and objectives.

Chapter 2: Literature Review

The relevant literature of paper degradation mechanism is presented. It also looks at the sizing used in paper manufacturing and the history of the different sizes used over time. Finally the chapter looks at the different spectroscopic techniques used to determine and characterise paper constituents.

Chapter 3: Methodology

This chapter describes the sampling method used as well as the sample preparation. It also gives a detailed description of the measurement methods used to determine transition metals in paper, valence state of iron in paper samples, composition of the paper samples as well as the optical characteristics of the fibres of the samples.

Chapter 4: Results and Discussion

This chapter presents the detailed results of all the experiments carried out in this study. The pH test results are given first because they represent the immediate threat to paper longevity. The elemental composition results are then discussed together with the results for the determination of the valence state of iron, one of the transition metals found in paper samples. Finally the results for paper fillers and sizes are presented and discussed.

Chapter 5: Conclusion

A summary of the significance of this research is presented together with proposed recommendations.

Appendix A

This section consists of all the FTIR spectra of the studied samples.

Appendix B

This appendix has the two publications that came out from this thesis. The first paper titled *Energy Dispersive X-ray Fluorescence Analysis of Pre- and Post-1850 Historical Documents Obtained from the National Library of South Africa* was published in the Asian Journal of Chemistry in 2013. The second paper whose title is *Mössbauer spectroscopy analysis of the valence state of iron in historical documents obtained from the National Library of South Africa*, was published in the Journal of Cultural Heritage in 2014.

References

This consists of all the literature consulted in this thesis.

CHAPTER 2: LITERATURE REVIEW

2.1 Introduction

This chapter first gives the detailed description of the structure and composition of paper. An understanding of the backbone material of paper together with its fillers and additives is important in understanding the chemical reactions that may occur during the life span of historical documents. The chapter will also trace the time line of the paper manufacturing technology as this will be a valuable tool in dating and authenticating historical documents. The paper degradation mechanisms are also explained as they are currently understood. These degradation mechanisms are known to produce by-products that tend to fuel further paper degradation. Finally the methods of detecting these byproducts and the rest of the components that make up historical documents are also discussed.

2.2 The Structure of Paper

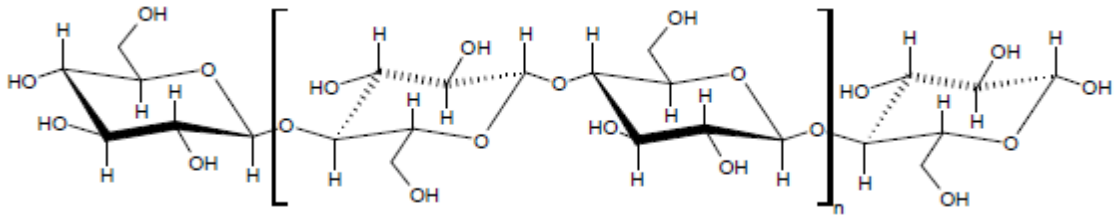

Figure 2.1: The chemical structure of cellulose macromolecule [20].

Cellulose (Figure 2.1) is the major structural component of paper. It is a fibrous, tough, water-insoluble substance, which is found in the protective cell walls of plants, particularly in stalks, stems, trunks and all woody portions of plant tissues. Cellulose is made up of β-D-glucopyranose elements joined by (1 → 4) glycosidic bonds [21]. These pyranose rings have been found to have the hydroxyl groups in an equatorial position. Cellulose chains have a degree of polymerization (DP) of approximately 10 000 glucopyranose units in wood cellulose and 15 000 in native cotton cellulose [22].

The degree of polymerization is low in primary cell walls (a thin, flexible and extensible layer formed while the cell is growing) as compared with secondary cell walls (layered sheaths of cellulose microfibrils). Chain lengths of large, insoluble molecules are difficult to measure because of enzymic and mechanical degradation which normally occur during analysis. The degradation of cellulose will also lead to the degradation of mechanical paper properties, relevant to the users of historical documents. Other components of paper also influence its stability, the major one being another natural polymer, lignin. Since cellulose is a macromolecule, many aspects of its degradation are common to degradation of other polymers. The methods of study are identical, and so are some of the degradation mechanisms.

The polymorph of cellulose and its derivatives has been well documented [23]. Two forms of cellulose exist in nature. Simon et al. [23] postulate that a form of crystalline cellulose existed near the surface of a crystal which differed from the structure to be found at the centre of the crystal. These two crystalline forms were termed celluloses Iα and Iβ [24-25]. Celluloses produced by primitive organisms were said to have the Iα component dominant, while those produced by the higher plants have the Iβ form dominant. Cellulose Iα and Iβ were found to have the same conformation of the heavy atom skeleton, but to differ in their hydrogen bonding patterns. Since paper is derived from plants, its cellulose polymorph is Iβ.

2.3 Sizing

Sizing refers to the process of imparting to paper some degree of resistance to the absorption or penetration of liquids. In paper production, sizing exists in two forms namely surface and internal sizing. Surface sizing entails application of chemicals to the surface of the paper after it has been formed rather than adding chemicals to the wet pulp. Internal sizing is used to describe the practice of adding chemicals to the aqueous slurry that contain cellulose fibres to improve paper hydrophobicity [26].

The first paper made by the Chinese was not sized [27]. It was very soft and absorbent, allowing the ink to diffuse through the paper easily. In the 8th century, the Chinese began to apply gypsum and later an adhesive like substance made from

lichen to the surface of their paper [27]. Later in the same century, they made a size from flour starch which was added to the paper as internal sizing or surface sizing.

In the middle of the 8th century papermaking technology reached the Arab world. Arabic papers were sized with a thick starch and afterwards glazed to produce a highly burnished surface that physically resembled parchment. The surface of an unsized sheet of Arabic paper was very irregular, reflecting the impressions left by the reeds used to construct the paper mould and the effects of drying with little or no pressing. The Arabs brought the papermaking technology to Spain as they expanded their empire [27].

The first paper used in early Spanish manuscripts was similar to traditional Arabic paper. This paper, like its traditional Arabic counterpart, was sized with a thick starch that had been spread over the sheet so that the surface was smooth and even. This method of sizing, and in fact Arabic papermaking practices in general, were continued in Spain into the 14th century [27]. In Europe, the first sized paper was made at Fabriano in Italy in the late 13th century. Hide glue or gelatine was used as the sizing material. The reason for choosing this type of sizing agent is not clear but it gave the paper a hard and opaque surface. In the 14th century the use of gelatine sizing had become widely accepted. Other sizing material like starch was however still being used.

Gelatine was very frequently applied as an external, surface size on finished sheets of paper. It was prepared by boiling animal hides, horns, hooves and bones in a large cauldron. Periodically, the solution was skimmed and filtered through cloths. When the gelatine was ready, it was transferred to a tub to cool and again heated before being used. The gelatine was applied to finished paper either alone or in combination with alum. One of the major problems encountered with gelatine size was that it deteriorated quickly, especially when the weather was hot. In a practice that began in the 16th century and was widely used by the middle of the 17th century, papermakers added potassium aluminium sulphate (alum) to the size to control the growth of mould and bacteria. Prominent paper historian, Henk Voorn [28] states that in hot weather sometimes as much as 20% alum was added to the sizing tub. Two other reasons given for the use of alum are that it stabilized the viscosity of the size at various concentrations and temperatures and increased the ability of a gelatine

sized sheet to resist ink penetration. The earliest use of alum in combination with gelatine is believed to have occurred during the 1500's [29]. Most of the time, alum was added directly to the sizing tub. Occasionally, it was added separately to the sized sheet itself.

As a sizing ingredient, alum has been one of the most important materials in the history of papermaking. Since the late 19th century, it has also been mentioned as a primary cause of paper degradation, but little detailed information on the manufacture and use of alum has been available in the readily accessible literature. The two major alum varieties (aluminium potassium sulphate and aluminium sulphate) employed in papermaking have not always been distinguished for their different properties. Aluminium potassium sulphate was used throughout the history of papermaking until the 19th century. It was then replaced by the newly developed aluminium sulphate, a cheaper and more concentrated source of aluminium compounds. Although both aluminium potassium sulphate and aluminium sulphate tended to introduce different impurities into paper, the negative effect of aluminium sulphate on the overall degradation of paper is more significant. An understanding of the characteristics of the two compounds can provide certain insights into the aging properties of paper containing either alum variety.

Aluminium potassium sulphate was the first alum used in papermaking. It could be obtained from minerals such as alunite which occurs in sulphur-containing volcanic sediments. Mining sites were sometimes located in volcanic crater bottoms where the stones were extracted with naturally heated water, with alum crystals forming in the evaporating solution [30]. Iron oxides and iron sulphates were the most common contaminants of aluminium potassium sulphate which were more likely to discolour gelatine-alum sizes. A process of repeated re-crystallisation of the alum was used to effectively remove the iron contaminants [27]. According to the 18th century writer Lalande [31], there were two types of alum namely Roman alum which was preferred by papermakers and rock alum which was cheap and of inferior quality.

Alum-rosin size which was invented by Moritz Friedrich Illig in Germany in 1807, eventually replaced alum-gelatine size due to its lower cost [30,32]. Paper mills were commonly adding alum-rosin size to the papermaking stock by the 1840's. The alum used was aluminium sulphate which could not be purified through re-crystallisation

because of its greater solubility in water. Rosin is an amber-coloured, natural resin present in pine. The rosin was tapped from trees, extracted from stumps, or processed from tall oil [33]. Aluminium is the active component in alum, and its properties are important to the sizing process. The aluminium ion has a high charge of +3, and a small ionic radius of 0.50 angstrom, which results in a high charge density. The high charge density is responsible for the diverse chemical reactions of Al^{3+} because the ion readily reacts with other species to form a lower energy state. Much of the complexity of alum-rosin chemistry is due to the many possible reactions of Al^{3+} with other constituents in paper pulp. The occurrence of specific reactions, and the types of aluminium compounds formed are dependent on many variables. One of the most important variable influencing alum-rosin chemistry is the pH of the paper pulp. The reactions most favourable to alum-rosin sizing of paper occur in a pH range of 4.0-5.5 [34]. This ultimately led to the production of acidic paper.

Aluminium ions also act as deflocculating agents in pulp slurries. They react with the paper fibres and give them electrical charges of the same sign. The repulsion of the like charges on the fibres keeps the fibres apart and in even suspension. On the other hand, alum helped to increase bonding between fibres during sheet formation on the paper machine. This increased the wet strength of the paper. Aluminium ions show a characteristic strong affinity for cellulose and a complex behaviour under various papermaking conditions. The bonding of alum-rosin is shown in figure 2.2:

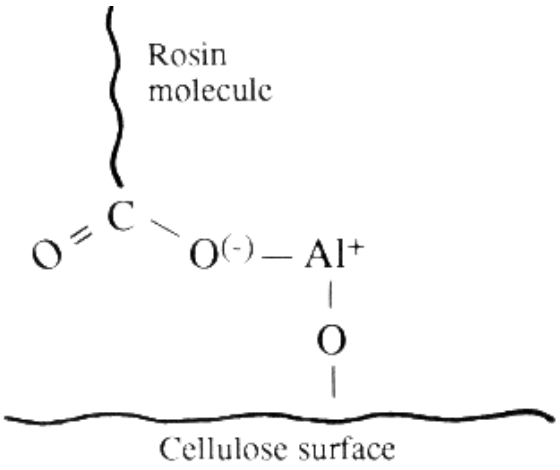

Figure 2.2 : Example of rosin-alum bonding to cellulose [35].

The basic mechanism of rosin sizing involves, among a variety of other possible reactions, the formation of cationic aluminium salts from the rosin soap and the

aluminium ions. The aluminium salt "can then react with the cellulose to provide a bridged complex" between the cellulose and the rosin as shown in fig 2.2 above.

The use of alum increased between the 16th and the 20th century as shown in figure 2.3.

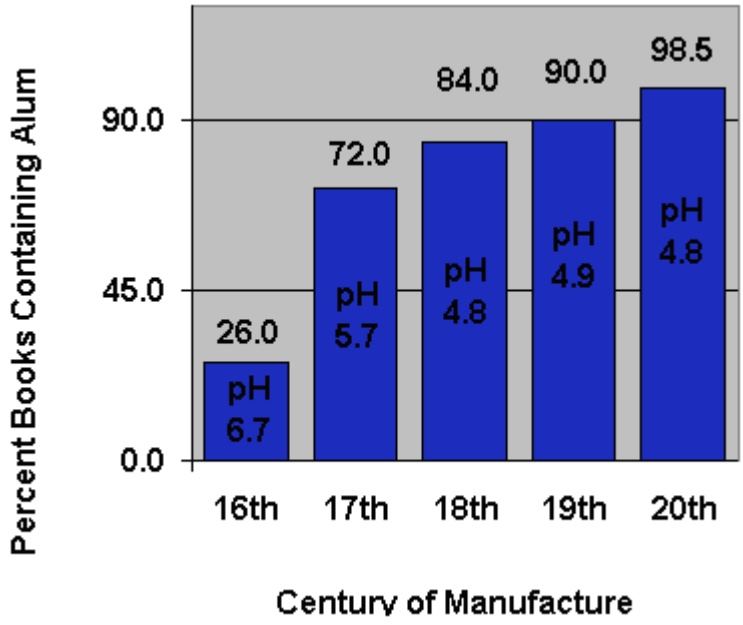

Figure 2.3: Presence of alum in historic book papers [30].

It is clear from figure 2.3 that as the use of alum increased, it was associated with a general decrease in the pH level of the paper. Thus the use of alum generally led to the production of acidic paper. Barrett [36], in X-ray fluorescence analysis of book papers from 1500 to 1800, found that papers in good condition contained less aluminium, potassium and sulphur than those in poor condition. The timeline of the use of alum is shown in figure 2.4.

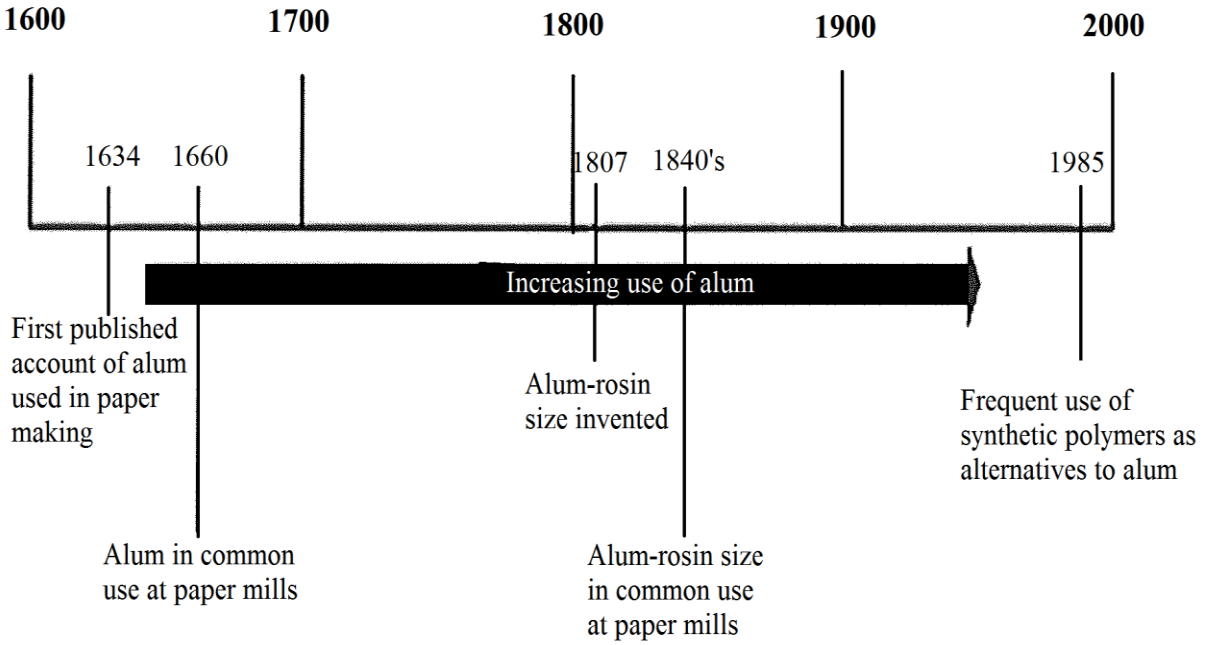

Figure 2.4 : Time line of the use of alum from year 1600 until today.

This timeline is normally used as a date marker for the purpose of dating and authenticating documents.

2.4 Paper Degradation Processes

Paper degradation or ageing can be defined as the irreversible changes that occur slowly over time [37], resulting in the deterioration of useful properties that can render it unsuitable as an information carrier. The understanding of the ageing of paper requires the study of the ageing of its main component, namely cellulose, and how certain inclusions with concentrations ranging from traces to substantial percentages can affect it. These inclusions are varied and include trace transition metals, the sizing in the paper together with the additives.

Degradation reduces the degree of polymerisation and deteriorates the mechanical and optical properties of cellulose and paper. The degree of polymerisation is a measure of the average number of glucose molecules in a polymer chain. It has been recognised that the degradation of cellulose is essentially due to the scission of

polymeric chains [38]. The characterisation of degradation of paper involves choosing the proper variable to define the defects that develop in cellulose at molecular level and to establish how the defects affect the macroscopic behaviour of cellulose. This involves either the determination of the Chain Scission Number (CSN) or the Scission Fraction of Cellulose Unit (SFCU) as a function of Degree of Polymerisation (DP). CSN represents the average number of chain scissions per cellulose chain unit during the time course of the degradation and can be calculated as

$$CSN = \frac{DP_0}{DP} - 1$$

where DP_o and DP are the degree of polymerisation before and after the degradation respectively. The SFCU is the ratio of the broken glucose units to the total glucose units in a cellulose chain, that is

$$SFCU = \frac{CSN}{DP_0} = \frac{1}{DP} - \frac{1}{DP_0} \qquad (2.1)$$

In most of the literature surveyed, the kinetics of cellulose degradation involves the determination of SFCU as a function of the ageing time (*t*). This is assumed to be a random first order chain scission reaction relationship of the form

$$ln\left(1 - \frac{1}{DP_0}\right) - ln\left(1 - \frac{1}{DP}\right) = kt \qquad (2.2)$$

k is the reaction rate constant. For large values of DP_o and DP, equation (2.2) can be reduced to

$$\frac{1}{DP} - \frac{1}{DP_0} = kt \qquad (2.3)$$

Equations (2.2) and (2.3) are for a homogeneous cellulose system and are called the Ekenstam equations [38]. In a heterogeneous cellulose system, the common approach is to introduce the accessible fraction of bonds (α) in a practical cellulose system in the determination of the rate of bond scission. Equation (2.3) can then be written as

$$\frac{1}{DP} - \frac{1}{DP_0} = \alpha kt \qquad (2.4)$$

It has been observed [39] that when DP approaches the levelling-off degree of polymerisation (LODP) Ekenstam equation (2.4) becomes invalid. It was then proposed that the reaction rate *k* should not be a constant but decrease with the ageing time

$$\frac{1}{DP} - \frac{1}{DP_0} = \frac{k_{10}}{k_2}[1 - \exp(-k_2 t)] \qquad (2.5)$$

,where k_{10} and k_2 are constants. More recently Calvini and Gorassini [40] proposed a rate equation of cellulose degradation of the form

$$\left(\frac{DP_0}{DP} - 1\right) = \left(\frac{DP_0}{LODP} - 1\right) * (1 - e^{-kt}) \qquad (2.6)$$

Equations (2.1) to (2.6) have been used to characterise cellulose degradation and develop cellulose degradation evolution equations. These equations have been successful in different applications but quantitative understanding is still limited due to the complex nature of the cellulose degradation problem.

The ageing or deterioration of paper has been in the focus of cellulose studies not only because of its chemical and structural complexity and its economic importance but also because it is the substrate for carrying information. The task of preserving paper has been entrusted to the libraries and archives and paper conservation scientists have studied the influence of the environmental factors on the stability of cellulose. The main process responsible for natural cellulose ageing is the acid hydrolysis of the glycosidic linkages between the glucose monomers in the macromolecule of cellulose. Oxidation and probably cross linking also contribute to the deterioration process [41]. It has been shown that the temperature and the relative humidity of the repositories play a crucial role in the longevity of paper. Paper degradation processes can be classified into two broad categories namely endogenous (pH, metal ions, lignin and degradation products) and exogenous (heat, humidity, pollutant gases and light).

Most cellulosic material consists of crystalline and amorphous domains whose proportions depend on both history and source of the material. The physical properties, chemical behaviour and reactivity of cellulose depends on the arrangement of the cellulose molecules with respect to each other and with respect to fibre axis. It has also been shown that the higher the accessibility (the ease with which cellulose is exposed to degradation agents) and the lower the crystallinity of cellulose, the higher the susceptibility to deterioration [42]. Most of the reactants can penetrate only the amorphous regions and it is only in these regions with a low level of order that the reactions take place leaving the crystalline regions unaffected. This therefore means that in order to check the degradation potential of the sampled documents, it is necessary to check the crystallinity of the cellulose that forms the

matrix of the paper sample. This has been done by determining the crystallinity index. The crystallinity index is inferred from the ratio of the integrals of the FTIR band at 1370 cm^{-1} to that at 2900 cm^{-1} [43-44]. The FTIR absorption broadband in the region 3600-3100 cm^{-1} is due to O-H stretching vibrations and gives considerable information concerning the hydrogen bond in the cellulose. The peaks characteristic of the hydrogen bonds from amorphous cellulose become sharper and are of lower intensity compared to the crystalline cellulose. In the amorphous cellulose, the peak is shifted to higher wave numbers. The band at 2900 cm^{-1} corresponds to the C-H stretching vibrations. The shift of this band to higher wavenumbers also confirms the presence of amorphous cellulose. The shift is normally accompanied by a strong decrease in the intensity of this band. In addition, the intensity of the FTIR absorption band at 1430 cm^{-1} due to the CH_2 bending vibrations decreases due to reduction in crystallinity. This band is also called the crystallinity band. The absorption band at 898 cm^{-1} is called the amorphous band. This band is assigned to the C-O-C stretching at the β-(1-4)-glycosidic linkages. The intensity of this band increases in amorphous samples [42].

Another parameter that can be used to measure the degradation status of the historical documents is the oxidation index. This is deduced from the carboxyl or aldehyde groups band at 1730 cm^{-1} and the band at 1620 cm^{-1} due to the carbonyl groups. The ratio of these two integrals can serve as an index defining an oxidation state of cellulose [1].

2.4.1 Acid Hydrolysis

The prevalent deterioration mechanism responsible for the natural and accelerated ageing of paper and cellulose is the acid hydrolysis of the glycosidic bonds of the cellulose macromolecule [42]. The loss of strength and the brittleness of aged paper are due to the loss of fibre strength, resulting from the acid-catalyzed hydrolysis of cellulose and not bond strength loss. Molecular mass distribution suggests that the chain scission occurs at random positions. A molecular approach is usually used to describe acid hydrolysis of cellulose. In the presence of an acid, glycosidic bond is hydrolysed and the macromolecule splits into two shorter units, as shown by the scheme in figure 2.5.

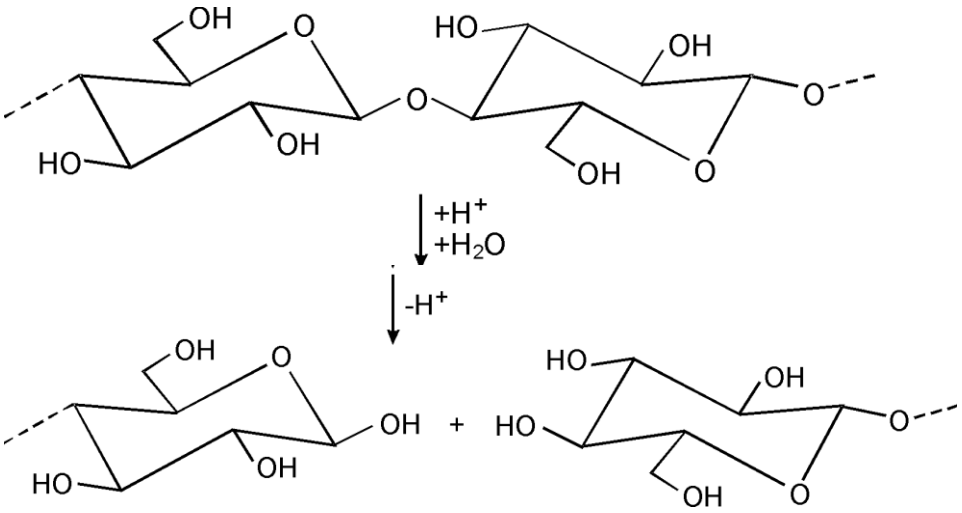

Figure 2.5: Schematic representation of acid-catalysed hydrolysis of the glycosidic bond [43].

The degradation mechanism consists of some elementary steps. They are depicted in figure 2.6. In the first step, the addition of a proton takes place, while later it is removed from the reaction product, thus acting as a catalyst [20]. According to this scheme, all glycosidic bonds between anhydroglucose monomer units are equivalent in the ideal cellulose structure, and their splitting occurs randomly.

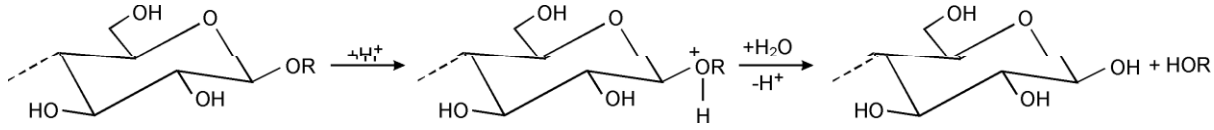

Figure 2.6: Some elementary steps of acid-catalysed hydrolysis of cellulose [20].

The acid-catalysed reaction rate is proportional to the number of available glycosidic bonds, expressed by the numerical value of cellulose degree of polymerisation (DP). This means that a first-order reaction takes place in the ideal cellulose structure. However, in reality some bonds are weaker than others, that is why frequently an initial fast reaction period is observed, followed by a slower one, especially in cellulose samples of high molecular mass [20]. In order to explain this concept of weak links in terms of acid hydrolysis, various ideas have been put forward. The most plausible explanation is that some hydroxyl groups are oxidized to carbonyl and/or carboxyl groups in the real cellulose structure. The glycosidic bonds in their vicinity become weak due to the action of these carboxyl and/or carbonyl groups.

This shows that degradation of cellulose is a symbiotic process with the degradation mechanisms feeding off one another. The existence of carbonyls, with or without ring opening, on the cellulose chain at random positions enhances the sensitivity of the adjacent glycosidic bonds and the overall liability to acid hydrolysis [44]. It has been shown that at the early stages of deterioration, chain scission occurs at random positions of the amorphous cellulose areas, while later the process becomes progressively less random [45].

The use of alum-rosin sizing has been identified as the major cause of paper degradation [46]. The typical aluminium compounds used in papermaking hydrolyse with the release of acidity. Acid conditions are known to promote cellulose degradation by reducing its degree of polymerisation. Acidity in paper can be attributed from the following sources:

Hydrolysis of Metal Ions

Aluminium ions Al^{3+} come from alum which was used mainly in the precipitation of rosin. Fe^{3+} is the most stable form of iron and is found as such in most paper samples. It may also be produced by the oxidation of Fe^{2+} which is a component of iron-gall inks that were used between the 9^{th} and early 20^{th} century for writing in Europe and its colonies [47]. These metal ions react with water to form solvated ions which act as proton donors that initiate the hydrolysis of cellulose.

Degradations/ageing Products

The degradation of cellulose and paper produces a large number of compounds which not only originate from the hydrolysis and oxidation of cellulose, but also from the degradation of hemicelluloses and lignin. The products of degradation can be classified in four categories, according to the compound class, its origin and method of identification:

- Simple sugars and cellulose oligomers: The main products of paper degradation include glucose and cellulose oligomers with DP up to 10 which originate from the hydrolysis of cellulose and hemicelluloses and are identified as products of both natural and accelerated ageing [48,49]. Their identification was accomplished by gas chromatography [50], ion chromatography [1],

capillary zone electrophoresis [49] and electrospray ionization-mass spectroscopy (ESI-MS) [51].

- Aliphatic organic acids: They are determined from the water extracts of naturally or artificially aged paper by capillary electrophoresis [48,49]. They include acetic, formic, oxalic, lactic, glycolic, succinic and malic acids [48,49]. Their mechanism of formation has not been determined in detail, but they are considered as products of the combined action of hydrolysis and oxidation [52].
- Phenolic products of lignin degradation: They have been determined by capillary electrophoresis of methanol or water extracts of aged paper [48,49].
- Volatile organic compounds (VOCs), determined from the ambient atmosphere of aged paper by gas chromatographic-spectroscopic techniques. Compounds classified in other categories such as volatile aliphatic acids and lignin degradation products are also determined together by those methods [52]. Methanol production has also been reported from the ageing of kraft paper in transformer oil.

Atmospheric Pollutants

It is well known that paper is able to absorb gaseous contaminants such as sulphur dioxide (SO_2), nitrogen oxides (NO_x) and ozone (O_3). Due to the presence of residual moisture in paper, these compounds lead to formation of acids, or react with paper components directly. Sulphur dioxide (SO_2) can be oxidized to sulphur trioxide (SO_3) and form sulphuric acid (H_2SO_4) in the presence of moisture. Ozone and various VOCs can oxidize cellulose and other paper components to acidic compounds.

2.4.2 Transition Metal Catalyzed Oxidation

In a recent study [53] degradation of pure cellulose was shown to strongly depend on pH value in the acidic region of the pH scale, which is a well-known and quantified fact [54,55] whereas there was no difference between the reaction rate constants at pH 7.3 and 8 (Figure 2.7). In the pH region around neutral, the degradation thus slows down, and two phenomena are thought to play a major role: oxidation and alkaline degradation.

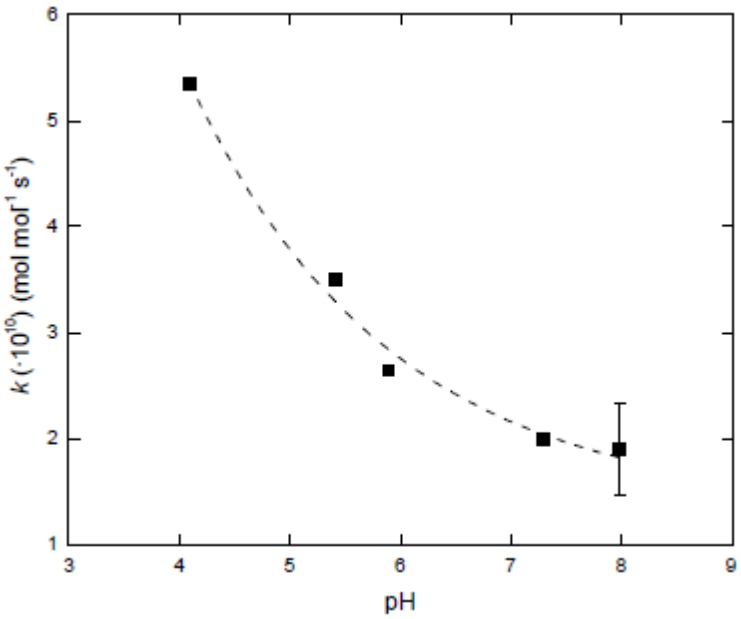

Figure 2.7 : Degradation rate constant for cellulose samples with different pH of aqueous extracts. The rate constants were obtained using the Ekenstam Equation [20].

Cellulose oxidation is a long-studied subject yet mostly in connection with pulping processes, where high temperature, pressure, pH and high concentrations of the oxidant regulate the kinetics [56]. The processes taking place in conditions of atmospheric oxidation, i.e. with atmospheric oxygen, were reviewed recently [57], and then further discussed by Kolar [58]. While the oxygen-independent alkaline degradation [59] proceeds in the vicinity of carbonyl functional groups, formed during oxidation, it is the latter process that has to be targeted in order to achieve a stabilisation effect. Judging from Figure 2.7, de-acidification of paper, that is, an increase of pH from 4 to 7.3, will lead to a three times lower rate of degradation at a temperature of 90 °C and relative humidity of 65%. The thermo oxidation scheme shown in figure 2.8 below adequately describes the process of oxidation in organic polymers including cellulose.

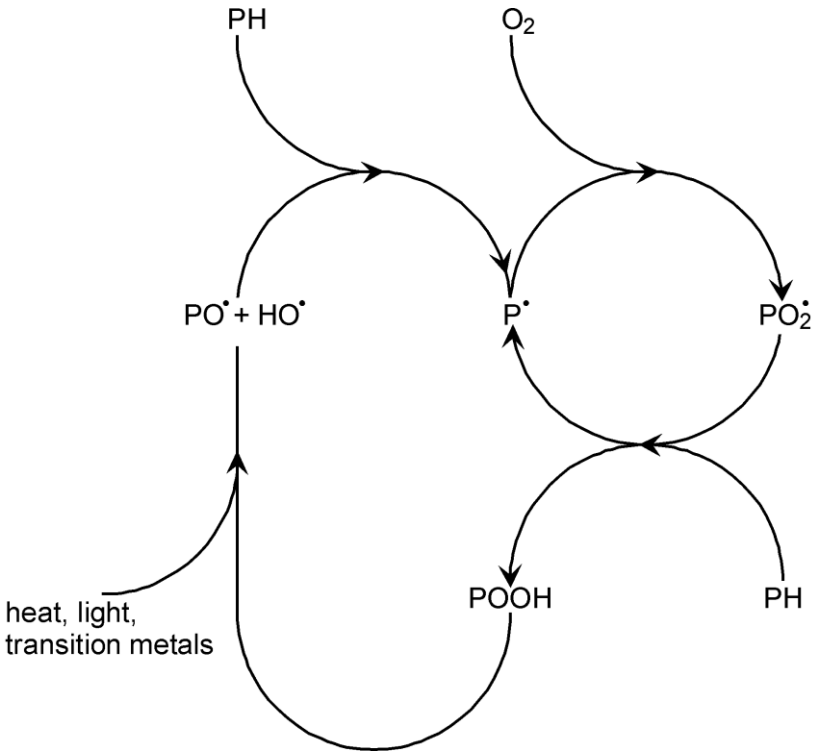

Figure 2.8: The Bolland-Gee autoxidation reaction scheme with the individual reactions outlined. The native cellulose polymer is denoted as PH [20].

The Bolland-Gee autoxidative reaction scheme shown in figure 2.8 can be explained by the general autoxidation scheme for oxidative degradation of hydrocarbons (PH) listed below.

$$PH \xrightarrow{w_i} P\cdot + products \quad (2.7)$$

$$P^* + O_2 \xrightarrow{k_3} {PO_2}^* \quad (2.8)$$

$${PO_2}^* + PH \xrightarrow{k_4} POOH + P^* \quad (2.9)$$

$$POOH \xrightarrow{k_{mono}} PO^* + HO^* \quad (2.10)$$

$$2POOH \xrightarrow{k_{bi}} {PO_2}^* + PO^* + H_2O \quad (2.11)$$

$$PO^* + PH \xrightarrow{k_{4a}} POH + P^* \quad (2.12)$$

$$PO\cdot \xrightarrow{k_{fragm}} P\cdot + products \quad (2.13)$$

$$2{PO_2}\cdot \xrightarrow{k_{61}} O_2 + products \quad (2.14)$$

$$2{PO_2}\cdot \xrightarrow{k_{62}} 2PO\cdot + O_2 \quad (2.15)$$

$${PO_2}\cdot + P\cdot \xrightarrow{k_7} POOP \quad (2.16)$$

Some reactions, for example reaction (2.13), result in embrittlement due to the reduction in molar mass. The relative importance of certain reactions is different for certain polymer systems. In cellulose, the large content of functional groups has its influence. It is almost never studied as a chemically pure compound, so it naturally contains a number of functional groups other than hydroxyl, e.g. carbonyl, aldehyde and carboxyl. This is even more pronounced in bleached wood pulp, where the remains of lignin may also play an important role. The situation is even more complex in paper, where additives, fillers, coatings, and other mixtures further complicate the system. Even fully delignified pulps contain non-cellulosic components, e.g. hemicelluloses, whose chemical structure and composition has nothing in common with cellulose, apart from being a polysaccharide. The closest model for pure cellulose is probably filter paper, which is made of cotton and extensively purified in alkalis and acids.

A direct reaction between ground state oxygen molecule and cellulose is unlikely, as it is a spin-forbidden process. The more common reactive oxygen species are superoxide anion with its conjugated acid, i.e. hydroperoxyl radical ($HOO^{\bullet}$), hydrogen peroxide (H_2O_2) and hydroxyl radical ($HO^{\bullet}$). In aqueous solutions, at the partial pressure of oxygen above the solution 1 atm and pH of 7, the following reduction potentials have been established [60]:

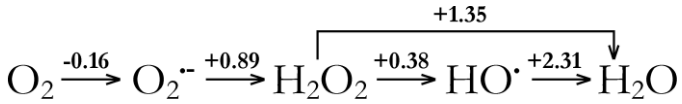

The mobility of superoxide in a hydrated cellulose molecule must therefore be high, provided that the content of water is sufficient. On the other hand, hydroxyl radicals are unspecific due to their high reactivity and react at an almost diffusion-controlled rate with a variety of compounds [61]. In a cellulose macromolecule probably only the aldehyde end groups are capable of spontaneous reaction with oxygen, which is promoted by alkalinity. The mechanisms of carbohydrate oxidation in alkaline media were reviewed in [62] and the reaction scheme as in figure 2.9 may be put forward [62,63].

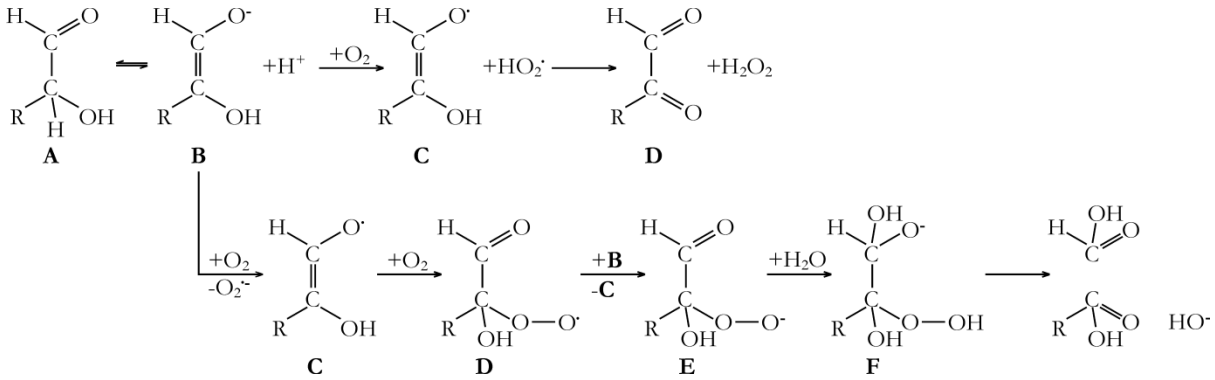

Figure 2.9: Two possible reaction pathways for oxidation of carbohydrate end-groups by oxygen in a mildly alkaline environment. R denotes the rest of a monosaccharide [62,63].

The above reaction scheme was not applied to polysaccharides successfully until recently. A satisfactory model for such studies would be cellulose of different molecular weight, in which the only aldehyde group would be the end result. However, cellulose cannot be obtained in narrow distribution of molecular masses and of sufficiently high purity, so other polysaccharides were studied instead. The polysaccharide that has been studied using artificial ageing is pullulan. Pullulan differs from cellulose only in geometry of the glycosidic bonds, which is not expected to affect the mechanisms in question, considerably. In a recent study [64] pullulan samples of different molecular weights and thus different content of aldehyde end-groups were used. In this study, pullulan samples were aged in a mildly alkaline environment ensured by surplus $CaCO_3$. During a 13-day degradation period at a temperature of 80 °C and relative humidity of 65%, the Ekenstam plots were composed of two distinct parts: during an initial period the degradation was faster, while during the advanced period, the degradation of most samples proceeded at a similar rate indicating that a steady-state content of aldehydes had formed.

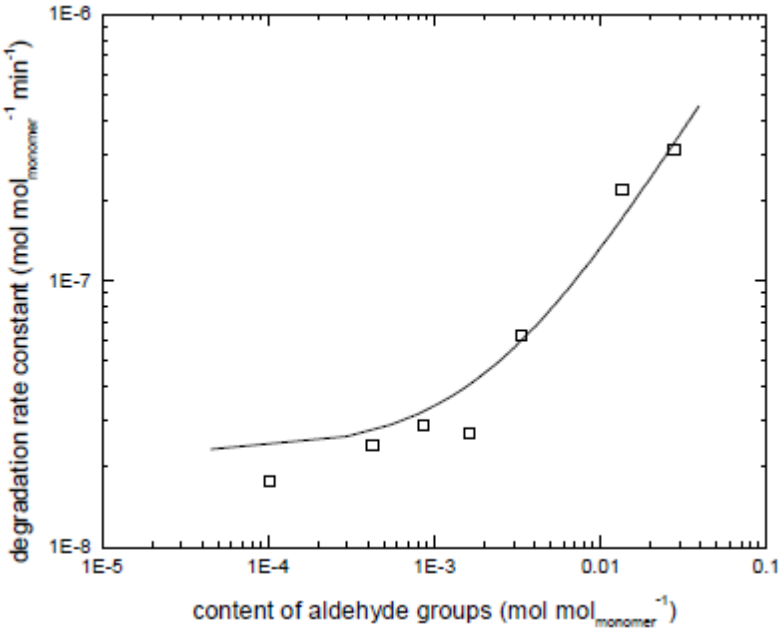

Figure 2.10: First-order degradation rate constants for pullulan samples in a mildly alkaline environment in air, 80 °C, 65% RH. The line represents a fit of the experimental data in the log-log scale [64].

A comparison of the initial degradation constant rates shows (figure 2.10) that the content of aldehydes decisively influences the degradation rate.

In paper, aldehyde groups may originate from components other than cellulose. The addition of glucose to paper is known to accelerate the degradation considerably [58]. Since aldehyde group-containing compounds, among them glucose, are products of acid-catalysed hydrolysis, it is therefore extremely important that they are washed out of paper during stabilisation treatments (washing, de-acidification). During delignification, wood pulps are subjected to various processes, during which a variety of oxidised groups on cellulose can be formed. Considering the above findings, bleached chemical pulps are thus especially prone to auto-oxidation. This was recently demonstrated in a study of a variety of differently de-acidified pulps with different contents of carbonyl groups [65]. It was observed that the percentage change in DP is proportional to the content of carbonyl groups in the cellulose. It was also observed that the content of the carbonyls also depend on the type of de-acidification implemented. The use of $MgCO_3$ produces more carbonyls compared to using $CaCO_3$. It is important to realise that by reducing the carbonyls, we may

thus greatly reduce the rate of degradation. Since these carbonyls are by-products of de-acidification process, there has to be a way of reducing the content of carbonyls after de-acidification.

Among the more important oxidative species, hydroperoxides (HOOR) and hydroxyl radicals ($HO^{\bullet}$) are two oxidative species that play a very important role. Peroxides are formed during cellulose oxidation [66]. In fact, the reactions in Figure 2.9 lead to production of a number of radicals, including the possibly long-lived superoxide. Peroxides (hydrogen peroxide, hydroperoxyl and organic peroxyl radicals and hydroperoxides) have thus been shown to take part in the process of cellulose oxidation. Other reactive species may be formed from hydroperoxides, especially if transition metals are present in the material, at least in traces:

$$Me^{n+} + H_2O_2 \rightarrow Me^{(n+1)+} + HO^{\bullet} + HO^{-}. \qquad (2.17)$$

This is called the Fenton reaction. In paper [58, 67], it is most often referred to in studies of metal tannate (iron gall) inks [68]. The activity of transition metals in paper depends on many parameters, including complexation with various ligands [69], pH and type of metal [70]. The effects of different metals in paper samples may even be synergistic [70-71].

2.4.3 Cross Linking Reactions

It is well known that when paper is exposed to heat in an accelerated ageing test the light scattering ability of the sheet is not changed [72]. This means that the bonded area of the sheet is unchanged after the heat treatment. Page [73] has also shown that the fibre bonding strength of paper increases during heat treatment whereas the fibre strength decreases. These results also agree with the fact that the wet strength of paper increases during heat treatment [74]. The wet strength can increase up to 40% of the dry strength of the paper [75]. It has also been shown that the wet strength of paper increases during natural ageing, and it is probable that it is a matter of similar mechanisms. The wet strength increase is assumed to depend on cross linking in the cellulose wall of the fibres and in the fibre-fibre bonding surfaces.

Cross linking reactions in cellulose lead to embrittlement. It is probable that these cross linking reactions contribute to the increase in specific modulus of paper during natural and accelerated ageing [76] although it has not yet been possible to separate the physical and chemical influences on the elasticity modulus. Back [74] has suggested that aldehyde groups can react with hydroxyl groups in a cross linking reaction and thereby form hemi-acetal bonds. A keto-group on carbon atom 2 or 3 in a cellulose chain would similarly be able to form hemiketal bonds to other cellulose chains. A high content of carbonyl groups is therefore favourable for cross linking reactions. It is also probable that carbonyl-containing hydrolysis and decomposition products from the cellulose, hemicellulose etc can crosslink the cellulose chains in acetal- and ketal-forming reactions.

2.5 Dating of Historical Documents

The dating of historical documents is often used as a means of determining their authenticity. The age of any document is usually associated with a typical ink composition and specific writing support. The writing support is the material on which inks and pigments form the matter of the text and pictures. These materials are of organic origin, and thus their dating is relatively simple, using ^{14}C radiocarbon dating.

The majority of texts on historical manuscripts are written using iron gall ink, which is the most important ink in Western history [77]. The ink is produced from four basic ingredients: galls, vitriol of iron (iron sulphate), gum Arabic as a binding medium, and an aqueous medium, such as wine, beer, or vinegar to prevent moulding of the ink. By mixing gallic acid with iron sulphate, a water-soluble ferrous gallate complex is formed. Due to its solubility, the ink penetrates the writing support, making it difficult to erase. When exposed to atmospheric oxygen, a black ferric gallate pigment is formed. This complex is not water soluble, which contributes to its indelibility as a writing matter. Normally, the presence of oxygen directly leads to the formation of the ferric gallate pigment when gallic acid and iron sulphate are mixed. In order to slow down the precipitation of this insoluble complex, a binding material, such as gum arabic, is added to the mixture. The iron gall ink is very slowly decomposed by atmospheric oxygen and this leads to changes in the ink colour and,

occasionally, to complete degradation of the writing support by increasing its acidity [78].

Colour pigments are used as materials for manuscript decoration, such as rubrication or illumination [79 - 81]. The pigments are water-insoluble, and are mixed with a binding material (gum arabic, egg yolk, gum resin) in order to be useable for drawing. The pigments are either inorganic or organic; their origin could be natural (minerals, substances isolated from animals) or synthetic. The medieval illustrators preferred the use of inorganic pigments, as these were, even then, well known to be less fugitive and more stable than organic ones. Some pigments are either of modern manufacture or, for other reasons, are unlikely to have been used for the manuscript decoration at a particular time or place. Therefore, the identification of the chemical composition of the pigment used could serve as date-marker, or if the modern pigment is identified, it could indicate a forgery or at least a recently restored work. Examples of historical and modern pigments are given in Table 1.

Table 2.1: Examples of historical and modern pigments used for decoration of manuscripts [82].

Color	Pigment	Chemical composition	Origin, date of use/production
	Lead white	$2PbCO_3 \cdot Pb(OH)_2$	Mineral, antiquity
	Barytes	$BaSO_4$	Antiquity
White	Calcite (chalk)	$CaSO_4$	Mineral, antiquity
	Zinc white	ZnO	1834
	Anatase	TiO_2	1923
	Azurite	$2CuCO_3 \cdot Cu(OH)_2$	Mineral, antiquity
	Lazurite (lapis lazuli)	$Na_8[Al_6S_6O_{24}]S_n$	Mineral, antiquity/Synthetic 1828
Blue	Prussian blue	$Fe_4[Fe(CN)_6]_3 \cdot 14–16H_2O$	1704
	Cobalt blue	$CoO \cdot Al_2O_3$	1775
	Winsor blue	Copper(II) phthalocyanine	1936
	Malachite	$CuCO_3 \cdot Cu(OH)$	Mineral, antiquity
	Green earth	$K[(Al^{III} \cdot Fe^{III})(Fe^{II} \cdot Mg^{II})](AlSi_3 \cdot Si_4)O_{10}(OH)_2$	Mineral, antiquity
Green	Scheele's green	$CuHAsO_3$	1775
	Cobalt green	$CoO \cdot nZnO$	1780
	Phtalocyanine green	Copper(II) chlorophthalocyanine	1938
	Orpiment	As_2O_3	Mineral, antiquity
	Lead tin yellow	Pb_2SnO_4	Synthetic, antiquity
Yellow	Cadmium yellow	CdS	Mineral/synthetic 1845
	Chrome yellow	$PbCrO_4$ or $PbCrO_4 \cdot 2PbSO_4$	1809
	Cobalt yellow	$K_3[Co(NO_2)_6]$	1861
	Sienna	$Fe_2O_3 \cdot H_2O$ +clay	Synthetic, antiquity
Orange	Ochre	Fe_2O_3 +clay	Mineral
	Cadmium orange	Cd(S, Se)	Late 19th century
	Minium	Pb_3O_4	Synthetic, antiquity
Red	Vermilion (cinnabar)	HgS	Mineral/synthetic, 13th century
	Cadmium red	$CdSe$	1910
	Ivory black	$Ca_3(PO_4)_2$ +C +$MgSO_4$	Synthetic, antiquity
Black	Magnetite	Fe_2O_3	Mineral, antiquity
	Mineral black	$Al_2O_3 \cdot nSiO_2$ +C	Mineral, antiquity

On the other hand, some pigments, for example, lazurite, vermilion and orpiment, have been in use for a long time and their identification could not be related to a particular period of time. Pigments are relatively chemically stable, nevertheless, the following processes could happen:

1. A change in the crystal structure, for example, the hexagonal structure of vermilion could be changed to cubic if the pigment is preserved in dark for a long time, resulting in darkening of the red shade of vermilion.

2. Microscopic cracks on the picture surface are formed due to motion of the writing support (especially parchment is a hygroscopic material reacting to the fluctuation in the humidity).

3. A chemical change of the pigment, for example, the lead(II) sulfide could be formed from lead white ($2PbCO_3.Pb(OH)_2$) by action of polluted air.

2.6 Spectroscopic Techniques

The following spectroscopic techniques can be used to determine the composition of both ink pigments and writing support for the purpose of document dating and preservation. Compositional make-up is important if a comprehensive preservation method is to be prescribed. These methods were employed in analysing the paper samples in this study. With the exception of Raman spectroscopy, the rest os the techniques presented in this section have been employed in this thesis. The considerable amount of background fluorescence made it impossible to obtain useable Raman spectra of the sapmles.

2.6.1 Infrared spectroscopy

A molecule produces infrared spectrum when it absorbs a photon of energy $E = hv$ at the frequencies that correspond to vibrational energy states of the molecule. The absorbed energy is distributed in the molecule according to the following equation

$$E_{total} = E_{electronic} + E_{vibrational} + E_{rotational} + E_{transitional} \qquad (2.18)$$

The translational energy relates to the displacement of molecules in space as a function of the normal thermal motions of matter. Rotational energy, which gives rise to its own form of spectroscopy, is observed as the tumbling motion of a molecule, which is the result of the absorption of energy within the microwave region. The vibrational energy component is a higher energy term and corresponds to the absorption of energy by a molecule as the component atoms vibrate about the mean centre of their chemical bonds. The electronic component is linked to the energy transitions of electrons as they are distributed throughout the molecule, either

localized within specific bonds, or delocalized over structures, such as an aromatic ring. In order to observe such electronic transitions, it is necessary to apply energy in the form of visible and ultraviolet radiation as shown in equation (2.19):

$$E = h\nu \qquad (2.19)$$

The fundamental requirement for infrared activity, leading to absorption of infrared radiation, is that there must be a net change in dipole moment during the vibration for the molecule or the functional group under study. The basic model of the simple harmonic oscillator and its modification to account for anharmonicity suffices to explain the origin of many of the characteristic frequencies that can be assigned to particular combinations of atoms within a molecule. From a simple statement of Hooke's law one can express the fundamental vibrational frequency of a molecular ensemble according to equation:

$$\nu = \frac{1}{2\pi}\sqrt{\frac{k}{\mu}} \qquad (2.20)$$

where ν is the fundamental vibration frequency, k is the force constant, and μ is the reduced mass. The reduced mass for a molecule made up of two atoms of masses m_1 and m_2 is given by , $\mu = m_1 m_2/(m_1 + m_2)$. This simple equation provides a link between the strength (or springiness) of the covalent bond between two atoms (or molecular fragments), the mass of the interacting atoms and the frequency of vibration.

FTIR (Fourier Transform InfraRed) is a method of obtaining infrared spectra by first collecting an interferogram of a sample signal using an interferometer, and then performing a Fourier Transform (FT) on the interferogram to obtain the spectrum. An FTIR Spectrometer collects and digitizes the interferogram, performs the FT function, and displays the spectrum. The interpretation of FTIR spectra and assignment of group frequencies is treated in depth in reference [83].

Infrared spectroscopy is a very useful tool for obtaining rapid information about the structure of paper constituents and chemical changes taking place in paper due to various degradation processes. Ever since the advent of the Fourier transform infrared (FTIR) spectrometer, this technique has been used for paper surface characterization. This has an advantage over conventional chemical methods, which

are time-consuming and also result in a concomitant degradation of natural polymers. Measurements can be done in transmission or diffuse reflectance infrared (DRIFT) modes. The DRIFT technique has an advantage over other methods because it is a quick, easier, and non-destructive method. FTIR has been used to determine the sizing used during the production of paper that makes up the historical documents [84]. It has also been used to determine most of the inclusions found in the paper matrix.

FTIR spectroscopy has also been frequently used for protein analysis [84, 85]. The Amide I band, near 1650 cm^{-1}, is associated with C=O stretching vibration of peptide groups and presents several frequencies that depend upon the chemical environment and consequently upon the conformational state of polypeptides. The Amide II band, near 1550 cm−1 is associated with C–N stretching and N–H bending vibrations of peptide groups. These two bands are usually considered to be valuable indicators of the presence of gelatinee in original paper [86]. Determination of gelatinee content in paper with infrared spectroscopy, in Attenuated Total Reflectance (ATR) and diffuse reflectance mode, was also done by Rouchon [87]. FTIR can also be used for the identification of plant fibres in paper [88]. The predominant component of plant fibres is cellulose. Other major constituents (hemicelluloses and pectins) are also polysaccharides, whose spectra are similar. Band assignments of these fibres are presented in Table 2.2

Table 2.2: Infrared band assignments for cellulosic fibres [89].

Position (cm^{-1})	Assignment
~ 3335	ν(OH) free
~ 2900	ν(C-H)
~ 2850	ν(CH_2) symmetrical stretching
~ 1735	ν(C=O) ester
~ 1635	adsorbed water
~ 1595	ν(C=C) aromatic in-plane
~ 1505	ν(C=C) aromatic in-plane
~ 1475	δ(CH_2) scissoring
~ 1455	δ(C-H); δ(C-OH) 1° and 2° alcohol
~ 1420	δ(C-H)
~ 1365	δ(C-H)
~ 1335	δ(CH_2) wagging
~ 1315	δ(C-H)
~ 1280	δ(CH_2) twisting
~ 1235	δ(C-OH) out-of-plane
~ 1200	δ(C-OH); δ(C-CH)
~ 1155	ν(C-C) ring breathing, asymmetric
~ 1105	ν(C-O-C) glycosidic
~ 1050	ν(C-OH) 2° alcohol
~ 1025	ν(C-OH) 1° alcohol
~ 1005	ρ(-CH-)
~ 985	ρ(-CH-)
~ 895	ν(C-O-C) in plane, symmetric

The spectra of these fibres cannot be readily distinguished by eye, and library search techniques have also been found to be of limited value. However, there are certain 'signatures' that can be assigned to specific components. The relative intensity of each component can be considered as representative of the proportion of that component within the fibre:

- the C=O ester band at 1735 cm^{-1}, from pectin (however, this band can also be strengthened by the carbonyl groups of oxycelluloses found in degraded materials)
- the C=C in-plane aromatic vibrations at 1595 cm^{-1} and 1505 cm^{-1}, from lignin
- the C-C ring breathing band at 1155 cm^{-1} and the C-O-C glycosidic ether band at 1105 cm^{-1}, both of which arise from the polysaccharide components (that is, largely cellulose).

The intensity of the C-H stretching vibration at 2900 cm^{-1} was taken as a measure of the general organic material content of the fibre.

2.6.2 Raman Spectroscopy

When light is scattered from a molecule most photons are elastically scattered. The scattered photons have the same energy (frequency) and, therefore, wavelength, as the incident photons. However, a small fraction of light (approximately 1 in 10^7 photons) is scattered at optical frequencies different from, and usually lower than, the frequency of the incident photons. The process leading to this inelastic scatter is termed the Raman effect. Raman scattering can occur with a change in vibrational, rotational or electronic energy of a molecule. The difference in energy between the incident photon and the Raman scattered photon is equal to the energy of a vibration of the scattering molecule. A plot of intensity of scattered light versus energy difference is a Raman spectrum.

The Raman effect arises when a photon is incident on a molecule and interacts with the electric dipole of the molecule. It is a form of electronic (more accurately, vibronic) spectroscopy, although the spectrum contains vibrational frequencies. In classical terms, the interaction can be viewed as a perturbation of the molecule's electric field. In quantum mechanics the scattering is described as an excitation of an electron to a virtual state either lower or higher in energy than a real electronic transition with nearly coincident de-excitation and a change in vibrational energy. The scattering event occurs in 10^{-14} seconds or less. The virtual state description of scattering is shown in Figure 2.11a.

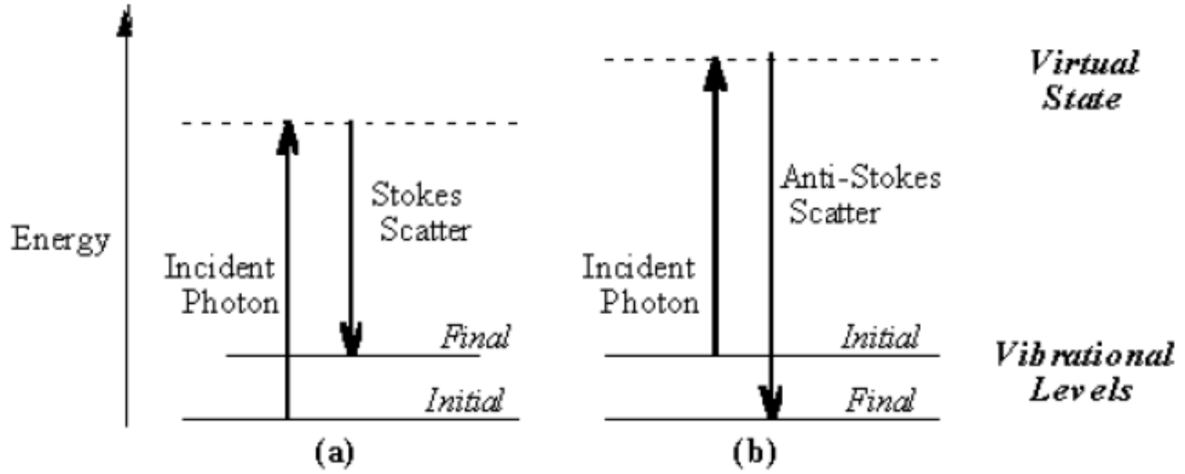

Figure 2.11: Energy level diagram for Raman scattering; (a) Stokes Raman scattering (b) anti-Stokes Raman scattering [90].

The energy difference between the incident and scattered photons is represented by the arrows of different lengths in Figure 2.11a. Numerically, the energy difference between the initial and final vibrational levels, $\bar{u}$, or Raman shift in wave numbers (cm^{-1}), is calculated through equation (2.21)

$$\bar{u} = \frac{1}{\lambda_{incident}} - \frac{1}{\lambda_{scattered}} \qquad (2.21)$$

in which $\lambda_{incident}$ and $\lambda_{scattered}$ are the wavelengths (in cm) of the incident and Raman scattered photons, respectively. The vibrational energy is ultimately dissipated as heat. Because of the low intensity of Raman scattering, the heat dissipation does not cause a measurable temperature rise in a material.

At room temperature the thermal population of vibrational excited states is low, although not zero. Therefore, the initial state is the ground state, and the scattered photon will have lower energy (longer wavelength) than the exciting photon. This Stokes shifted scatter is what is usually observed in Raman spectroscopy. Figure 2.11(a) depicts Raman Stokes scattering. A small fraction of the molecules are in vibrationally excited states. Raman scattering from vibrationally excited molecules leaves the molecule in the ground state. The scattered photon appears at higher energy, as shown in Figure 2.11(b). This anti-Stokes-shifted Raman spectrum is always weaker than the Stokes-shifted spectrum, but at room temperature it is strong enough to be useful for vibrational frequencies less than about 1500 cm^{-1}. The Stokes and anti-Stokes spectra contain the same frequency information. The ratio of anti-Stokes to Stokes intensity at any vibrational frequency is a measure of temperature. Anti-Stokes Raman scattering is used for contactless thermometry. The anti-Stokes spectrum is also used when the Stokes spectrum is not directly observable, for example because of poor detector response or spectrograph efficiency.

The energy of a vibrational mode depends on molecular structure and environment. Atomic mass, bond order, molecular substituents, molecular geometry and hydrogen bonding all effect the vibrational force constant which, in turn dictates the vibrational energy. For example, the stretching frequency of a phosphorus-phosphorus bond ranges from 460 to 610 to 775 cm^{-1} for the single, double and triple bonded moieties

respectively [90]. Much effort has been devoted to estimation or measurement of force constants. For small molecules, and even for some extended structures such as peptides, reasonably accurate calculations of vibrational frequencies are possible with commercially available software. Vibrational Raman spectroscopy is not limited to intramolecular vibrations. Crystal lattice vibrations and other motions of extended solids are Raman-active. Their spectra are important in such fields as polymers and semiconductors. In the gas phase, rotational structure is resolvable on vibrational transitions. The resulting vibration/rotation spectra are widely used to study combustion and gas phase reactions generally. Vibrational Raman spectroscopy in this broad sense is an extraordinarily versatile probe into a wide range of phenomena ranging across disciplines from physical biochemistry to materials science.

A simple classical electromagnetic field description of Raman spectroscopy can be used to explain many of the important features of Raman band intensities. The dipole moment, **P**, induced in a molecule by an external electric field, **E**, is proportional to the field as shown in equation (2.22).

$$\boldsymbol{P} = \alpha \mathbf{E} \qquad (2.22)$$

The proportionality constant α is the polarizability of the molecule. The polarizability measures the ease with which the electron cloud around a molecule can be distorted. The induced dipole emits or scatters light at the optical frequency of the incident light wave. Raman scattering occurs because a molecular vibration can change the polarizability. The change is described by the polarizability derivative, $\frac{\partial \alpha}{\partial \boldsymbol{Q}}$, where **Q** is the normal coordinate of the vibration. The selection rule for a Raman-active vibration, that there be a change in polarisability during the vibration, is given in equation (2.23)

$$\frac{\partial \alpha}{\partial Q} \neq 0 \qquad (2.23)$$

The Raman selection rule is analogous to the more familiar selection rule for an infrared-active vibration, which states that there must be a net change in permanent dipole moment during the vibration. From group theory it is straightforward to show that if a molecule has a centre of symmetry, vibrations which are Raman-active will

be silent in the infrared, and vice versa. Scattering intensity is proportional to the square of the induced dipole moment, that is to the square of the polarisability derivative, $\left(\frac{\partial \alpha}{\partial Q}\right)^2$. If a vibration does not greatly change the polarisability, then the polarisability derivative will be near zero, and the intensity of the Raman band will be low. The vibrations of a highly polar moiety, such as the O-H bond, are usually weak. An external electric field cannot induce a large change in the dipole moment and stretching or bending the bond does not change this. Typical strong Raman scatterers are moieties with distributed electron clouds, such as carbon-carbon double bonds. The π-electron cloud of the double bond is easily distorted in an external electric field. Bending or stretching the bond changes the distribution of electron density substantially, and causes a large change in induced dipole moment. Physicists generally prefer a quantum-mechanical approach to Raman scattering theory, which relates scattering frequencies and intensities to vibrational and electronic energy states of the molecule. The standard perturbation theory treatment assumes that the frequency of the incident light is low compared to the frequency of the first electronic excited state. The small changes in the ground state wave function are described in terms of the sum of all possible excited vibronic states of the molecule.

Raman spectroscopy has been applied to different types of artwork. In the case of artwork on paper supports, the presence of fillers in the cellulose can be detected. A Raman analysis of a map from the XVII century [91] showed that gypsum ($CaSO_4.2H_2O$) was used as filler in the cellulose. Moreover, the sensitivity of this Raman technique also allowed the degradation mechanisms of some cultural heritage materials to be determined. Bicchieri [92] examined degraded papers with several non-destructive spectroscopic techniques, including Raman spectroscopy. This work is a contribution to a better understanding of the degradation pattern of historical samples in order to be able to choose the most appropriate restoration treatment using non-destructive spectroscopic techniques. Cellulose undergoing accelerated hydrothermal ageing gives rise to a pattern of carbonyl groups; their vibrational modes were observed in Raman spectra by Lojewska et al. [93].

Raman spectroscopy probes molecular and crystal-lattice vibrations and is therefore sensitive to the composition, bonding, chemical environment, phase and crystalline structure of the sample material. Raman spectroscopy is a fingerprinting technique, and materials are identified by comparing their characteristics vibrational spectra with those in databases [94]. The characteristics of the Raman spectroscopy that make it well suited for analysis of historical documents include its molecular specificity, non-destructiveness, applicability to samples of large or non-uniform shapes and relative immunity to interference.

2.6.3 X-ray Fluorescence

X-Ray Fluorescence spectroscopy (XRF) is a widely used technique in museum laboratories for the analysis of artefacts. The technique most commonly used involves the exposure of unprepared or minimally prepared surfaces to the X-radiation [95, 96]. X-rays emitted from atoms by fluorescence carry elemental information. Each element thus emits a characteristic X-ray spectrum. This fact has been used to investigate solid materials by obtaining qualitative and quantitative information for most of the elements of the periodic table. However, the difficulty met in detecting light elements such as C, N and O coupled with the fact that this method cannot provide molecular information make it unsuitable for the study of organic material [97]. The main advantage of this technique is that it is mostly non-destructive which makes it the perfect tool for elemental analysis of cultural heritage. Experimental setups can be categorized according to the way in which X-rays are generated and how the emitted radiation is energetically selected. XRF is involved whenever high energy radiation is used to irradiate the sample; X-ray emission is, in contrast, involved when charged particles such as electrons, protons or ions are used as the bombarding beam. The emitted radiation is wavelength dispersed (WD) according to Bragg's law by means of a suitable crystal which is sequentially tilted towards or away from the beam or is energy dispersed (ED) by means of solid state lithium-drifted [Si(Li)] detectors. The use of a collimated X-ray beam makes it possible to direct the incoming beam at an extremely low glancing angle (< 0.1°) so as to interact with the surface of the sample alone,. Modern micro-XRF spectrometers provide spatial resolution in the range of 5–10 μm and are suitable for mapping experiments. The potential of direct imaging has also been demonstrated.

Moreover, the use of synchrotron radiation has led to improvements both in intensity and the beam diameter of the stimulating radiation,
thus reducing the achievable lateral resolution to 2–5 μm for synchroton radiation XRF.

In a study done by Manso et al [98] it was shown that the elemental composition of some newspapers depended with the year of publication. This means that the composition and concentration of specific elements in a writing support can give an indication of when that writing support was made.

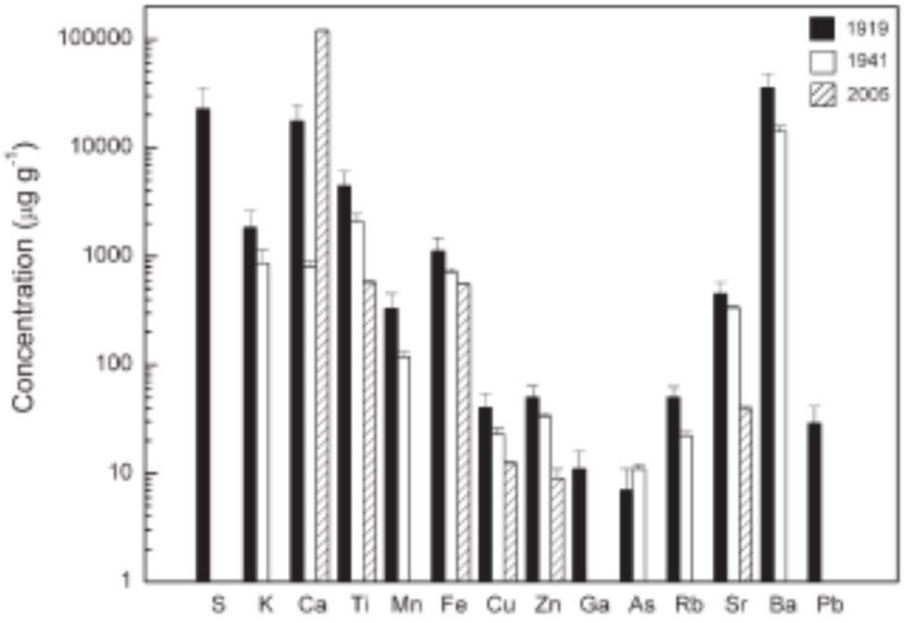

Figure 2.12: Mean elemental concentration in newspaper from different years obtained by EDXRF [98].

Except for Ca, the most recent newspaper presents lower elemental concentration levels and elemental variability than the older ones. The number of detected elements depended on the newspaper age, and decreases from the oldest to the most recent as shown in figure 2.12. Similar results were obtained in [99] when analyzing different types of paper from the XVI to XXI century. Rozic et al. [100] determined the concentrations of Pb, Rb, Sr, Y, Zr, K, Ca, Ti, V, Cr, Mn,Fe, Ni, Cu, Zn and Co by EDXRF in ash samples of modern papers. The obtained results can serve as useful information for examination of properties of the office papers, as well as for investigation of possibilities for recycling of the same papers. In reference

[101], the elemental composition of the paper sheets from an Italian book (Rivista del Diritto Comerciale, 1941) was determined by EDXRF.

On the other hand, the presence of unusual elements in either handmade or machine made historical documents allowed for the identification of the paper maker. The study reported in reference [102] highlights the presence of Co, Ni, As and Bi in paper composition of 18th and 19th century Dutch manuscripts, allowing easy identification of the manufacturer. These four elements together in such high concentration levels have never been reported before. Taking into account the strong Spearman correlation [102] coefficients between these four elements, the author suggested the use of a mineral containing Co, Ni, As and Bi in paper composition.

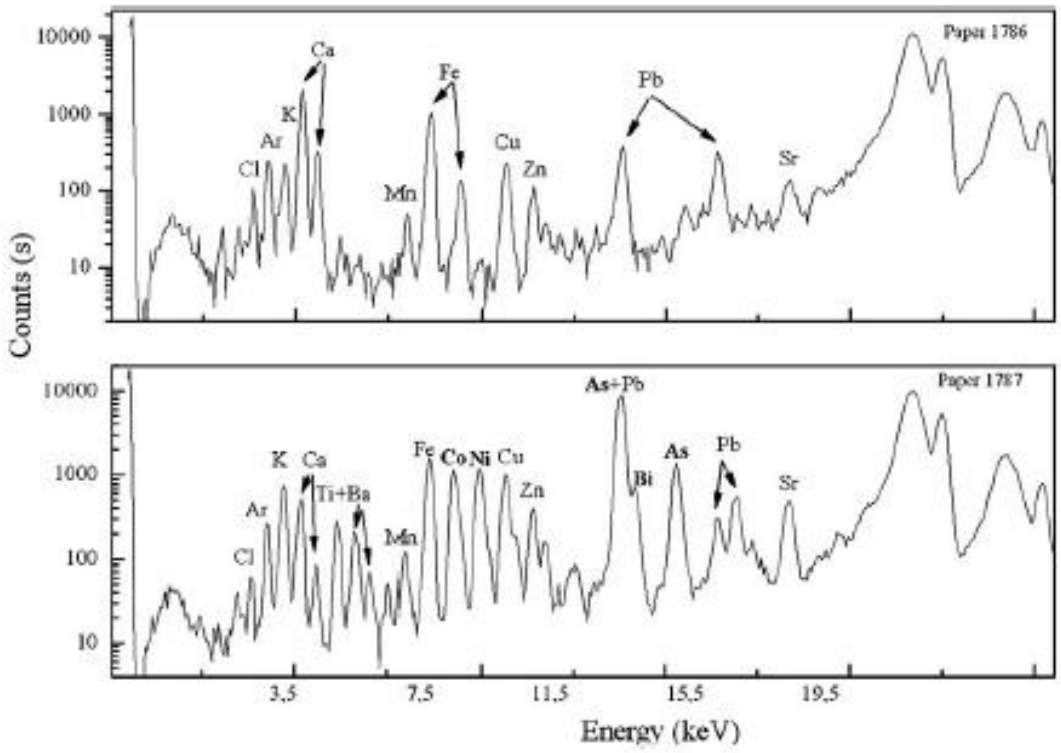

Figure 2.13: Spectra of 1786 and 1787 paper obtained by EDXRF. The unusual presence of the elements in bold allowed the identification of the papermaker [102].

In figure 2.13 the spectra of the two analyzed papers obtained by EDXRF can be seen where these elements are highlighted in bold. The levels of Ca, and K also allowed differentiation between Dutch and the rest of the analysed manuscripts.

2.6.4 Polarised Light Microscopy (PLM)

The cellulose fibres of paper samples can also be uniquely identified by PLM. These fibres have optical characteristics that can be used to determine the nature of the paper matrix. Many transparent solids are optically isotropic, meaning that the index of refraction is equal in all directions throughout the crystalline lattice. Many polymers, including cellulose, and a wide variety of both organic and inorganic compounds are isotropic [103, 104]. Crystals are classified as being either isotropic or anisotropic depending upon their optical behaviour and whether or not their crystallographic axes are equivalent. All isotropic crystals have equivalent axes that interact with light in a similar manner, regardless of the crystal orientation with respect to incident light waves. Light entering an isotropic crystal is refracted at a constant angle and passes through the crystal at a single velocity without being polarized by interaction with the electronic components of the crystalline lattice. Anisotropic crystals, on the other hand, have crystallographically distinct axes and interact with light in a manner that is dependent upon the orientation of the crystalline lattice with respect to the incident light. When light enters the optical axis of anisotropic crystals, it acts in a manner similar to interaction with isotropic crystals and passes through at a single velocity. However, when light enters a non-equivalent axis, it is refracted into two rays each polarized with their vibration directions oriented at right angles to one another, and travelling at different velocities. This phenomenon is termed double or birefraction and is seen to a lessor or greater degree in all anisotropic crystals [103-105]. When anisotropic crystals refract light, the resulting rays are polarized and travel at different velocities. One of the rays travels with the same velocity in every direction through the crystal and is termed the ordinary ray. The other ray travels with a velocity that is dependent upon the propagation direction within the crystal. This light ray is termed the extraordinary ray. The retardation between the ordinary and extraordinary ray increases with increasing crystal thickness. The two independent refractive indices of anisotropic crystals are quantified in terms of their birefringence, a measure of the difference in refractive index. Thus, the birefringence (B) of a crystal is defined as the difference between $\mathbf{n}_{high}$ and $\mathbf{n}_{low}$. $\mathbf{n}_{high}$ is the largest refractive index and $\mathbf{n}_{low}$ is the smallest. This

expression holds true for any part or fragment of an anisotropic crystal with the exception of light waves propagated along the optical axis of the crystal. As mentioned above, light that is doubly refracted through anisotropic crystals is polarized with the vibration directions of the polarized ordinary and extraordinary light waves being oriented perpendicular to each other. We can now examine how anisotropic crystals behave under polarized illumination in a polarizing microscope. A polarizer placed beneath the sub stage condenser is oriented such that polarized light exiting the polarizer is plane polarized in a vibration direction that is east-west with respect to the optic axis of the microscope stand (Fig. 2.4). Polarized light enters the anisotropic crystal where it is refracted and divided into two separate components vibrating parallel to the crystallographic axes and perpendicular to each other. The polarized light waves then pass through the specimen and objective before reaching a second polarizer (usually termed the analyser) that is oriented to pass a polarized vibration direction perpendicular to that of the sub stage polarizer. Therefore, the analyser passes only those components of the light waves that are parallel to the polarization direction of the analyser. The retardation of one ray with respect to another is caused by the difference in speed between the ordinary and extraordinary rays refracted by the anisotropic crystal [104, 105]. A schematic illustration of microscope configuration for crossed polarized illumination is presented in figure 2.14.

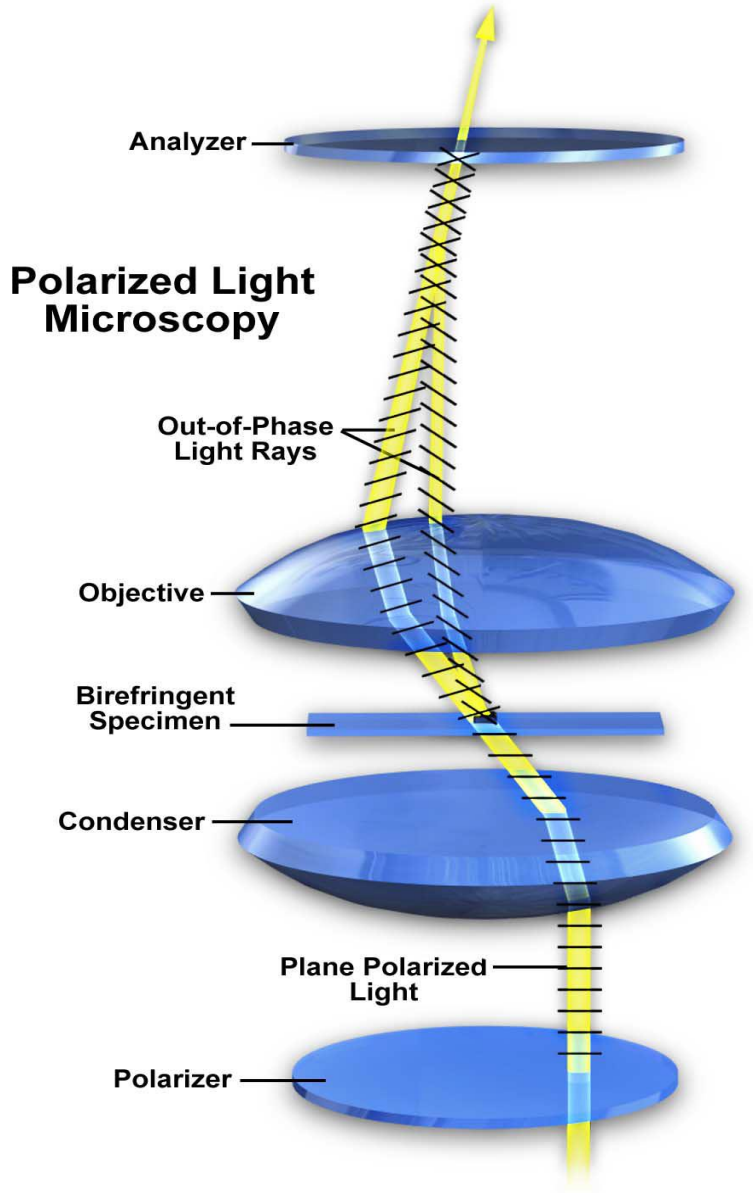

Figure 2.14: Schematic microscope configuration for observing birefringent specimens under crossed polarized illumination [106].

The difference in refractive indices will cause one ray to pass through the crystal at a slower rate than the other ray. In other words, the velocity of the slower ray will be retarded with respect to the faster ray. This retardation is the measure of the physical distance between the fast and the slow components can be quantified using the equation:

$$\Gamma = t \times |n_{high} - n_{low}|$$

Γ is the retardation and *t* is the thickness of the sample.

More than 95% of all particles and fibres can be identified and characterised by PLM alone. In order to understand the particle and fibre identification process, it is important to understand the characteristics of particles and fibres that will be observed by the polarized light microscope. The observed characteristics are

(i) *Morphology* : The shape of the fibre. This can be equant (same dimension in all directions), acicular (needlelike), rodlike, plate, tablet, flake, cylindrical or spherical. For fibres, morphology refers to cross-sectional shape

(ii) *Size*: The particle's dimensions and thickness. This will be limited to thickness for fibres

(iii) *Surface texture and hardness*: Surface smoothness or porosity of the particle. Description of any surface spines, ridges or furrows. Also include the elasticity of the particle when deformed.

(iv) *Refractive index*: The most important identifying characteristic of transparent particles. The internal atomic structure of the particle may result in one, two or three refractive indices

(v) *Pleochroism*: A change in colour in a coloured transparent particle of fibre that has more than one refractive index when its position is changed relative to the vibration direction of the polarizer. Used to determine whether the particle is anisotropic\isotropic

(vi) *Birefringence*: Numerical difference between the principal refractive indices. This may be determined through a measurement of the refractive indices or through observation and interpretation of the dispersion staining colours. It can also be obtained qualitatively through observation of the retardation in conjunction with particle thickness.

(vii) *Extinction angle*: The angle between the particle's extinction position and some prominent crystal face, length or cleavage plane.

(viii) *Sign of elongation*: In fibres or particles which are elongated, the location of high and low refractive indices relative to the direction of elongation.

2.6.5 Mössbauer Spectroscopy

The theory behind Mössbauer spectroscopy has been described in detail in numerous texts [107-110]. There are certain nuclides, called Mössbauer nuclides,

that exhibit a nuclear decay scheme where the transition from the first excited nuclear level (14.41keV for Fe-57) and sometimes from second excited nuclear levels to the ground state may occur with the recoilless emission of ɣ-ray. This gamma ray is uniquely capable of raising a similar nucleus in the same type of environment from ground state to the first (or second) excited nuclear level by recoilless absorption. Elements with one or more Mössbauer nuclides are shown in figure 2.15.

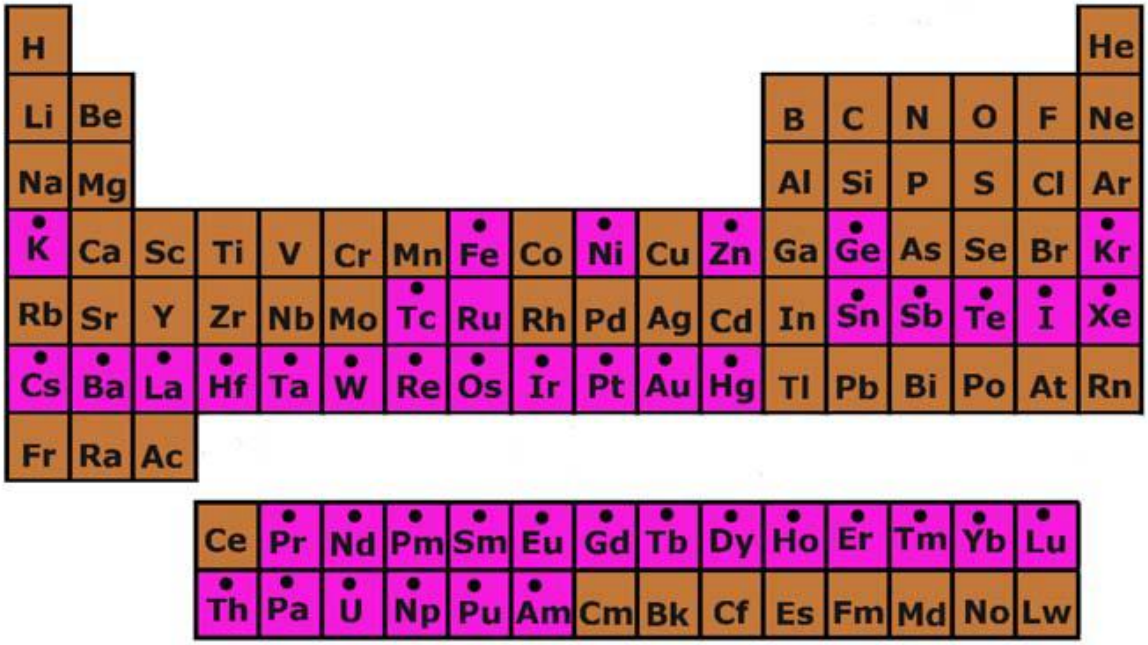

Figure 2.15: Elements with Mössbauer nuclides (the dotted elements) [111].

The recoilless absorption process depends on the fact that the emitting (source) and absorbing (sample) species are bound in a crystal lattice. Recoilless absorption may be destroyed by means of Doppler effect. If either the source or the absorber moves relative to the other, the conditions necessary for resonant or recoilless absorption are destroyed. By moving either the source or absorber toward the other the energy of the gamma ray is increased as seen by the absorbing species. By moving one away from the other the energy of the gamma ray as seen by the absorbing species is decreased. A complete Mössbauer spectrum would therefore have a plot of the rate of transmission of the gamma ray through the absorbing sample as a function of the Doppler velocity.

Recoilless absorption occurs at zero velocity only if both the emitting and absorbing species are in the same physical environment. If this is not the case then the recoilless absorption will occur at a non-zero Doppler velocity. Such a displacement of recoilless absorption from zero velocity is called isomer shift (IS) and is shown in figure 2.16. Three parameters of importance in describing a Mössbauer spectrum are the isomers shift (δ), electric quadrupole splitting (Δ) and magnetic hyperfine splitting (MHS). The description of these parameters and the standard experimental setup for Mössbauer spectroscopy measurements are treated in depth elsewhere [107,113–114].The IS value is a function of the *s* electron density and for Fe-57 decreases with increasing *s* electron density [112]. The *d* electron density affects the isomer shift mostly by shielding the *s* electrons from the nucleus. The contribution from the *p* electrons is very small [110]. The electron density at the nucleus is a function of the oxidation state of the absorbing atom and of the electronegativity of its nearest neighbours. This therefore provides the means of qualitatively identifying compounds, determining the valence or oxidation states and structural information concerning the absorbing material.

Quadrupole splitting (Δ) is due to the interaction of the inhomogeneous electric field at the nucleus with the electric quadrupole moment of the excited nucleus. The result is a doublet or two resonant peaks. This occurs because the first nuclear excited level splits into two sublevels and two transitions of slightly different energy may occur. Δ is measured as the distance between two resonant peaks as shown in figure 2.16:

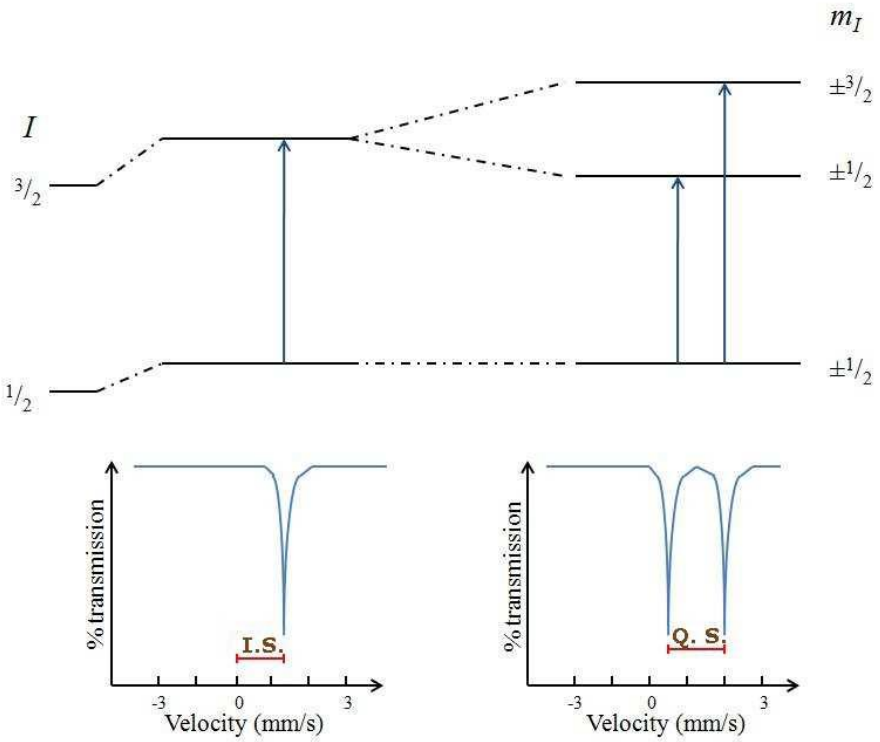

Figure 2.16: The Isomer Shift and Quadrupole Splitting of the nuclear energy levels and corresponding Mössbauer spectra [115].

Quadrupole splitting may be related quantitatively to the oxidation state and the nature of the chemical bonding of the absorbing atom [107]. It may also be used as a method of determining the symmetry of crystals and crystal distortions incurred by substitution in compounds. The isomer shift of a quadrupole split spectrum is taken as the displacement of centroid from zero velocity. The nuclear states have spin, and associated magnetic dipole moments. The spins can be oriented with different projections along a magnetic field. The energies of nuclear transitions are therefore modified when the nucleus is in a magnetic field. The energy perturbations caused by this Hyperfine Magnetic Fields (HMF) are sometimes called the “nuclear Zeeman effect,” in analogy with the more familiar splitting of energy levels of atomic electrons when there is a magnetic field at the atom. A hyperfine magnetic field lifts all degeneracies of the spin states of the nucleus, resulting in separate transitions identifiable in a Mössbauer spectrum. In the case of iron a spectrum with six resonances can be obtained as shown in figure 2.17:

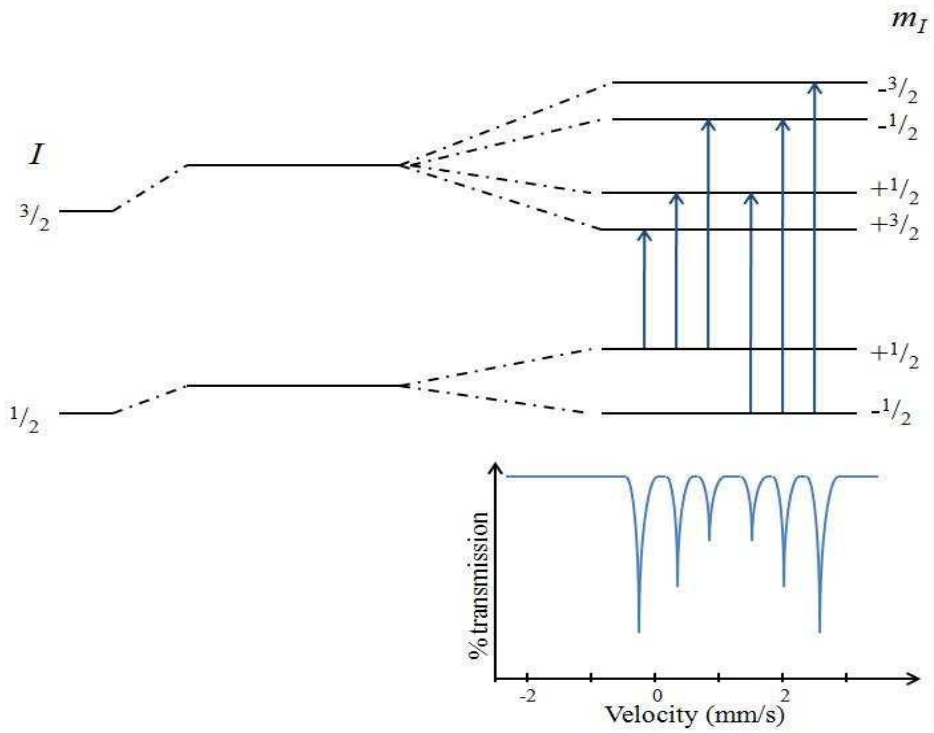

Figure 2.17: Mössbauer Magnetic Hyperfine Splitting (MHS) spectrum from bcc Fe [111].

Identification of magnetically ordered structures and determination of Currie and Neel temperatures for many materials may be accomplished by studying their MHS spectra.

The isomer shift, with supplementary information provided by the quadrupole splitting, often can be used to determine the valence and spin of ^{57}Fe and ^{119}Sn atoms. The isomer shift is proportional to the electron density at the nucleus, but this is influenced by the different σ- and π-donor acceptance strengths of surrounding ligands, their electro negativities, covalence effects, electronic screening, and other phenomena. It is usually best to have some independent knowledge about the electronic state of *Fe* or *Sn* in the material before attempting to determine valence. Nevertheless, even for unknown materials, valence and spin can often be determined reliably for the Mössbauer isotope. It is sometimes possible to use isomer shifts (IS) to find the number of 4*s* and 3*d* electrons at an Fe atom. This however requires calibration curves. For ^{57}Fe, the calibration curves are plots of the IS versus the number of 4*s* electrons at the iron atom. These plots however do not consist of just one curve. The 3*d* electrons screen the 4*s* electrons from the nucleus, and with more 3*d* electrons on the Fe atom, there is a more shallow slope of IS

versus 4*s* count. The ^{57}Fe isomer shifts shown in Figure 2.18 are useful for determining the valence and spin state of Fe ions. If the ^{57}Fe isomer shift of an unknown compound is +1.2 mm/s with respect to bcc Fe, for example, it is identified as high spin Fe(II). Low-spin Fe(II) and Fe(III) compounds show very similar isomer shifts, so it is not possible to distinguish between them on the basis of isomer shift alone.

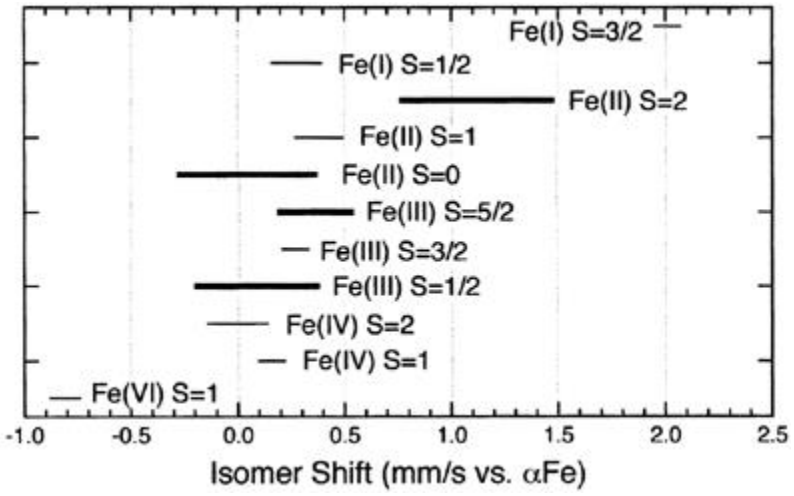

Figure 2.18: Ranges of isomer shifts in Fe compounds with various valences and spin states, with reference to bcc Fe metal at 300 K [111].

Fortunately, there are distinct differences in the electric quadrupole splitting of these electronic states. For low spin Fe(II), the quadrupole splitting are rather small, being in the range of 0 to 0.8 mm/s. For low spin Fe(III) the electric quadrupole splitting are larger, being in the range 0.7 to 1.7 mm/s. The other oxidation states shown in Figure 2.18 are not so common, and tend to be of greater interest to chemists than materials scientists.

CHAPTER 3: METHODOLOGY

3.1 Introduction

This chapter gives a detailed description and explanation of the methods and the experimental set ups performed to determine the elemental composition of the paper as well as the filler material of the samples investigated. ED-XRF technique was used for the determination of metal elements in the samples. A description of the sample analysis of oxidation state of the most abundant metal element is also given. Knowledge of the oxidation/valence state of the most prevalent metal element in paper samples is important from a document preservation perspective. This was done using the Mössbauer spectroscopy technique. This technique was chosen because of the availability of this spectrometer. This method has also never been used before to study paper samples. It provided an opportunity to try a new technique in historical document analysis and conservation. Finally polarized light microscopy and FTIR spectroscopy were used to investigate the fibres, fillers and sizing in the samples.

3.2 Sampling Method

Sampling, in this study, is defined as the process of selecting and collecting the sample for analysis. The samples were obtained from documents of historical value therefore sampling was limited to sizes that do not considerably affect the integrity of the documents. The samples of cross-sectional area of not more than 5mm^2 were cut from bottom corners of the first page, centre page and last page of each document. Figure 3.1 below shows a typical sample size used in this investigation.

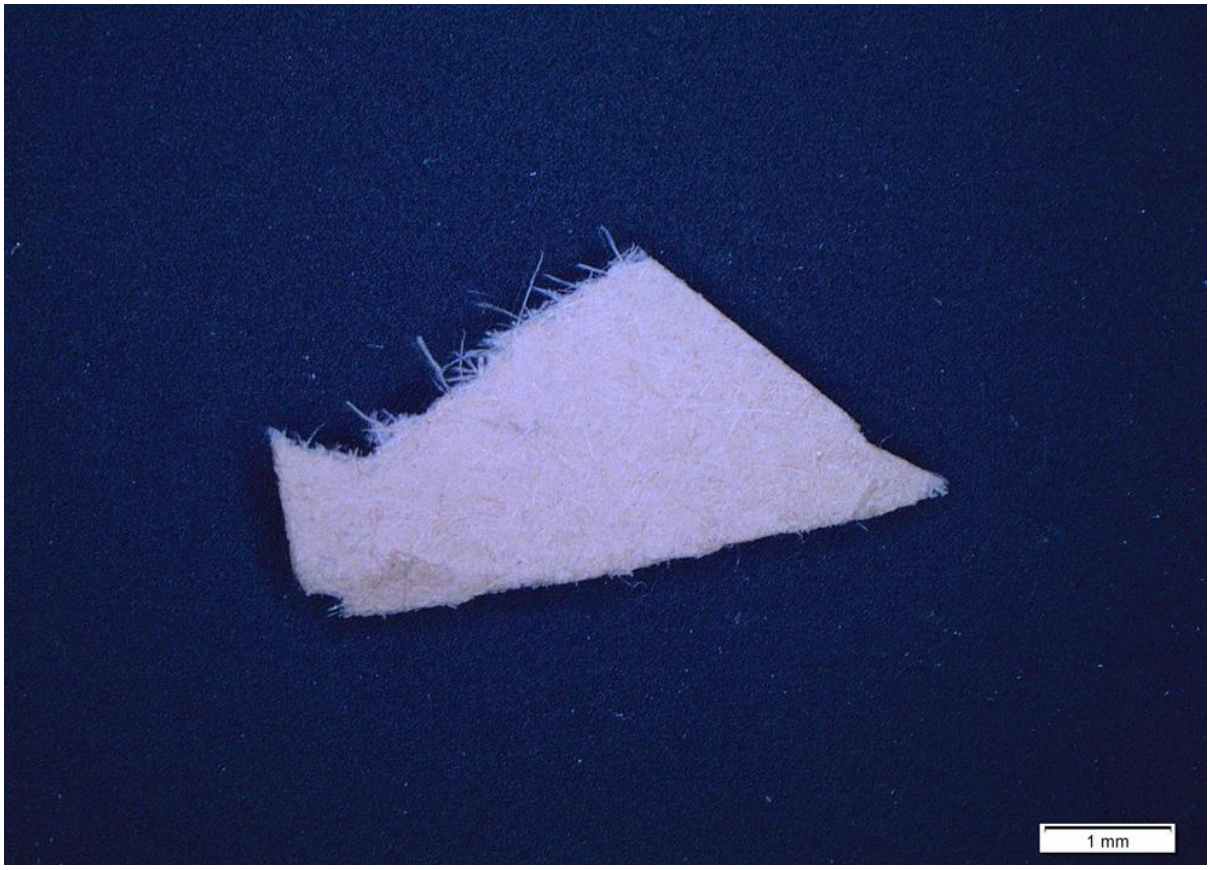

Figure 3.1: Typical sample size (*Wildsport of Africa*).

Three (3) samples were therefore cut from each document for further analysis. This sampling design was adopted to ensure that the samples are representative of the document from which they have been removed. The samples were then sealed in plastic sample holders and labeled with the name of the document from which they were obtained. Table 3.1 below shows the samples that were collected from the National Library of South Africa.

Table 3.1: Collection of samples studied.

Item	Title	Classification	Publication date
1	Het Leven en Bedryf van Michiel De Ruiter.	Book	1732
2	South Africa (Barrow)	Book	1803
3	The 19th Century (Volume 33)	Book	1893
4	The Press	Newspaper	1893
5	The 19th Century (Volume 39)	Book	1896
6	The Weekly Press	Newspaper	1897
7	Regulatien : Staatsbiblioteek	Periodical	1897

8	The Weekly Press	Newspaper	1899
9	Natal Almanac & Directory	Periodical	1901
10	Die Huisgenoot	Periodical	1918
11	The Standard & West Rand Review	Newspaper	1925
12	Wild sport of Africa	Book	1844
13	The Boeren in Zuid Africa	Book	1897
14	The Courier	Newspaper	1946

In addition to these samples, other samples were also obtained from one of the local libraries in Timbuktu, Mali. The Timbuktu manuscript sample cannot be identified with any particular manuscript as it was obtained from left over material during restoration at a private library in Timbuktu. These samples therefore do not have any known date associated with them.

Most of the spectroscopic techniques used in the analysis of the samples required micro samples, therefore. These micro samples were obtained from the primary samples without any additional intrusion on the original documents. Any other subsequent sample preparation that was carried out was therefore specific to the spectroscopic technique being used and is therefore discussed in the following sections.

3.3 Determination of pH Levels of Samples

An Abbey pH pen was used to determine the pH levels of the paper samples studied. A very small line was drawn on the paper sample using the Abbey pen. Colour changes were observed as the ink dried. A colour change of the drawn line from orange to purple would mean that the sample is neutral to alkaline with a pH value of above 6.5. If the colour of the ink becomes yellow to colourless, then the sample is acidic. If the ink becomes yellow, then the pH is below 6.0. If the ink becomes colourless then the sample has a pH value of less than 5.0. The observed colour changes are presented in Section 4.2.

3.4 Determination of Elemental Composition

The elemental composition of the document samples was determined by energy dispersive X-ray fluorescence (ED-XRF) analysis. This method was chosen for the elemental analysis of the solid paper/document samples because it requires little or no sample treatment or preparation. An energy dispersive X-ray fluorescence spectrometer[1], EDX-720 Shimadzu, was used for XRF measurements.

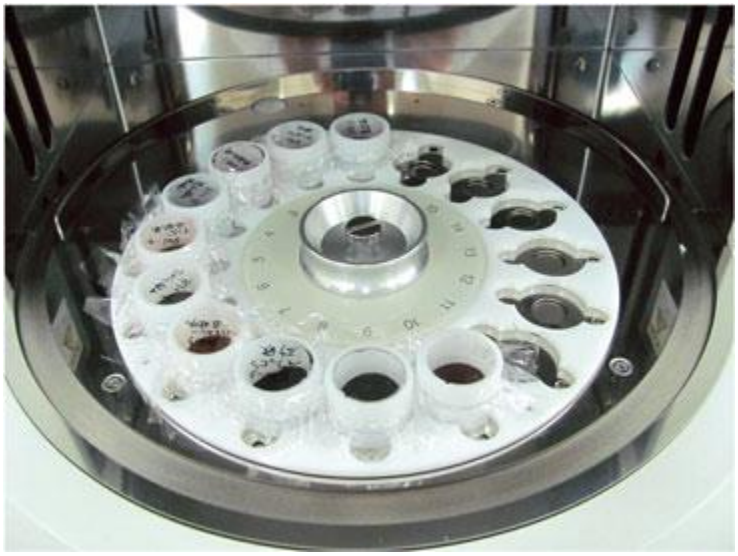

Figure 3.2: A 16-turret solid sample holder for EDX-720 with samples in place.

The samples were carefully placed into the sample holder of the X-ray spectrometer. The 16-turret solid sample holder is shown in figure 3.2. The surface of the sample was irradiated by an X-ray beam. When an appropriate energy was applied, a photoelectron was emitted. The vacancy left by the ejection of a photoelectron is filled by an outer electron while the energy difference is emitted in the form of X-ray fluorescence radiation. The excitation energies correspond to the emission lines of the elements in the sample while the intensity of the emission provides information about their concentration on the sample surface. The spectra were recorded in air and the instrument energy range was automatically set at 0 to 40 keV. The spectra recorded are shown in Section 4.2.

[1] It was made available by the department of Chemistry, NWU (Mafikeng Campus)

3.5 Determination of Valence State of Iron in Paper Samples

The valence state of each sample with trace amounts of iron was determined using Mössbauer spectroscopy. The Mössbauer spectrometer used is located at the iThemba laboratories in Cape Town. Based on the results of XRF analysis, samples with considerable amount of iron were selected for valence state determination. Mössbauer spectra of all samples were measured in constant acceleration transmission mode with instrumentation shown in figure 3.3. The sample was folded in the sample holder to increase the beam interaction with the iron in the sample. This was done because the iron in the sample was in trace quantities, therefore the folding would also reduce the spectrum collection time.

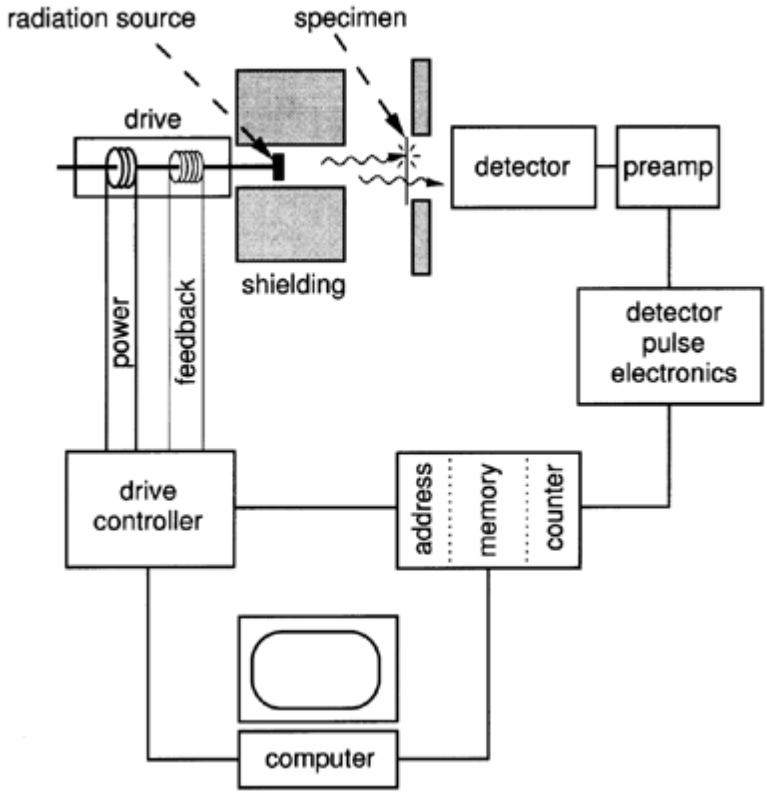

Figure 3.3: Experimental set-up for the determination of Mössbauer spectra of paper samples [114].

The ɣ-ray energy,E_{γ}, is tuned with a drive controller that imparts a Doppler shift, Δ*E*, to the ɣ- ray in the reference frame of the sample:

$$\Delta E = \frac{v}{c} E_{\gamma}$$

where v is the velocity of the drive and *c* is the speed of light. The radiation source for this ^{57}Fe Mössbauer spectrometer is the ^{57}Co isotope with a half-life of 271 days.

Most components for the Mössbauer spectrometer in figure 3.3 are standard items for x-ray detection and data acquisition. The items specialized for Mössbauer spectrometry are the electromagnetic drive and the radiation source. The unstable ^{57}Co nucleus absorbs an inner-shell electron, transmuting to ^{57}Fe and emitting a 122-keV gamma ray. The ^{57}Fe nucleus thus formed is in its first excited state, and decays about 141 ns later by the emission of a 14.41-keV gamma ray. This second gamma ray is the useful photon for Mössbauer spectrometry. While the 122-keV gamma ray can be used as a clock to mark the formation of the ^{57}Fe excited state, it is generally considered a nuisance in Mössbauer spectrometry, along with emissions from other contamination radioisotopes in the radiation source. A Mössbauer radiation source is prepared by diffusing the ^{57}Co isotope into a matrix material such as Rh, so that atoms of ^{57}Co reside as dilute substitutional solutes on the fcc Rh crystal lattice. Being dilute, the ^{57}Co atoms have a neighbourhood of pure Rh, and therefore all ^{57}Co atoms have the same local environment and the same nuclear energy levels. They will therefore emit gamma rays of the same energy. Although radiation precautions are required for handling the source, the samples (absorbers) are not radioactive either before or after measurement in the spectrometer.

The spectrum was obtained by counting the number of ɣ-ray photons that pass through the sample as a function of the ɣ-ray energy. At energies where the Mössbauer effect is strong, a dip was observed in the ɣ-ray transmission.

3.6 Paper Fillers and Size Determination

A number of spectroscopic techniques can be used to identify the filler material and sizing used in historical documents. Size and filler material are important in that they give an indication of the most likely degradation mechanism in these documents. This will in turn inform the document curators and conservators of the most appropriate methods to look after these documents. The initial plan was to use both Raman and FTIR spectroscopy to analyse the paper fillers. The Raman analysis was however producing too much background fluorescence for both the 532nm and 785nm laser sources. It was therefore finally resolved to use only the FTIR analysis. The FTIR measurements were done in reflection mode by use of Attenuated Total

Reflection (ATR). ATR is a reflection technique where the Infrared (IR) beam is directed through the internal reflection element (IRE) with a high index of refraction. The method requires no sample preparation. The IR light is totally reflected internally off the back surface which is in contact with the sample as shown in figure 3.4 below.

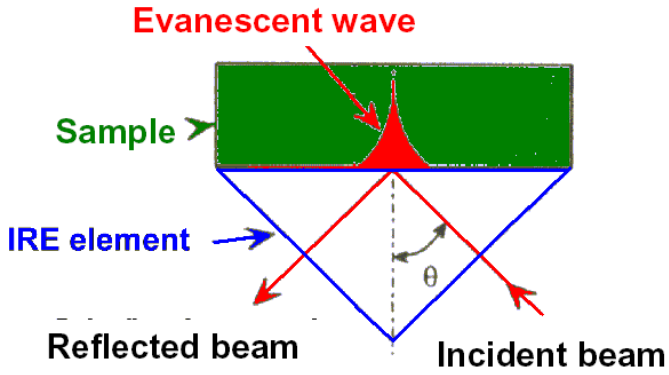

Figure 3.4: Single bounce ATR [116].

The sample must have a lower index of refraction than the IRE to achieve total internal reflection. Upon reflection at the IRE/sample interface, the IR light penetrates the sample to a small degree and the IR data from the sample is obtained. This evanescent wave that penetrates the sample decays exponentially. The depth of penetration is determined according to reference [116]. ATR has been used by Cain and Kalansky [117] to determine gelatine size in paper samples.

A ZnSe ATR crystal was used on a Bruker FTIR machine[2]. This crystal has a refractive index of 2.4 at wavenumber of 1000cm^{-1} and a cutoff spectral range of 520cm^{-1}. The penetration depth for this crystal is stated as 2µm meaning that it is a surface analysis instrument. The crystal was pressed against the sample to ensure that there is sufficient contact between the crystal and sample. The angle of incidence of the incoming IR for the ATR crystal is greater than the critical angle to ensure total internal reflection. This method is fairly routine and the results are highly reproducible due to the controlled presentation of the sample to the IR radiation by ATR crystal. FTIR spectra were collected for analysis for all samples and the results are presented in Chapter 4.

[2] Made available by the department of Physics – University of Pretoria

3.7 Optical characteristics

3.7.1 Sample Preparation

A glass dropper was used to transfer a small drop of the standard refractive index liquid of $n = 1.550$ onto the center of a cleaned microscope slide. The dropper was wiped on the edge of the refractive index bottle several times before quickly touching the dropper on the slide. This was done to ensure that only the minimum amount of the liquid was transferred to the microscope slide. The sample was placed on another pre-cleaned microscope slide and the slide holding the sample was put under the stereo microscope. Using a small steel needle, a single fibre was scratched off the paper sample and transferred onto the refractive index liquid drop previously put on the centre of the first slide. The surface tension helped wash the fibre off as the needle was withdrawn from the liquid. This process was repeated until a representative amount of fibre was transferred to refractive index liquid drop on the first slide. A pre-cleaned cover glass was placed on a cardboard box and pressed down at its centre with a carbide scriber. This process broke down the cover glass into four or more small pieces. The cover glass fragment was then used to cover the refractive index fluid droplet with the fibre samples. There was enough liquid to completely fill the area beneath the cover glass. The excess liquid was absorbed using a membrane filter fragment. The prepared slide was then placed onto the microscope stage and the microscope focused on the particles ready for observation.

3.7.2 Observation Using Ordinary Light

The following procedures were adopted for making observations using ordinary light. Morphology was the only property that was determined using ordinary light. The prepared slide was placed onto the microscope stage and focused on a single fibre.

The general shape of the fibre was recorded together with a brief description of surface markings, texture, inclusions and surface roughness. Many fibres have characteristic morphology which can be recognized on sight. The observed characteristics were then compared with those documented in literature. The absorption colour was also recorded under transmitted light.

3.7.3 Observations Using Plane Polarized Light

The following properties were determined using plane polarised light namely, pleochroism and refractive index. Pleochroism is a change in colour of a fibre relative to the vibration direction of the plane polarized light. Coloured fibres that are anisotropic (have more than one refractive index) often exhibit different degrees of light absorption in different directions within the fibre resulting in the fibre showing different colours or different intensities of colour, when rotated in plane-polarised light. Ordinary light will not work for microscopic specimens such as fibres, because light vibrates in all directions and therefore the fibre will show the composite of all effects. This composite effect is not useful for sample analysis. For observing transparent coloured fibres, the stage was rotated at least 90^0. Alternatively the polarizer was rotated instead of the stage and the changes in colour or intensity were observed. The changes were recorded in a particle identification characteristics sheet. Since fibres are elongated, the colour changes seen are related to the shape. If the fibre length was oriented east/west, that is, parallel to the polarizer vibration direction, the observed colour was characteristic of the fibre length [106]. The stage was then rotated 90^0 so that the fibre was now oriented north/south, the colour of the fibre changed and that was characteristic of the fibre width, that is, the width was now parallel to the polarizer vibration direction. Thus two colours are recorded in the column under pleochroism.

Fibres can also be uniquely identified by their refractive indices together with other optical properties. Solids may have more than one refractive index namely α, β and ɣ depending on the orientation of the fibre to the plane of polarization of the light. By definition, α is the lowest refractive index and ɣ is the highest. It should be noted that β being the intermediate can be closer to α or closer to ɣ. The determination of the refractive index of a solid is based on the premise that if the solid is placed in a liquid of equal refractive index, the solid will be invisible in that liquid. Thus a repeated careful choice of refractive index liquids will result in the exact determination of the refractive index of a given fibre. This determination is done at a standard wavelength of 589 nm. In most cases however, it is sufficient just to know whether the refractive index of the fibre is greater than or lower than the medium in which it is mounted. This is done by using Becke lines. Becke line is a halo that forms around a particle as a result of using axial illumination achieved by closing the aperture diaphragm. An

orange interference filter (wavelength of 589 nm) was placed over the light exit port of the microscope so that all measurements were done at one wavelength. The Becke line halo is best produced with high numerical aperture objectives, usually with 40x/0.65 objective when a 589 nm filter is in place. The fibre image was brought into focus under these conditions. The fine adjustment was then suddenly turned in such a way that one was focused above the best focus. During this operation the Becke line will be seen to move either into the fibre or into the medium in which the fibre is mounted. On focusing above the best focus like this, the Becke line always moves towards whichever medium has the higher index. If one focuses below the best focus, the opposite effect occurs. The refractive index of the fibre was recorded as either greater than or less than the refractive index of the medium. The fibres were correctly oriented with respect to the polarizer vibration direction.

3.7.4 Observations Using Uncrossed Polarisers

Three optical fibre properties were determined using crossed polarisers namely birefringence, sign of elongation and extinction angle. Birefringence was determined using the Michel Levy colour chart. This required measuring the fibre thickness and estimation of the retardation using the colour chart. The fibre was rotated to a position of maximum brightness. At that position, the thickness of the fibre was measured directly by using the Stream particle characterization software. The retardation was obtained by matching colour at the point where the thickness is determined with the colour on the Michel Levy chart. The Michel Levy chart is actually a graphical solution to the birefringence equation up to the limit of 50µm of thickness. Going to the Michel Levy chart, one entered the thickness, moved along that thickness line to the right until one got to the retardation colour that the fibre was showing. There will be a diagonal line at the intersection of the thickness and retardation. Following the diagonal line up to the right, the birefringence can be read off.

The sign of elongation refers to the orientation of high and low refractive indices relative to the direction of elongation of the fibre. A fibre which has high refractive index parallel to its length has positive sign of elongation and is described as ‘length slow’. Fibres which have low refractive indices parallel to their length have negative sign of elongation and are described as ‘length fast’. The sign of elongation was determined by use of a compensator. A compensator is a device with a known fixed

retardation and vibration direction used to determine the amount of retardation of an anisotropic substance. The most common compensators are the first order red (530-550nm), quarter-wave (137-147 nm) and the Sernamont compensator. A fibre whose sign of elongation was to be determined was oriented 2 o'clock / 8 o'clock in the field of view (45^{o} to the cross hair) and viewed under crossed polarisers. The colour was noted and recorded. A quarter-wave compensator (137 nm) was inserted and the colour changes noted again. The compensator's retardation of 137nm can either add to or subtract from the observed fibre colour. The retardations are subtractive when slow is on fast or fast is on slow. The colours go down the scale towards the lower retardation values on the Michel Levy chart. On the other hand, if the slow is on slow or fast side is aligned with the fast side the retardation will be additive. This will mean going up the scale on the Michel Levy chart. The compensator was inserted into the beam path at 45^{o} to the vibration direction of the polarizer when it is at position 0^{o}. The compensator's slow direction is 2 o'clock/8 o'clock. By aligning the fibre at 45^{o} to the eye piece cross hairs, the fibre length was made to be parallel to the compensator slow direction. Thus if the fibre's colour goes down the Michel levy colour chart then it has negative sign of elongation. If the fibre's colour goes up the chart, then it has positive sign of elongation.

In order to determine the fibre extinction angle, the slide was moved until the fibre was under the crosshairs. By rotating the stage, the fibre was lined up with either the north-south or east-west crosshair. This aligned the length of the fibre to the crosshair. If the fibre cannot be seen at this position, then it is at its extinction angle and the internal vibration directions lie parallel to the length of the length of the fibre. This corresponds to the polariser and analyser vibration directions and the extinction angle is 0^{o}. The extinction direction was then recorded as either parallel or perpendicular to the polariser direction.

CHAPTER 4: RESULTS AND DISCUSSION

4.1 Introduction

This chapter presents the detailed results of all the experiments carried out in this study. The pH test results are given first because they represent the immediate threat to paper longevity. The elemental composition results are then discussed together with the results for the determination of the valence state of iron, one of the transition metals found in paper samples. Finally the results for paper fillers and sizes are presented and discussed.

4.2 pH Levels

The pH levels of the samples were determined using the Abbey pH pen (Chlorophenol red). This is a quick or spot test method that only gives an indication whether the paper sample is acidic or not. The indicator solution of the pH pen approximates the pH value obtained by extraction methods [29]. Table 4.1 below shows the Abbey pH pen test results obtained after following the procedure detailed in Section 3.3.

Table 4.1: pH test results obtained using the Abbey pH pen.

Sample No.	Title	Classification	Publication date	Observed Colour	pH level
1	Het Leven en Bedryf	Book	1732	Purple	Above 6.5
2	South Africa (Barrow)	Book	1803	Purple	Above 6.5
3	The 19th Century (Vol 33)	Book	1893	Yellow	Below 6.0
4	The Press	Newspaper	1893	Yellow	Below 6.0
5	The 19th Century (Vol 39)	Book	1896	Yellow	Below 6.0
6	The Weekly Press	Newspaper	1897	Yellow	Below 6.0
7	Regulatien:Staatsbiblioteek	Periodical	1897	Yellow	Below 6.0
8	The Weekly Press	Newspaper	1899	Yellow	Below 6.0
9	Timbuktu	Manuscript	Unknown	Colourless	Below 5.0
10	Natal Almanac & Directory	Periodical	1901	Yellow	Below 6.0
11	Die Huisgenoot	Periodical	1918	Yellow	Below 6.0
12	The Standard	Newspaper	1925	yellow	Below 6.0
13	The Courier	Newspaper	1946	yellow	Below 6.0
14	Wild Sport of Africa	Book	1844	yellow	Below 6.0

Table 4.1 shows that most of the samples are acidic because they turned colourless. Samples 1 and 2 are neutral or alkaline. This is because the chlorophenol red ink turned purple. They are therefore not experiencing acidic degradation. Based on the Abbey pH pen test chart, the Timbuktu manuscript sample is extremely acidic. The chlorophenol red ink became colourless in only a few seconds after being deposited on the sample. Such a colour transformation indicates pH levels of below 5.0. The sample itself was very brittle and had a brownish colour. This sample is therefore under more severe acid hydrolysis compared to the other samples. The colour transformation of the chlorophenol red ink to yellow of the other samples showed that these samples were acidic, with a pH level of less than 6.0. Their acidity is however less than that of the Timbuktu manuscript sample. The colour transformation from purple to yellow or colourless showed that such samples are acidic. Therefore, the most predominant degradation process is acid hydrolysis. This means that the first remedial action to save these documents is to adjust their pH level to archival levels of between 7 and 9. The de-acidification process can be done in a number of ways namely:

- Utilising aqueous processes with dissolved alkaline earth carbonates as a neutralisation agent. This is done in the Viennese treatment [118], paper splitting machine treatment [119] as well as in the Buckeburger method [120]. The three techniques use calcium hydroxide, calcium/magnesium carbonate and magnesium bicarbonate respectively as the effective de-acidifying agents.
- Non-aqueous processes using organo-metallic agents, usually magnesium alcoholates with organic solvents like alcohols,perfluoro alkanes etc.
- Utilisation of the Bookkeeper process [121]. This process features non-aqueous liquid phase impregnation. The de-acidifying agent is magnesium oxide submicron powder with perfluoroheptane as the suspension liquid.
- Treatment with ultrafine particles of de-acidifying agent usually magnesium oxide applied directly from a stream of air [122]

The techniques described above when correctly used will completely neutralise acidic paper and also incorporate an alkaline reserve. No method is however universally suitable to address all forms of deterioration. The applicability of each

method depends on the state of the document as well as its form. Some methods are suitable for bound papers like books where as some can only be applied on loose sheets of paper. Aqueous techniques for example are suitable for treating single sheets of paper and contain a paper-strengthening aspect [123]. The aqueous method however has a problem of bleeding the ink of the document being treated. This method is therefore used where the inks or dyes are absent or chemically fixed before the treatment. The paper splitting method is designed for the mechanical reinforcement of very fragile single sheets. This is usually achieved by lining brittle paper with translucent adhesives The Buckeburger method is designed for archival material which has to be taken apart in single sheets as a first step. The Vienesse is designed to de-acidify and re-strengthen newspapers after removing the covers. In the non-aqueous method, impregnation with treatment solution takes place in a vacuum. Books as well as loose sheets can be treated with this method.

4.3 Elemental Composition

As indicated in section 3.4, the ED-XRF spectroscopy method was used to determine concentrations of different elements found in the paper samples. The concentrations of the detected elements are shown in figure 4.1.

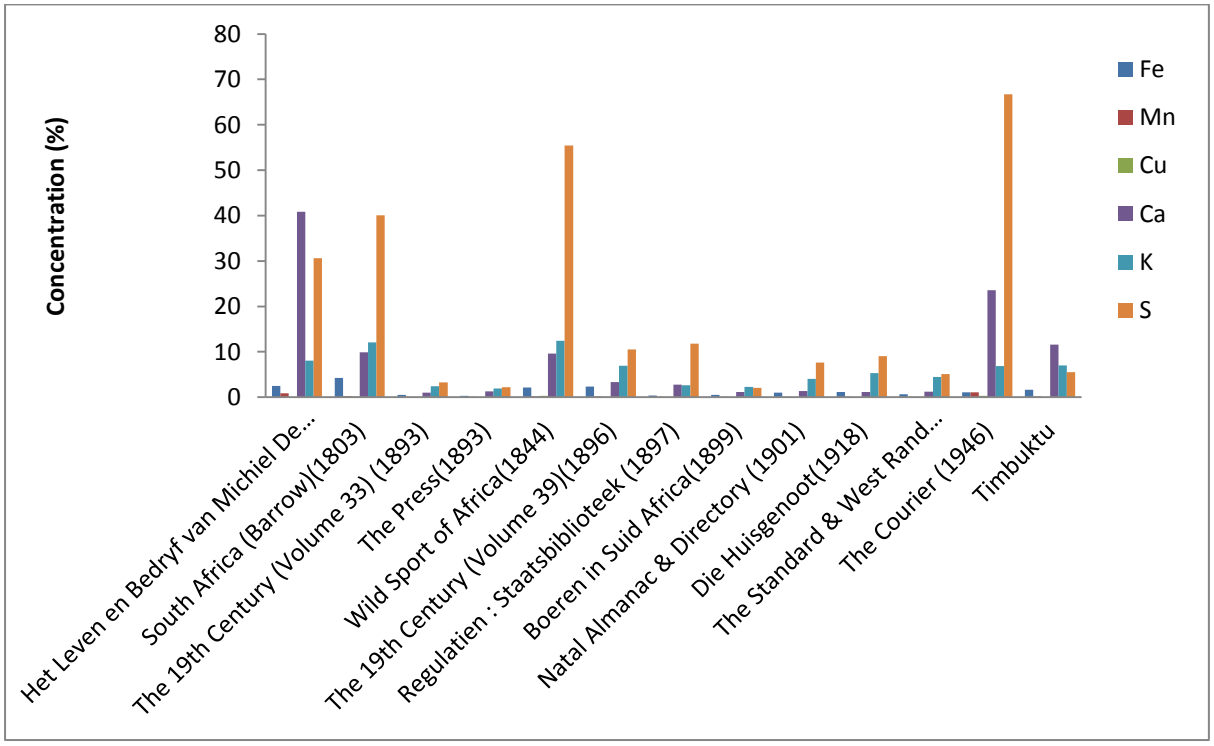

Figure 4.1: Elemental composition of Fe, Mn, Cu, Ca, K and S in the various paper samples.

The key transition metals of interest are Fe, Cu, and Mn while elements Ca, K and S give an indication of the macromolecular environment of the transition metals in the paper samples. Because of the large difference in concentrations between the transition metals and the macromolecular environment elements, it is necessary to plot these elements on different graphs with different scales.

In order to understand how effective the transition metals will be as oxidative agents, it is imperative that we have a clear understanding of their environment within the paper sample. All the samples studied had Ca present in them. A sample with the highest concentration of Ca of 41% was the of the book titled *Het Leven en Bedryf van Michiel*. This book had a publication date of 1732 making it the oldest dated sample that was studied. It is also worth noting that this book was still in good physical condition when compared to the other samples studied. The concentrations of the macromolecular elements in all the samples studied are shown in figure 4.2.

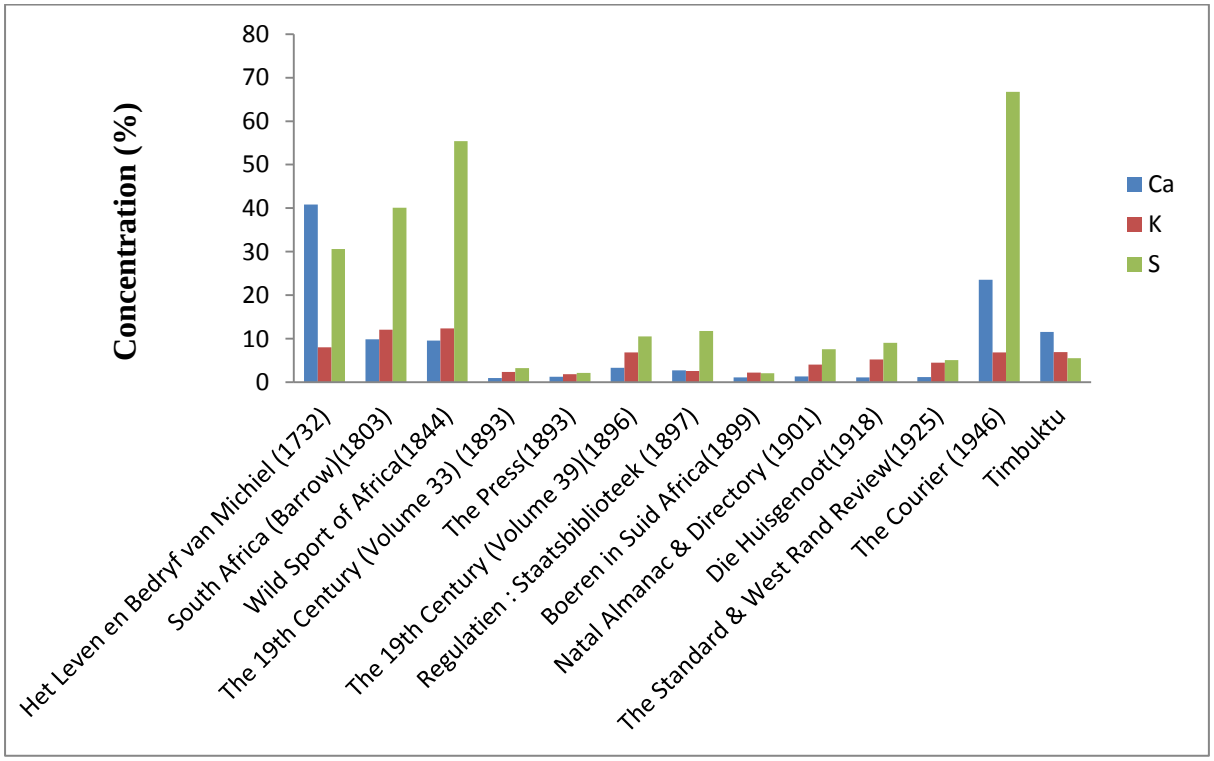

Figure 4.2: Concentrations of Ca, K and S in the samples.

There is a greater concentration of calcium in older samples than in the recent paper samples. Calcium is associated with alkaline carbonates such as $CaCO_3$ which is

generally regarded as beneficial to paper stability. High Ca concentration in the paper sample showed a large alkaline buffer and good archival quality [6]. This also means that the effectiveness of Fe as an oxidative catalyst is greatly reduced [124]. There is a notable drop in the concentration of Ca between 1803 and 1893 in the samples studied. This period coincide with the time paper making technology changed from external sizing to internal sizing.

Sulphur (S) and potassium (K) are the primary elements of alum. The concentration of alum in the samples studied is therefore inferred from the concentration of S and K. It can be observed from figure 4.2 that as the concentration of K decreased so did the concentration of S and that the concentration of S was always greater than that of K for all samples except that of the Timbuktu manuscript. This may mean that the technology used in the production of the Timbuktu manuscript may be different from the rest of the samples. The presence of alum also shows that gelatine may have been used for sizing in the paper samples. Gelatine has been known to play a protective role to cellulose through preferential hydrolysis of protein molecules over those of cellulose [125]. Gelatine can also bind transition metals such Cu and Fe, thus inhibiting their catalytic role in oxidative degradation of cellulose [126].

The concentrations of transition metals in the samples studied are shown in figure 4.3. It can also be observed that Fe is present in every sample and that very few samples had Cu and Mn. This means that iron plays a very important role in the chemistry of paper.

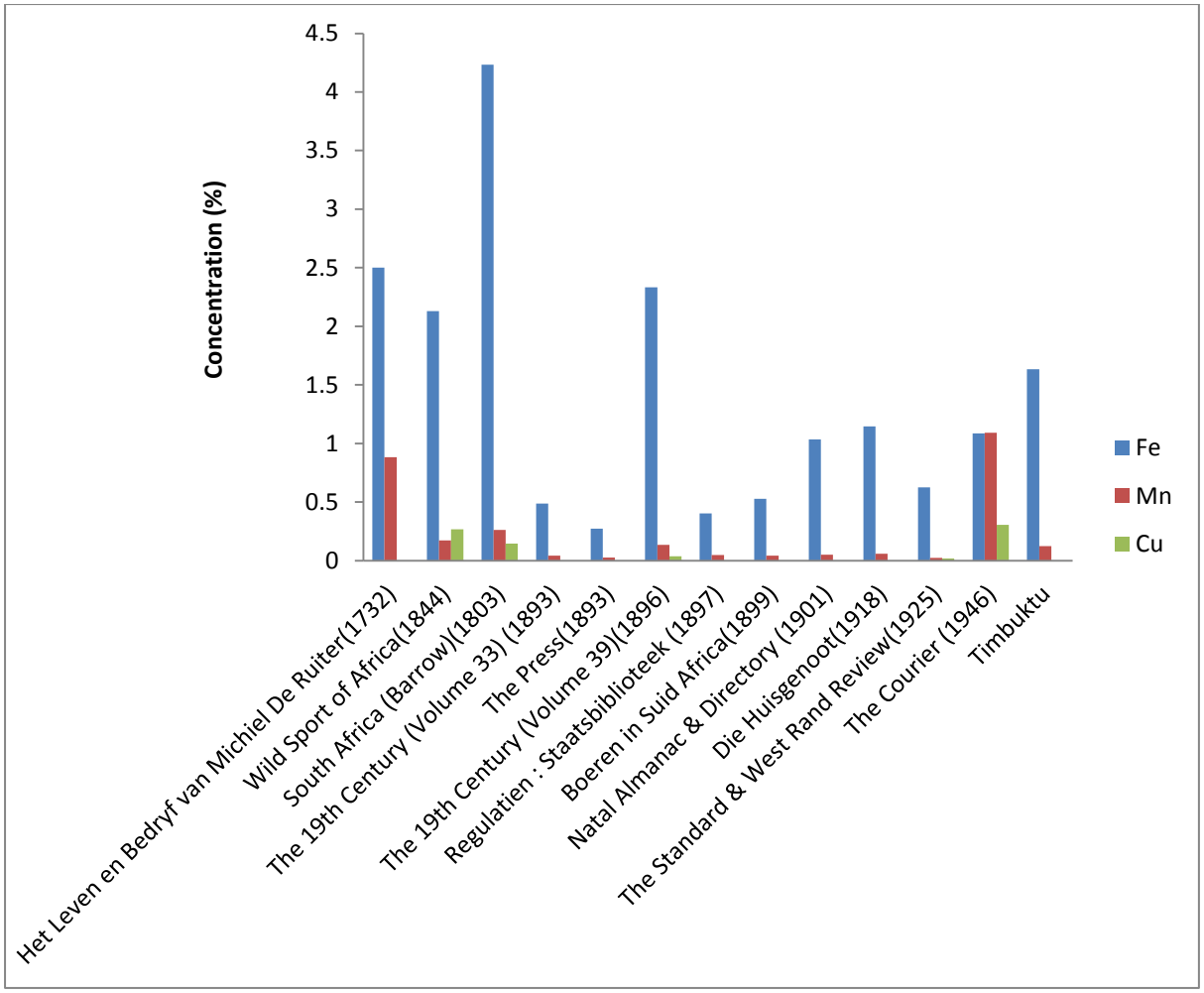

Figure 4.3: Transition metal concentrations of the paper samples.

Fe and Cu have been associated with paper foxing [127] regardless of their catalytic role in oxidative degradation of paper. Foxing is the term used to describe brown coloured spots that appear on paper surfaces. These spots are not due to molds. An alkaline macromolecular environment had been observed to inhibit the catalytic action of Fe but not of Cu [13]. Mn was found in much lesser conentrations than Fe and tended to be much less for the more recent documents.

4.4 The Valence State of Trace Iron

Mössbauer spectra (MS) of the samples investigated and presented in Dzinavatonga et al (2014) [128] (see also Appendix B), together with the fitted spectral components, are shown in figure 4.4 and the extracted MS parameters are listed in Table 4.2. The spectra were fitted using the Mössbauer analysis code RECOIL, and

are presented in Chapter 3. The fitting parameters and the identification of the Fe components are listed in Section 4.4. The velocity scale and isomer shifts were calibrated relative to an α-Fe absorber.

The isomer shift is estimated by the equation

$$\mathbf{IS} = K\,(R_e^{\,2} - R_g^{\,2})\,\{[\Psi_s^{\,2}(0)]_b - [\Psi_s^{\,2}(0)]_a\}$$

where K is a nuclear constant, the difference between $R_e^{\,2}$ and $R_g^{\,2}$ is the effective nuclear charge radius difference between excited state and the ground state, and the difference between $[\Psi_s^{\,2}(0)]_a$ and $[\Psi_s^{\,2}(0)]_b$ is the electron density difference on the nucleus. Subscripts *a* and *b* represent the source and sample respectively.

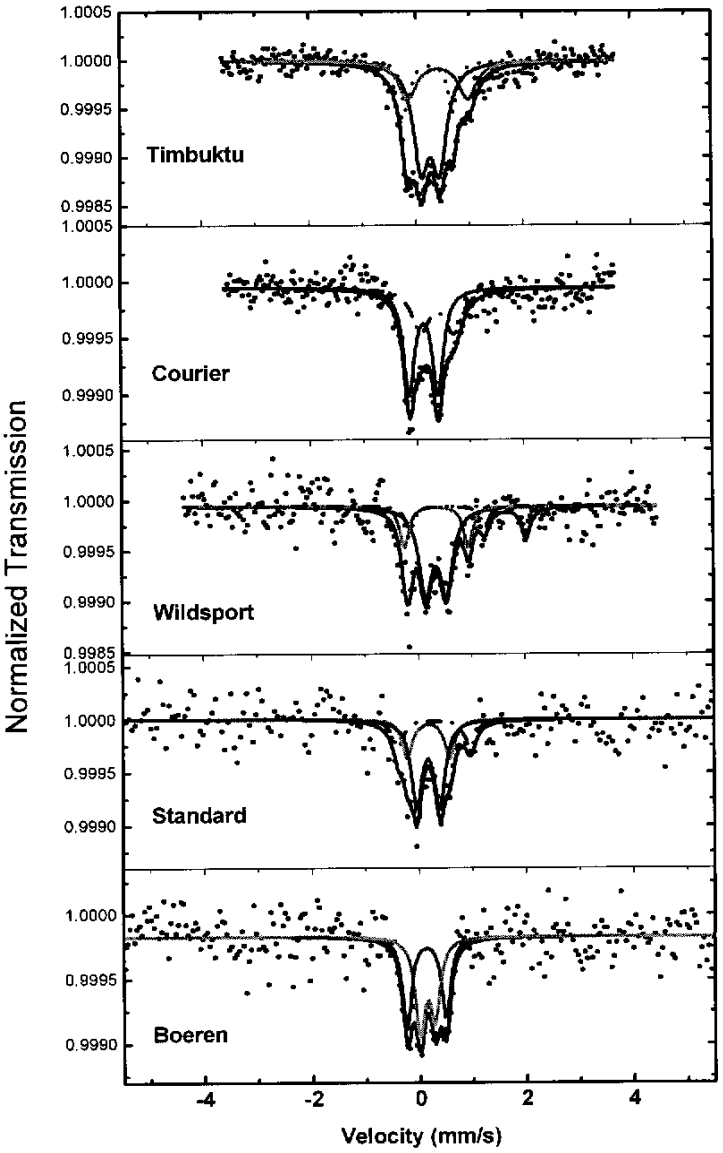

Figure 4.4: Mössbauer spectra of studied samples collected in transmission mode.

The identification of the Fe^{3+}/Fe^{2+} states is based on the characteristic values of isomer shift and quadrupole splitting of Fe^{3+} and Fe^{2+} [17]. Fe^{3+} is characterised by an isomer shift in the range 0.25 - 0.70 mm/s while Fe^{2+} is characterised by an

isomer shift of 0.6 - 1.4 mm/s and large quadrupole splitting. Only the *Wildsport of Africa* sample with isomer shifts (δ) of 0.7 mm/s and 1.09 mm/s and quadrupole splitting (Δ) of 1.12 mm/s and 1.89 mm/s for spectral components D3 and D4, respectively, shows the presence of Fe^{2+} , as shown in Table 4.2. There was no evidence of magnetic components in any of the samples investigated.

Table 4.2 Mössbauer parameters isomer shift (δ), quadrupole splitting (Δ), line width (Γ - FWHM) and areal fraction (*A*) extracted from fits to the spectra shown in Fig. 4.4. Isomer shifts are given relative to α-Fe. D1 – D4 are spectral bands

.

Sample	MS parameters	D1	D2	D3	D4
Timbuktu	δ (mm/s) Δ (mm/s) Γ (mm/s) *A* (%) **Fe**	0.27(4) 0.34(5) 0.32(3) 53(5) **Fe 3+**	0.26(4) 0.86(8) 0.24(2) 23(4) **Fe3+**	0.42(7) 1.12(10) 0.38(3) 24(4) **Fe3+**	
Courier	δ (mm/s) Δ (mm/s) Γ (mm/s) *A* (%) **Fe**	0.13(5) 0.54(8) 0.25(3) 60(5) **Fe3+**	0.39(4) 0.62(6) 0.40(4) 40(5) **Fe3+**		
Wildsport	δ (mm/s) Δ (mm/s) Γ (mm/s) *A* (%) **Fe**	0.17(5) 0.72(6) 0.26(3) 58(6) **Fe3+**	0.56(6) 0.78(8) 0.22(3) 21(6) **Fe3+**	0.70(8) 1.12(9) 0.22(3) 8(4) **Fe2+**	1.09(9) 1.89(9) 0.22(3) 13(3) **Fe2+**
Standard	δ (mm/s) Δ (mm/s) Γ (mm/s) *A* (%) **Fe**	0.17(5) 0.44(5) 0.24(3) 56(6) **Fe3+**	0.18(5) 0.79(8) 0.24(3) 24(6) **Fe3+**	0.42(10) 1.4(2) 0.24(3) 20(6) **Fe3+**	
Boeren	δ (mm/s) Δ (mm/s) Γ (mm/s) *A* (%) **Fe**	0.14(5) 0.28(5) 0.22(3) 51(6) **Fe3+**	0.12(5) 0.73(9) 0.20(3) 49(6) **Fe3+**		

The *Wildsport of Africa* sample was discoloured and yellowish showing that the sample is undergoing some chemical changes. The presence of Fe^{2+} in this sample

can accelerate oxidative degradation of cellulose by participating in two main processes, namely; formation of organic radicals and formation of hydroxyl radicals from hydrogen peroxide according to the Fenton reaction [18]. Hydroxyl radicals are very reactive and they easily abstract hydrogen from cellulose, leading to the formation of organic radicals, which then react in a chain reaction with oxygen and the next cellulose molecule in the cellulose structure. This leads to chain scission of the cellulose molecules, thus accelerating the degradation of paper. Surprisingly, the *Wildsport of Africa* sample, published in 1844, was still in good physical condition despite the presence of Fe^{2+}, indicating that the oxidation degradation is not yet fully advanced and remedial action can prevent any further damage to the cellulose macromolecules of this document. From a document degradation perspective, this means that both acid hydrolysis and catalytic oxidation mechanisms are occurring in this document.

All other samples have δ and Δ values that are less than 0.56mm/s and 0.86mm/s respectively showing that only Fe^{3+} is present in these samples, which is catalytically inactive. The only degradation mechanism in these other samples is therefore acid hydrolysis. This can be inhibited by a de-acidification process.

4.5 Paper Fillers and Sizing

The determination of both the nature of the cellulosic material and the sizing material of the samples was done using FTIR. The spectra of the analysed samples are shown in Appendix A. All spectra were acquired in absorbance mode and later converted to transmittance. Baseline corrections as well as spectral smoothing were done to all spectra. These spectrum manipulations are all available in the OPUS software that was used. No atmospheric compensations were done for all samples measured in ATR mode. This is because the measurements were carried out in a vacuum when the instrument was in ATR mode.

4.5.1 Cellulosic Material of the Samples

The degradation mechanism that is taking place in the sampled documents depends to some extent on the cellulosic material that makes up the document. The most common constituents of cellulosic paper are cellulose, hemicellulose and lignin. All

the samples observed had cellulose as shown in the spectra in Appendix A. All the samples had absorption peaks at 1365 cm^{-1} and 1315cm^{-1} assigned to δ(C-H) and 1155 cm^{-1} assigned to the asymmetric ring breathing as well as 1105cm^{-1} associated with the υ(C-O-C) glycosidic bonds. These absorption bands are associated with cellulose. Only one document namely *The Courier (1946)* had peaks at 808cm^{-1} which associated with hemicellulose and at 1505cm^{-1}- and 1595cm^{-1} that are assigned to lignin. The sample from the Timbuktu manuscripts also had cellulose only as the paper matrix.

The broad peak in the region 3600-3100 cm^{-1} is due to the O-H stretching vibrations and gives considerable information about the hydrogen bonds in the cellulose. The Timbuktu sample has a very broad and strong (20% transmittance) absorption in this region. The spectrum from the Timbuktu sample is shown in figure 4.5. This band is also shifted to higher wavenumbers peaking around 3333 cm^{-1}.

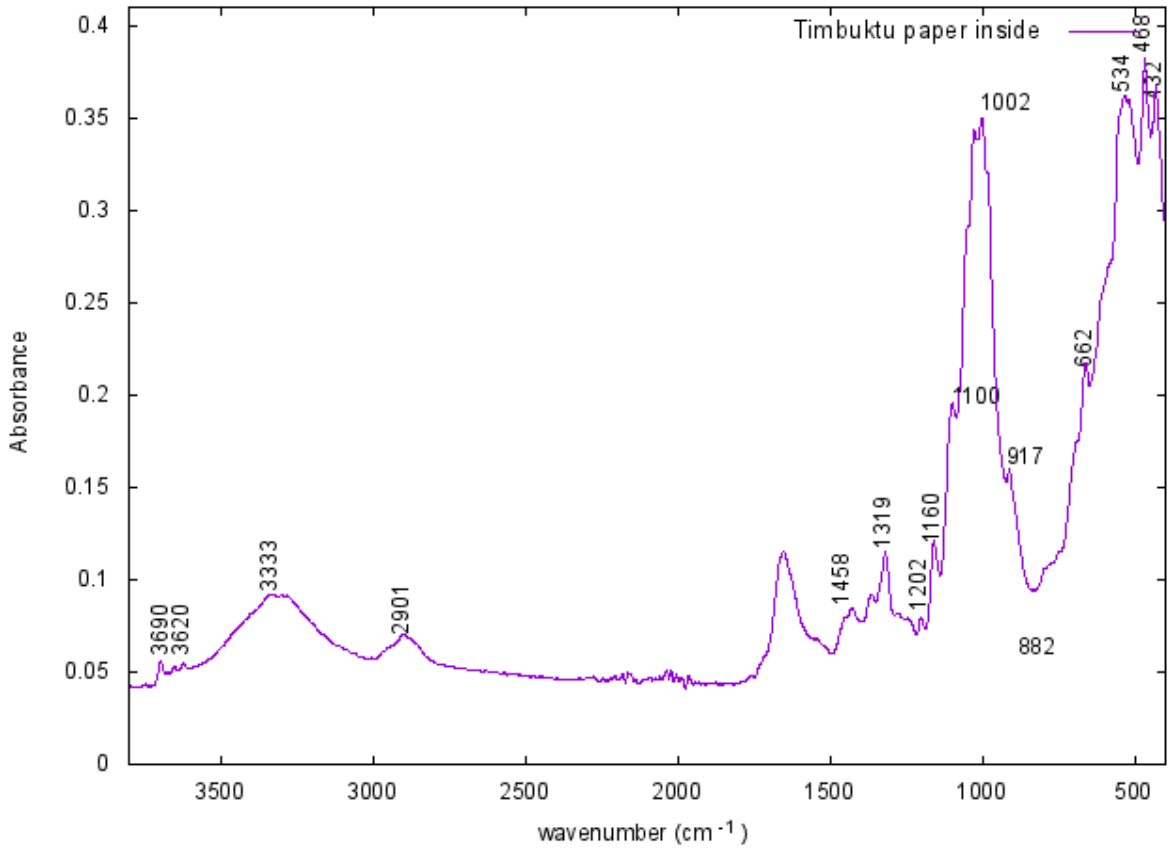

Figure 4.5: FTIR spectrum of the *Timbuktu manuscript* sample.

This shows that the Timbuktu sample has a significant region that is made up of crystalline cellulose. On the other hand all other samples have a sharper band with low intensity (not less than 90% transmittance) in this region as shown in figure 4.6.

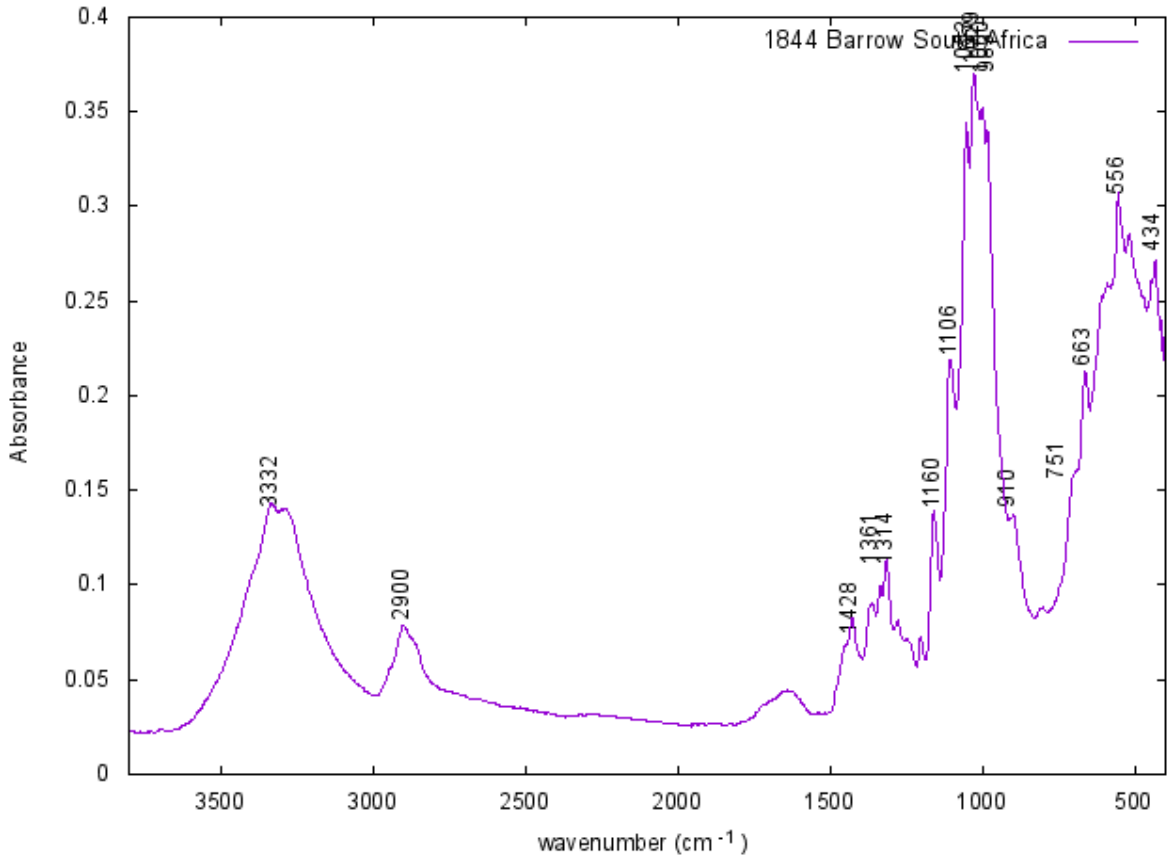

Figure 4.6: FTIR spectrum of the *Wild Sport of Africa* sample with relevant wave numbers.

This band is also shifted to lower wavenumbers at around 3285 cm^{-1} showing that the cellulose is amorphous. The FTIR spectra of all the other samples studied are given in Appendix A. The band at 2900 cm^{-1} corresponds to the C-H stretching vibrations. There is no significant shift of this band to higher wavenumbers to qualitatively confirm the presence or absence of amorphous region of the cellulose making up the Timbuktu samples. There is a significant shift to lower wavenumbers for The Courier sample. This is also an indication that this sample has a significant region that is amorphous

The Total Crystallinity Index (TCI) of each of the samples was also calculated in order to determine the susceptibility of cellulose to degradation agents. This index is the ratio of the integrals of the FTIR band at 1372 cm^{-1} to that at 2900 cm^{-1}. The integrals were taken over the ranges 1390 – 1339 cm^{-1} and 2959 – 2830 cm^{-1} for the bands at 1372 cm^{-1} and 2900 cm^{-1} respectively as shown in table 4.3 below.

Table 4.3: Measurement of Crystallinity Indices TCI and LOI.

Sample Name	**Publication date**	**I_{1372} (1339 - 1390) cm^{-1}**	**I_{2900} (2830 - 2959) cm^{-1}**	**Total Crystal .Index**	**I_{1420} (1458 - 1407) cm^{-1}**	**I_{1372} (917 - 882) cm^{-1}**	**LOI**
Het Leven en Bedryf	1732	0.432	0.054	0.125	0.121	0.04	3.03
South Africa (Barrow)	1803	0.814	0.134	0.165	0.206	0.087	2.37
Wild sport of Africa	1844	0.531	0.077	0.145	0.143	0.050	2.86
The 19th Century (Vol 33)	1893	0.712	0.083	0.117	0.179	0.144	1.24
The Press	1893	0.325	0.033	0.101	0.067	0.228	0.29
The 19th Century (Vol 39)	1896	0.164	0.012	0.073	0.030	0.031	0.97
Regulatien:Staatsbiblioteek	1897	0.512	0.056	0.109	0.128	0.097	1.32
Timbuktu	Unknown	0.528	0.106	0.200	0.103	0.295	0.35
Natal Almanac & Directory	1901	0.034	0.394	0.086	0.103	0.163	0.63
Die Huisgenoot	1918	0.716	0.094	0.132	0.145	0.296	0.49
The Standard	1925	0.291	0.051	0.175	0.074	0.164	0.45
The Courier	1946	0.265	0.073	0.275	0.053	0.025	2.12

The values of the TCI obtained ranged from 0.073 (*The 19th Century (Vol 39)*) to 0.275 *(The Courier)*. The Timbuktu sample has the greatest value of Total Crystallinity Index (TCI) of 0.2 for all the samples that are made up entirely of cellulose. This means that about 20% of the cellulose making up the Timbuktu sample is crystalline. A TCI of 0.275 was obtained for *The Courier* sample. It should be noted that this sample is different from the rest in that it is the only sample that contains cellulose, hemicellulose and lignin. The TCI results seem to agree with the observed spectral modifications.

The values of the calculated Lateral Order Index (LOI) are shown in the last column of Table 4.3. This index is the ratio of the integrals of the FTIR band at 1420 cm^{-1} to that at 898 cm^{-1}. The integrals were taken over the ranges 1407 – 1458 cm^{-1} and 882 – 917 cm^{-1} for the bands at 1420 cm^{-1} and 898 cm^{-1} respectively. The two bands from which LOI is obtained are sensitive to the amount of crystalline versus amorphous structure in the cellulose. These bands broaden in a more disordered structure. Thus the smaller the LOI, the more ordered the cellulose structure. *The*

Het Leven en Bedryf (1732) sample has the greatest LOI of 3.03 while the Timbuktu and The Press samples have the smallest LOI values of 0.35 and 0.29 respectively. LOI reflects the ordered regions perpendicular to the chain direction.

4.5.2 Sizing and Fillers

Table 4.4 below shows a summary of the filler material detected in the samples. None of the samples showed evidence of gelatine sizing except the Timbuktu sample. This is the only sample whose FTIR spectrum showed absorption bands of amide I and amide II bands at 1550 cm^{-1} and 1650 cm^{-1} respectively associated with gelatine. There is no evidence of starch which has absorption bands at 1148 cm^{-1}, 995 cm^{-1}, 933 cm^{-1} and 851 cm^{-1}. There is evidence of clay in the Timbuktu sample shown by the doublet at 3690 cm^{-1} and 3620 cm^{-1} together with sharp peaks at 910 and 1000 cm^{-1}. Clay was also found in all other samples except the *The Courier* sample. The clay absorption bands were not present in the sample's FTIR spectrum. This sample had absorption bands at 470 cm^{-1} and 524 cm^{-1}. These are the characteristic absorption bands of kaolin. There was evidence of kaolin in all other samples except *The Natal Almanac* and *The 19th Century Vol 33* samples shown in Appendix A. All the samples did not show any evidence of gypsum (typical wavy pattern in the OH region of 3700 – 3000 cm^{-1} together with a small but sharp peak at 1620 cm^{-1}).

Table 4.4: A summary of filler material detected in the samples under investigation. The detected fillers are with a tick (√)together with the observed absorption bands in cm^{-1}.

Sample	Filler												
	Kaolin				**Calcium Carbonate**			**Gelatine**		**Clay**			
	1032	**1004**	**524**	**470**	**1415**	**874**	**710**	**1650**	**1550**	**3690**	**3620**	**1000**	**910**
The Courier	√		√	√		√	√						
Timbuktu	√	√	√	√			√	√	√	√	√	√	√
The Standard			√	√						√	√	√	√

Die Huisegnoot	√	√	√	√						√	√	√	√
Natal Almanac										√	√	√	√
Regulatien	√	√	√	√						√	√	√	√
The Press	√	√	√	√						√	√	√	√
The19th Cent. (Vol 33)										√	√	√	√
Het Leven en Bedryf	√		√	√	√		√			√	√	√	√
Wild Sport of Africa	√	√	√	√						√	√	√	√
Barrow South Africa	√	√	√	√	√	√	√			√	√	√	√

Only four samples showed the presence of calcium carbonate namely; *The Courier, Het Leven en Bedryf, Timbuktu* and *Barrow South Africa*. These samples also showed high levels of calcium as shown in their XRF spectra. The Courier sample had absorption peaks at 874 cm^{-1} and 710 cm^{-1} that are due to out of phase CO_3 bending vibrations and in-plane CO_2 bending vibration respectively of calcium carbonate. On the other hand the *Het Leven en Bedryf* sample showed calcium carbonate peaks at 1415 and 710 cm^{-1}. The 1415 cm^{-1} absorption band is due to the asymmetric stretching CO_3 vibrations characteristic of calcium carbonate. The *Barrow South Africa* sample had three absorption peaks at 1415, 874 and 710 cm^{-1}.

4.5.3 Observed Degradation By-Products

The process of ageing often produces oxidised groups namely carbonyls and carboxyls on the cellulose chain. This means the detection of these oxidised groups is related to the conservation/degradation state of the sample. Table 4.5 shows the degradation by-products detected together with the oxidation index of each sample. The oxidation index was calculated using the FTIR spectra of the samples. It was calculated from the ration of the area under the peaks at 1730 cm^{-1} and 1620 cm^{-1}. Two samples namely *Natal Almanac* and *The Wild Sport of Africa* did not show any

by-products that are associated oxidative degradation. This means that there is no evidence of oxidative degradation that was observed on these two samples.

Table 4.5: Oxidation indices and the detected degradation by-products of the samples under study.

Sample	**Oxidation Index Calculation**			**Oxidation by-products**					
	I_{1730} (1710-1744) cm^{-1}	**I_{1620} (1598-1631) cm^{-1}**	**Oxidation. Index (I_{1730}/ I_{1620})**	1745 cm^{-1}	1710 cm^{-1}	1618 cm^{-1}	1685 cm^{-1}	1665 cm^{-1}	1236 cm^{-1}
Het Leven en Bedryf	0	0.008	0						√
Barrow South Africa	0.07	0.16	0.44	√	√	√	√		
The Standard	0.007	0.022	0.32			√			√
Die Huisegnoot	0.012	0.018	0.67		√	√	√		
Natal Almanac	0	0	0						
Regulatien	0.008	0.025	0.32	√		√	√		
The Press	0.008	0.019	0.42			√			
The19th Cent. (Vol 33)	0.008	0.019	0.42			√			
The Courier	0	0	0		√			√	√
Wild Sport of Africa	0.006	0.020	0.3						
Timbuktu	0	0	0						√

The Timbuktu and the Het Leven samples only had the 1236 cm^{-1} absorption band that is associated with the C-O stretching of the carboxyl group. According to the observed Abbey pen colour changes, the *Timbuktu* sample was extremely acidic while the *Het Leven* sample was neutral to alkaline. This therefore means that the Het Leven sample showed evidence of marginal oxidative degradation but no evidence of hydrolytic degradation. On the other hand the acidity of the Timbuktu sample suggested that acid hydrolysis was occurring on this sample as well as marginal oxidative degradation.

The *Barrow South Africa* sample had absorption peaks 1745 cm^{-1} representing the final oxidation stage of carbon in the glycopyranose rings, the carbonyl bands at

1710 $cm^{-1,}$ 1618 cm^{-1} and 1685 cm^{-1}. Its oxidation index was calculated to be 0.44 as shown in table 4.5. These detected bands showed that this sample had evidence of oxidative degradation. This sample also had the highest concentration of iron, which is a catalyst in oxidative degradation, as shown by the x-ray fluorescence results in Section 4.3. A relatively high value of oxidation index suggests that the cellulose of this sample had been significantly oxidised.

The *19th Century Vol. 33* and *The Press* samples had no detectable absorption bands associated with oxidation by-products except absorption peaks at 1730 cm^{-1} and 1620 cm^{-1} that were used in the determination of the oxidation index. These samples had the same oxidation index of 0.42. Table 4.5 shows that *The Standard*, *Die Huisegnoot* and *Regulatien* had quantifiable oxidation indices of 0.32, 0.67 and 0.32 respectively together with other oxidation by-products absorption bands. These bands showed evidence of oxidative degradation in these samples

4.6 Optical Properties of the Fibres

The samples were mounted in liquid whose refractive index was 1.55. It was observed by analysing the movement of the Becke lines that the refractive indices of all the fibres parallel to the fibre length ($n_{\parallel}$) is greater than 1.55.The refractive indices of all the fibres perpendicular to the fibre length ($n_{\perp}$) was less than 1.55. It was also observed that all the fibres showed colour pleochroism and positive sign of elongation. Table 4.6 below shows a summary of the optical properties under both plane and cross polarised light.

Table 4.6: Optical properties of samples investigated showing Morphology, thickness at point measurement (t, in μm), Retardation colour (Γ), Birefringence (Δn) fibre type, refractive index parallel to fibre length ($n_{\parallel}$) and refractive index perpendicular to fibre length ($n_{\perp}$).

Sample Name	**Morphology**	***t (μm)***	**Retardation Colour**	Δn	Fibre type	$n_{\parallel}$	$n_{\perp}$
Het Leven en Bedryf	Joints, colourless, with surface irregularities, fractures and swollen tissues	8.57	Brown yellow	0.060	Hemp	>1.55	<1.55
South Africa (Barrow)	Joints, colourless, with surface irregularities, fractures and swollen tissues	14.22	Light green	0.060	Hemp	>1.55	<1.55
Wild sport of Africa	Joints, colourless, with surface irregularities, fractures and swollen tissues	8.60	Brown yellow	0.060	Hemp	>1.55	<1.55
The 19th Century (Vol 33)	Transparent, colourless, cylindrical. Node like ridges and longitudinal striations	5.03	Orange	0.065	Rammie	>1.55	<1.55
The Press	Transparent, fuzzy, short. Has hooks and wart like growths	14.22	Brown yellow	0.032	Linters	>1.55	<1.55
The 19th Century (Vol 39)	Transparent, colourless, cylindrical. Node like ridges and longitudinal striations	5.49	Orange	0.065	Rammie	>1.55	<1.55
Regulatien:Staatsbiblioteek	Joints, colourless, with surface irregularities, fractures and swollen tissues	7.03	Brown yellow	0.060	Hemp	>1.55	<1.55
Timbuktu	Joints, colourless, with surface irregularities, fractures and swollen tissues	6.89	Brown yellow	0.060	Hemp	>1.55	<1.55
Natal Almanac & Directory	Joints, colourless, with surface irregularities, fractures and swollen tissues	4.96	Red orange	0.060	Hemp	>1.55	<1.55
Die Huisgenoot	Transparent,	10.01	Sky blue	0.065	Rammie	>1.55	<1.55

	colourless, cylindrical. Node like ridges and longitudinal striations						
The Standard	Transparent, colourless, cylindrical. Node like ridges and longitudinal striations	6.68	Bright yellow	0.065	Rammie	>1.55	<1.55
The Courier	Joints, colourless, with surface irregularities, fractures and swollen tissues	4.96	Red orange	0.060	Hemp	>1.55	<1.55

The fibre type was deduced by direct comparison with morphology of known reference fibres (Cargille Chemical Microscopy set). The Press is the only sample made of natural fibres called linters. This fibre is transparent, fuzzy and short. It also has crooks, hooks and wart like growths on the fibre surface as shown in figure 4.7.

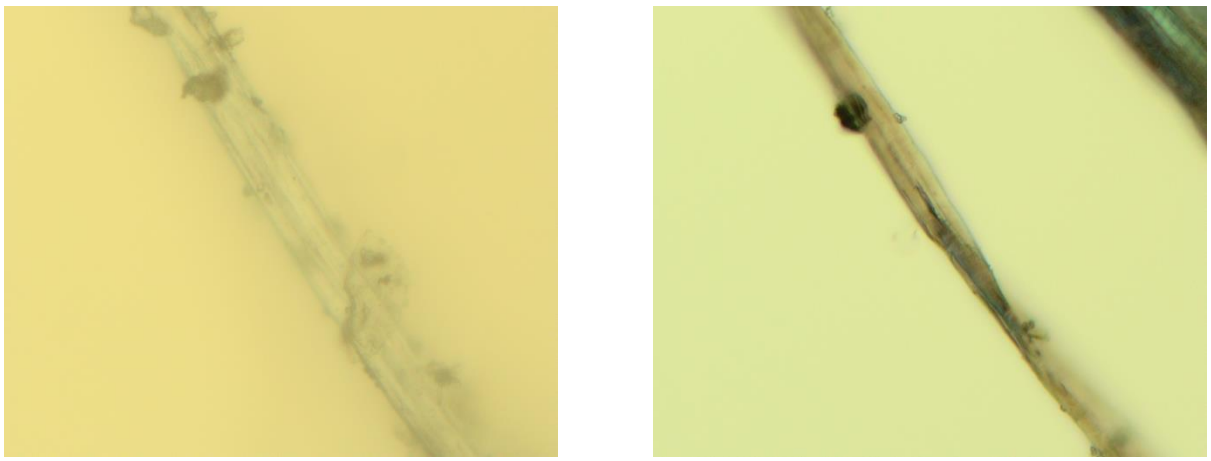

(a) (b)

Figure 4.7 Micrograph of the fibre from (a) *The Press* sample and (b) linters reference fibre.

The values of birefringence were deduced from the Michel Levy chart by noting the retardation colour and measuring the fibre thickness as described in Section 3.5. The sampled had a measured birefringence of 0.032. This is within the quoted range of

linters of 0.030 – 0.044 [129]. Four other samples namely *The Standard*, *19th Century Vol. 33, 19th Century Vol. 39* and *Die Huisegnoot* had a birefringence of 0.065. The samples had fibres that were colourless, transparent and cylindrical. They also had node like ridges and striations that were consistent with the natural fibre ramie. Figure 4.8(a) shows the micrograph of a fibre from *The Standard* sample.

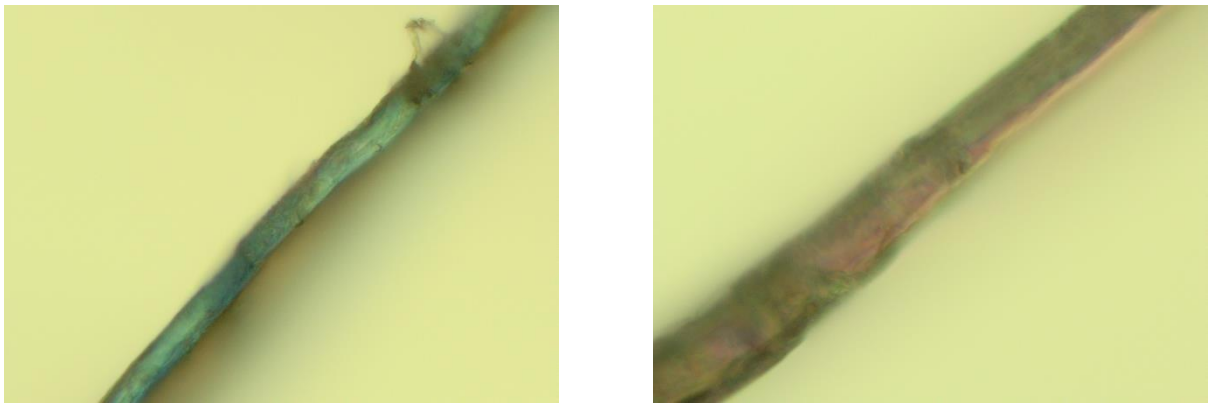

(a) (b)

Figure 4.8: Micrograph of the fibre from (a) *The Standard* sample and (b) rammie reference fibre.

The remaining eight samples namely *The Courier, South Africa (Barrow), Het Leven, Timbuktu, Wild Sport of Africa, Regulatien, Natal Almanac* and *Alweer*. were colourless with surface irregularities. They also had joints, fractures and swollen tissues. The birefringence of fibres from these samples was 0.060. This is consistent with hemp as shown in figure 4.9(a) and (b).

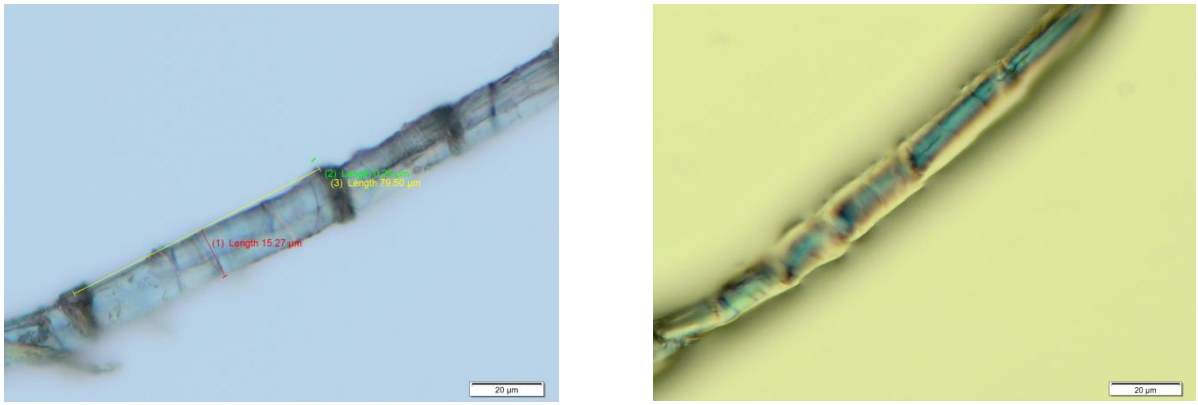

(a) (b)

Figure 4.9: Micrograph of the fibre from (a)*Timbuktu* manuscript sample and (b) hemp reference fibre.

These fibre samples are colourless hence all the observations were done under crossed polarisers. The birefringence values obtained agree with the ones quoted in literature.

CHAPTER 5 : CONCLUSION AND RECOMMENDATIONS

The aim of this research was to assess the risk of degradation of specific documents, the majority of which were from the National Library of South Africa with the ultimate goal of providing recommendations on possible remedial and preventative actions. This assessment was carried out by performing four spectroscopic tests on the samples as well as determining their pH levels.

The pH level of the samples was determined using the Abbey pen test. It was found that all the samples were acidic except two, namely; *South Africa (Barrow)* and *Het Leven.* The chlorophenol red ink turned purple on these samples indicating that their pH level was greater than 6.5. The *Timbuktu* sample was however extremely acidic. with pH level of less than 5.0 [130]. All other samples were also acidic and showed a pH level of below 6.0. The acidity of these samples can be corrected by an aqueous method such as the Bookkeeper process [121]. This process features non-aqueous liquid phase impregnation. The de-acidifying agent is magnesium oxide submicron powder with perfluoroheptane as the suspension liquid. There will no hydrolytic degradation occurring in the neutral samples. The only risk of degradation that the neutral samples may have is from catalytic oxidation that may be caused by the presence of trace quantities of transition metals in the samples. The effectiveness of these transition metals as oxidation catalysts depended on the environment and oxidation state. The elements Ca, K and S are usually found as fillers or part of the sizing material used in paper and therefore form part of the environment of the transition metals.

The concentrations of Fe, Cu, Mn, Ca, K and S in each sample were determined using XRF spectroscopy. This study gave an insight into the distribution of transition metals in paper samples studied. Iron was found to be present in all samples while Cu was found in less than a fifth of the samples. The concentration of Fe remained considerably high for all the samples studied. These results emphasize the importance of Fe in paper degradation and that conservation efforts should aim to slow down/arrest the adverse effects of Fe. The catalytic effect of Fe can be inhibited in an alkaline environment. This means that mass de-acidification undertaken by some libraries and archives can effectively extend the shelf lives of their collections. The presence of Ca also ensured that there is a sufficient alkaline buffer so that the

paper remains of archival quality. The drop in the concentration of Ca in the samples originating from around the period AD 1850 coincides with the time when paper making technology changed. That was the period during which most of the acidic paper started to be produced. Since the concentrations of Fe remained consistently high even after the notable decrease in Ca concentration, it means that Fe was now in an acidic macromolecular environment and its catalytic effect became more pronounced. The catalytic activity of Cu increases steadily in the pH range 7-9. A serious implication of this behaviour of Cu is that oxidative degradation of paper will persist even after de-acidification. K and S are the characteristic indicators for the presence of alum. Alum can also bind transition metals, therefore it is beneficial to paper permanence as long as the paper remains alkaline. By determining the elemental composition and concentration of paper and linking it to the history of paper production, one can determine the origin of the paper as well as estimate its age. Very little research has been done that connects elemental composition and concentrations to historical periods. Elemental analysis of paper together with knowledge of the elemental composition of the ink used in a historical document [131] can thus be used in dating and authenticating such documents.

It has been observed that the effectiveness of transition metals as oxidative agents depend on their oxidation states. The determination of these oxidation states in paper samples was the next logical step in order to fully understand the paper degradation mechanism. In this work, Mössbauer spectroscopy was successfully used to determine the valence state of iron within the paper of several historical paper samples. Spectra of trace quantities of iron in the samples with distinct signatures for Fe^{2+} and Fe^{3+} have been obtained. According to the literature studied, this was the first time MS was applied successfully on the study of iron in paper.Significant drawbacks encountered had been the very small sizes of available samples and the trace amounts of iron in the samples, which necessitated relatively long data acquisition times, often lasting several days. This is a major setback of this technique. It is not suitable for quick checks in libraries, museums or archives where there are large collections of books or historical documents. However, this method can still be valuable in assessing the oxidative degradation risk of rare and valuable historical documents and works of art. A direct implication of the results of this study is that MS analysis of any sample on paper substrate will also contain information

about the valence state of the iron in the substrate. This is particularly important in the MS analysis of inks on historical documents. If the analysis of the ink is done in situ, that is without removing the ink from the paper, it is necessary to separate the MS spectrum of the paper from that of the ink. The presence of Fe^{2+} in the *Wildsport of Africa* sample means that de-acidification alone will not be able to completely stop the degradation of this sample. There was a notable discolouration on the *Wildsport of Africa* sample that can be attributed to both acid hydrolysis and catalytic oxidation. Under such moderately acidic conditions, the use of an antioxidant such as a peroxide decomposer will be effective in inhibiting the oxidation of cellulose [20]. Other techniques that can be used to inhibit cellulose oxidation are chelation of transition metals and the use of radical scavengers.

FTIR analysis revealed that the samples are made mainly out of cellulose with the exception of *The Courier* sample. This sample also had absorption peaks at 808 cm^{-1} which is associated with hemicellulose and at 1505 cm^{-1} and 1595 cm^{-1} that are assigned to lignin. The samples studied had Total Crystallinity Index (TCI) values that ranged from 0.073 (*19th Century Vol. 39*) to 0.275 (*The Courier*). On the other hand, the Het Leven sample had the Lateral Order Index (LOI) of 3.03 while the Timbuktu and The Press samples had the lowest LOI values of 0.35 and 0.29 respectively. All the three methods used to estimate the degree of crystallinity seem to point to the fact that the Timbuktu sample had more crystalline regions than any of the samples studied. All samples except *The Courier* had clay as the filler material. Only the *Timbuktu* sample showed evidence of gelatine. Traces of $CaCO_3$ were found only in *The Courier, Timbuktu, Het Leven* and *South Africa (Barrow)*. *Het Leven* and *South Africa (Barrow)* also had high levels of Ca and a pH level of more than 6.5. These two samples are also in good physical condition. *The Timbuktu* sample had only a weak shoulder band at 710 cm^{-1}. This may mean that the detected $CaCO_3$ was in small concentrations. Such an interpretation has merit because the presence of $CaCO_3$ could not neutralise the acidity of this sample. Four samples namely; *Het Leven, The Courier, Timbuktu* and *Natal Almanac* samples had an oxidation index of zero. *The Courier* had zero oxidation index but with carbonyl absorption peaks at 1710 cm^{-1}, 1665 cm^{-1} and 1236 cm^{-1}. The sample therefore had evidence of oxidative degradation but the degree of oxidation could not be quantified using the peaks at 1730 cm^{-1} and 1620 cm^{-1}.

PLM analysis of the fibre showed that the samples were made up of three types of natural fibres namely linters, hemp and rammie. All sample fibres had positive sign of elongation and parallel extinction. It was also observed that ($n_{\parallel}$) of all the fibres was greater 1.55 and ($n_{\perp}$) of all the fibres was less1.55. It should be noted that there was no change in the value of the birefringence of all the samples over time. This means that the light scattering ability of the paper matrix does not change with time since the birefringence was invariant over time.

The assessment of the degradation potential of the samples was done and possible remediation methods were suggested. It must however be noted that the biggest threat of deterioration that needs immediate attention is the acidic nature of the samples. This can be easily achieved by mass de-acidification.

Appendix A : FTIR spectra of the samples studied

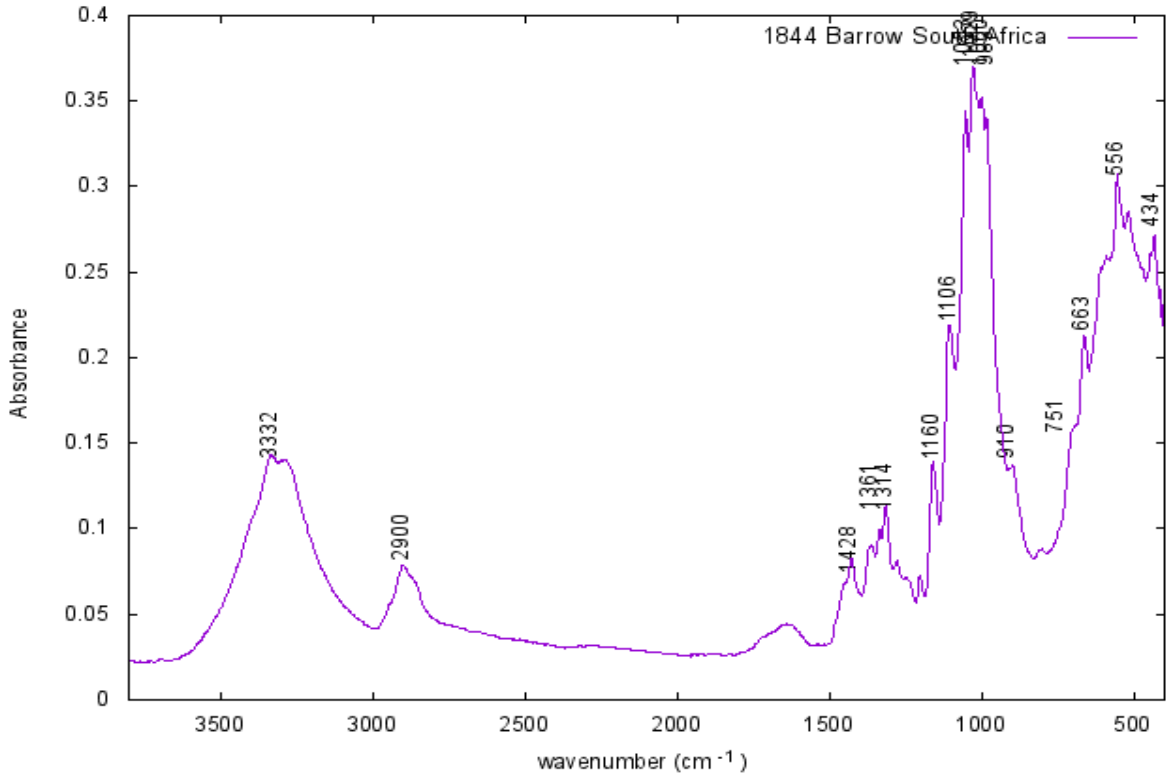

Figure A1: FTIR spectrum of the *Barrow South Africa* sample with relevant wave numbers.

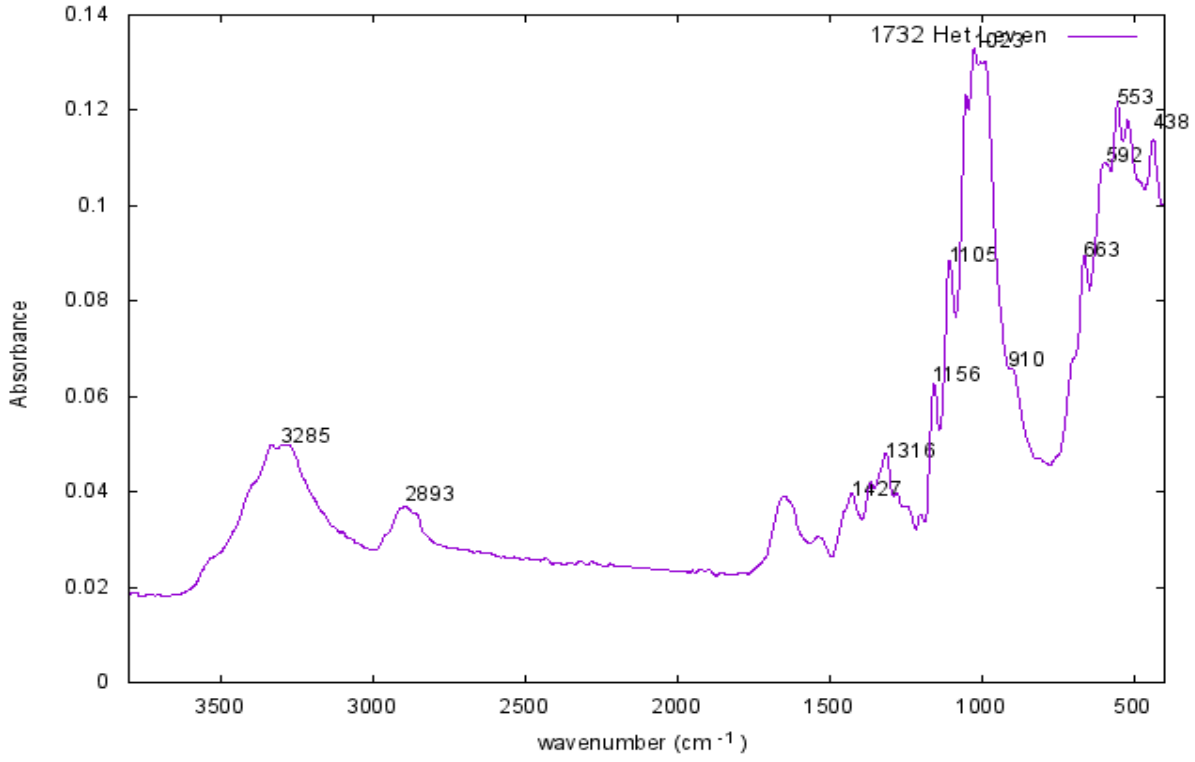

Figure A2: FTIR spectrum of the *Het Leven* sample with relevant wave numbers.

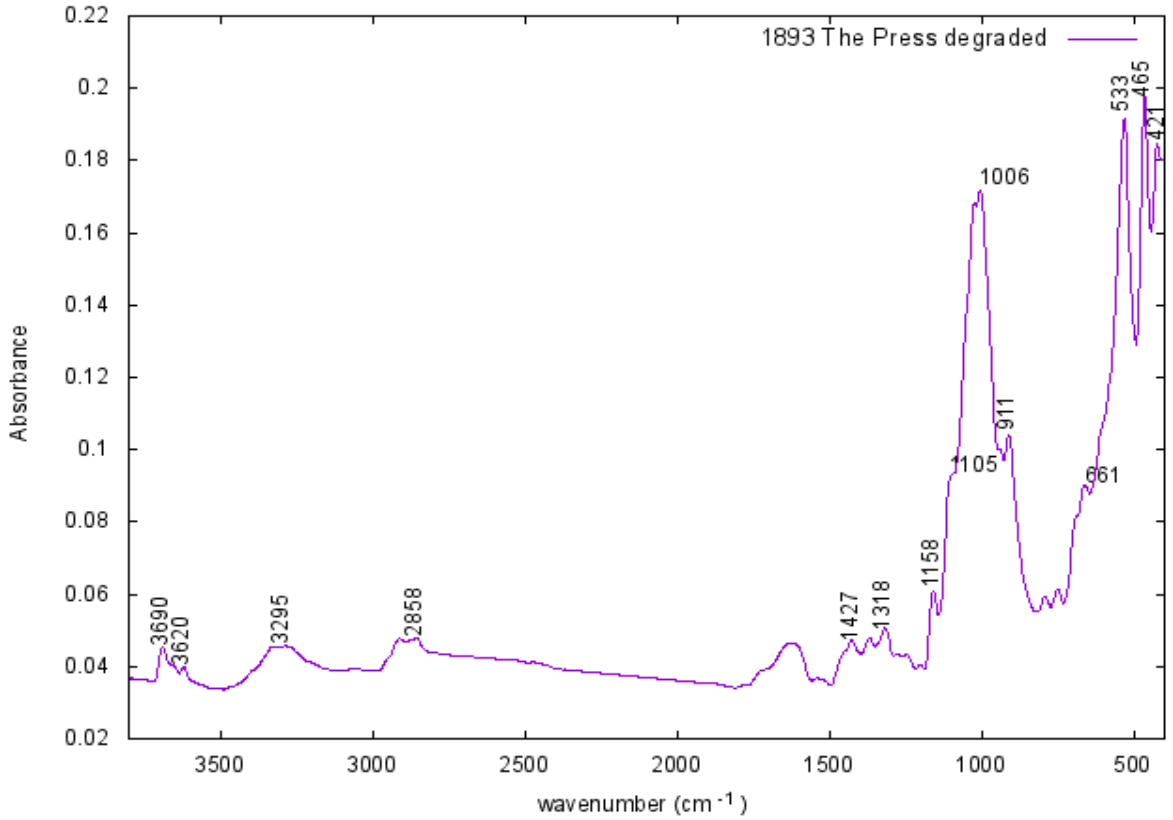

Figure A3: FTIR spectrum of *The Press(1893)* sample with relevant wave numbers.

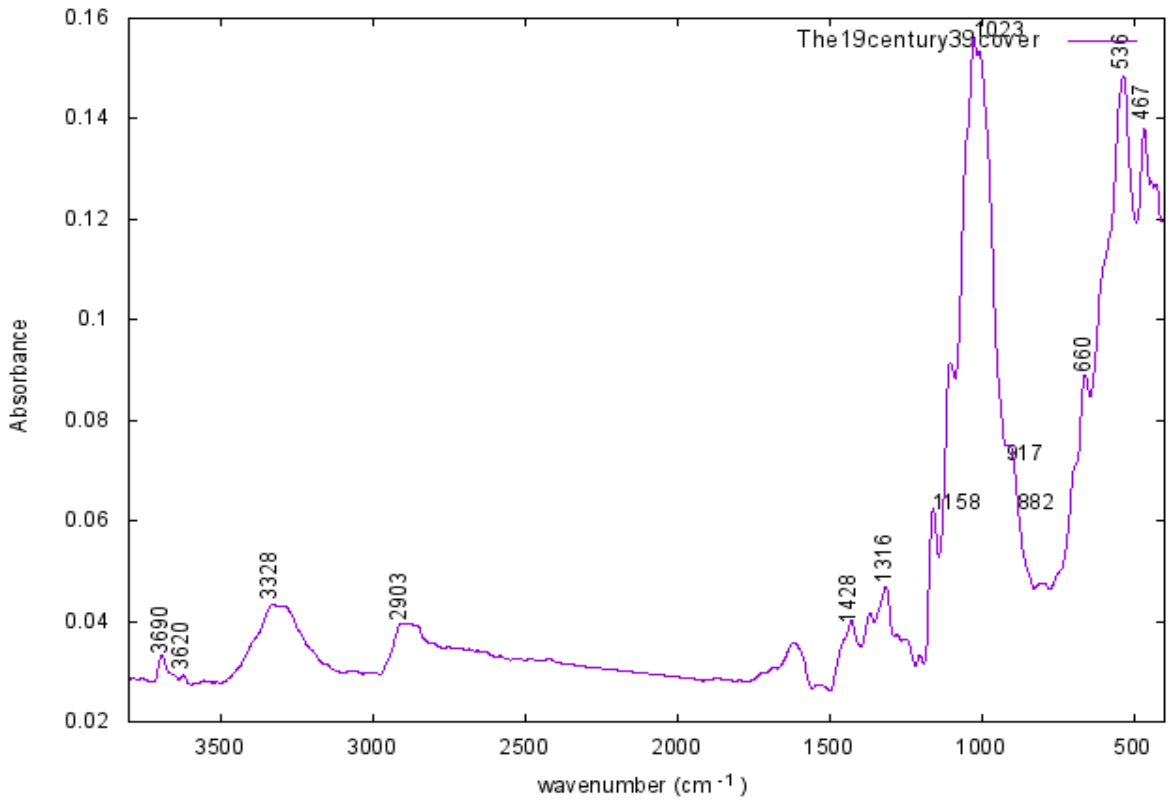

Figure A4: FTIR spectrum of *The 19th Century Vol 39* cover sample with relevant wave numbers.

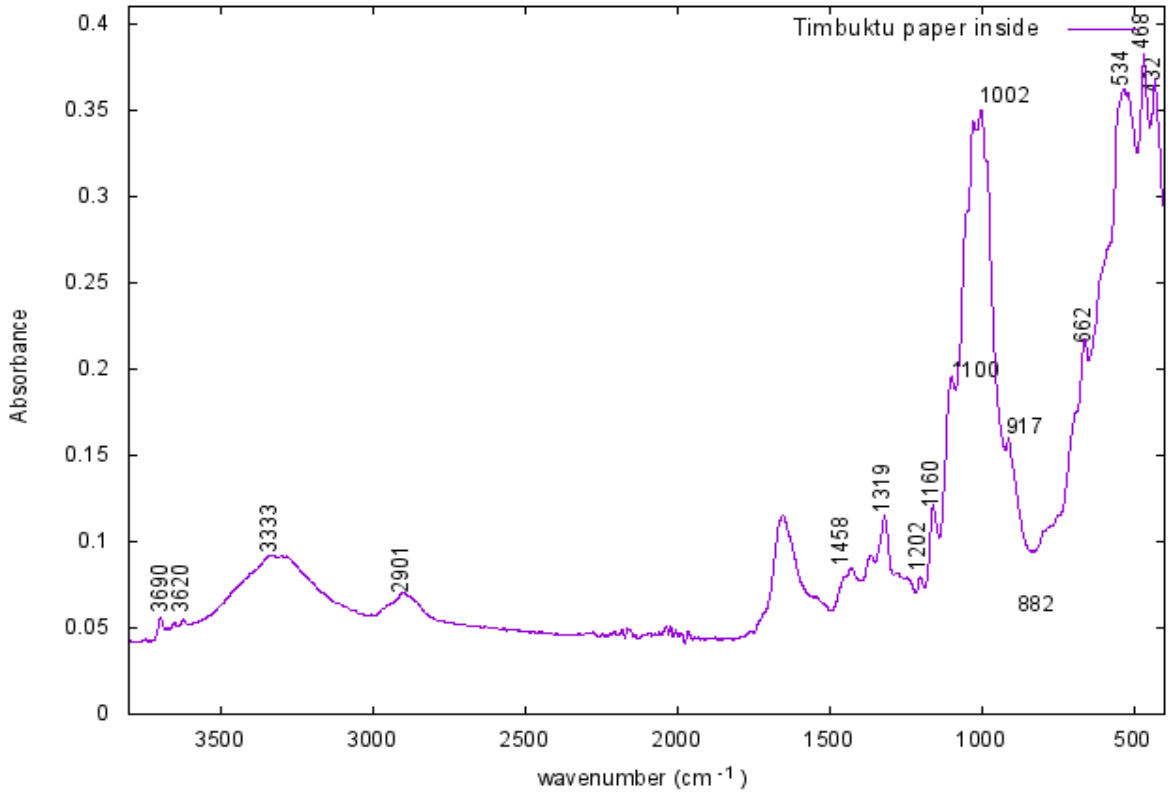

Figure A5: FTIR spectrum of the *Timbuktu* manuscript sample.

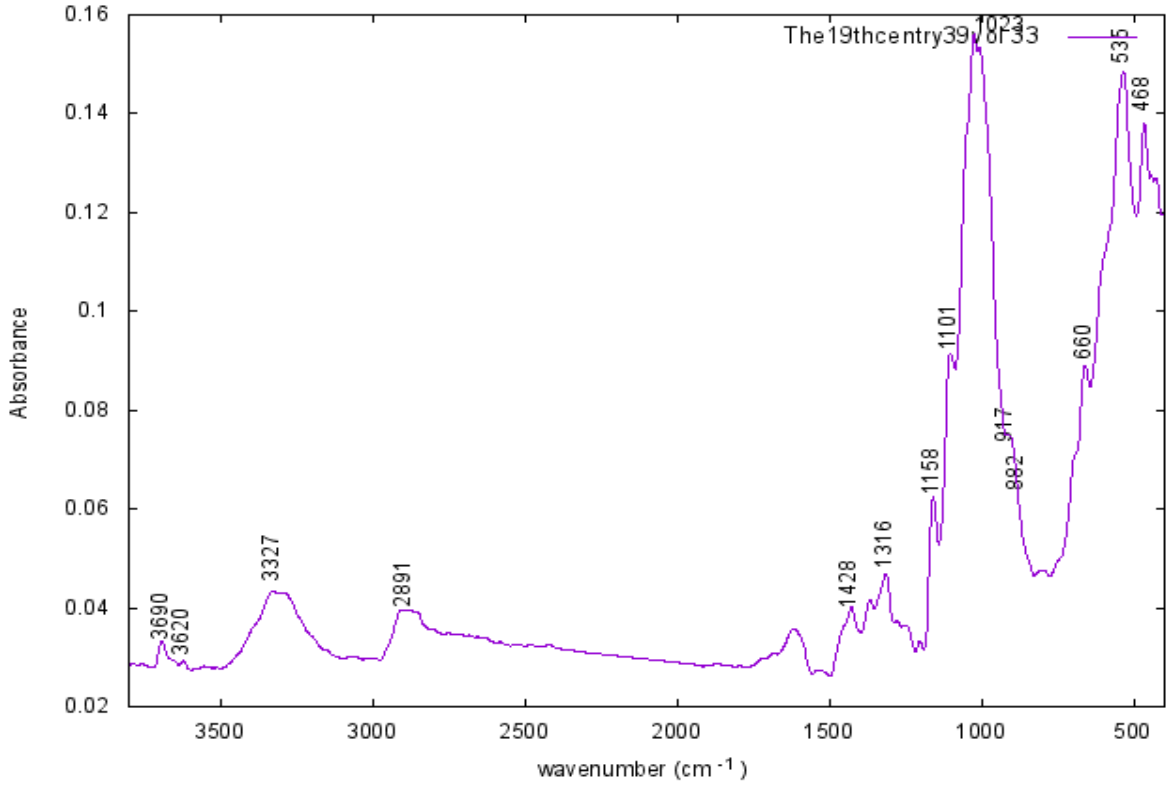

Figure A6: FTIR spectrum of *The 19th Century Vol 33* sample with relevant wave numbers.

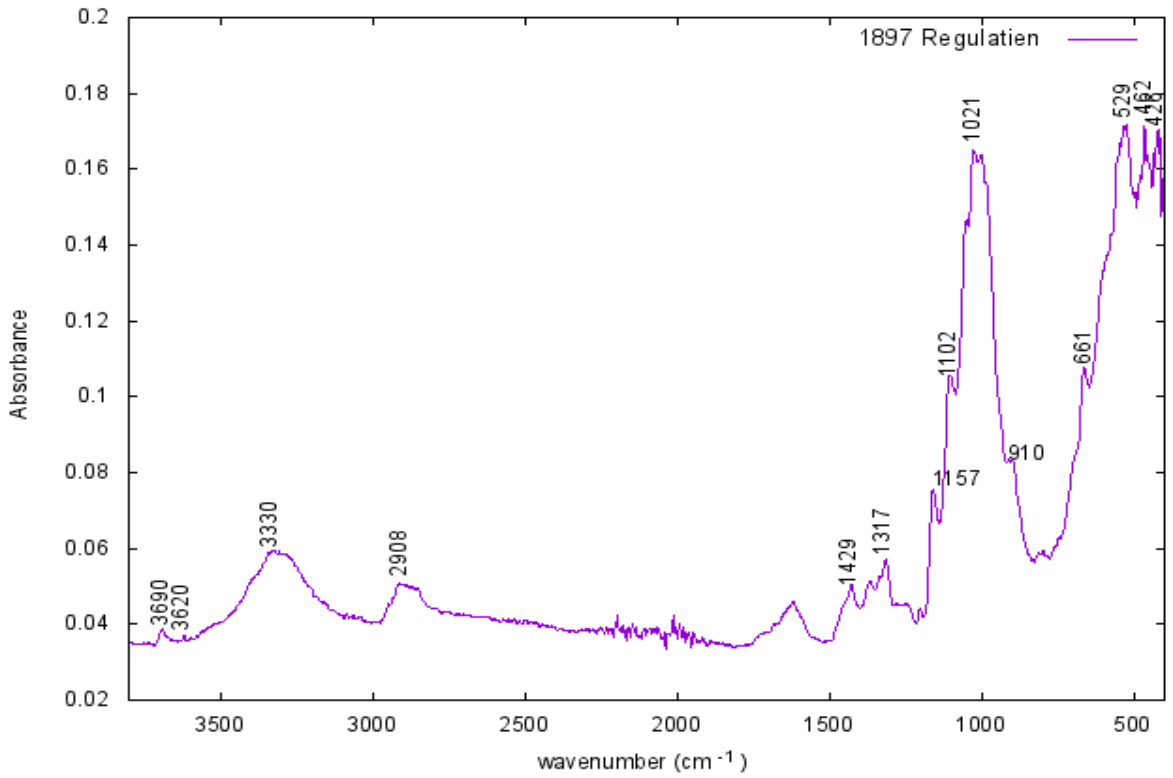

Figure A7: FTIR spectrum of *The Regulatien* sample with relevant wave numbers.

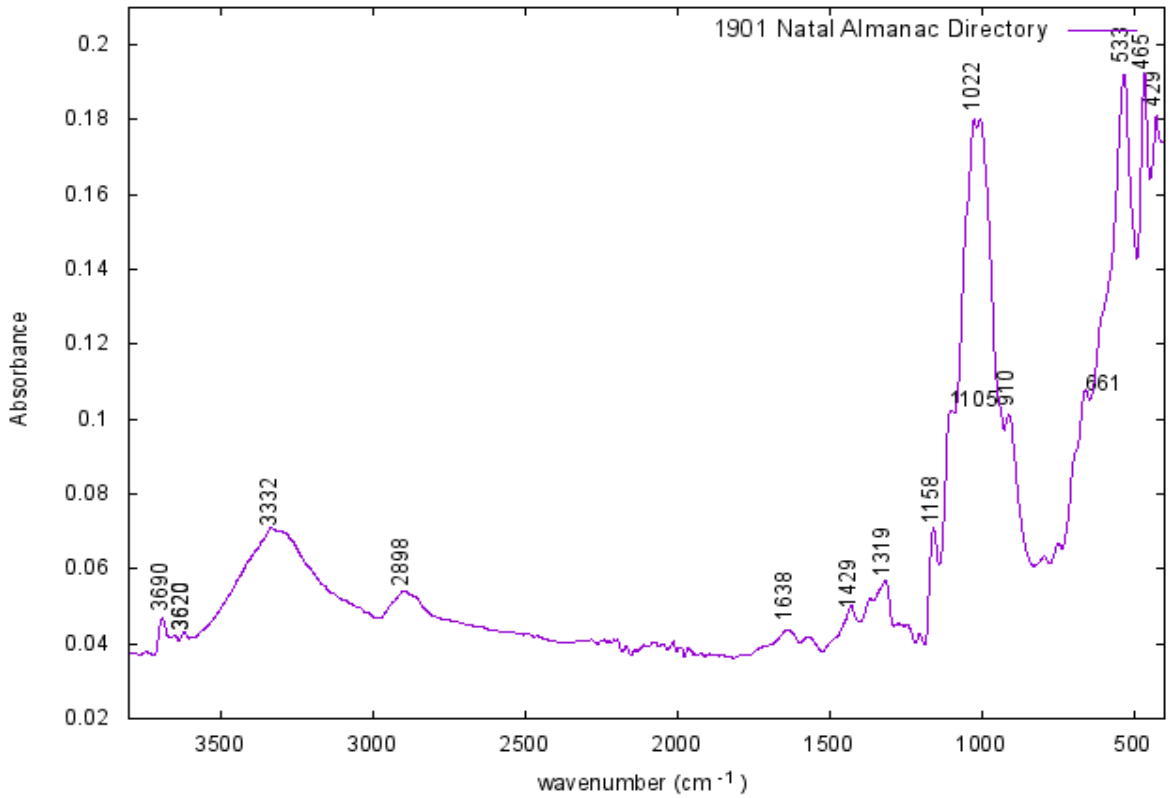

Figure A8: FTIR spectrum of the *Natal Almanac Directory* sample with relevant wave numbers.

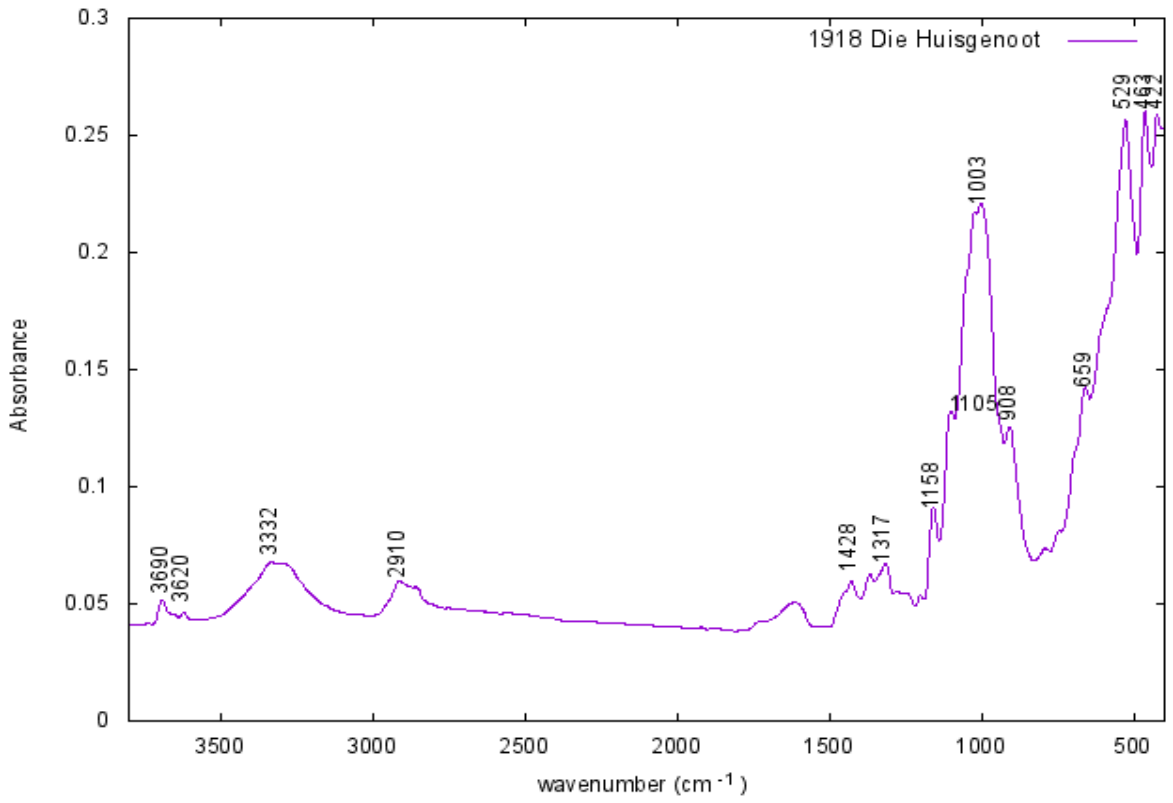

Figure A9: FTIR spectrum of the *Die Huisegnoot* sample with relevant wave numbers.

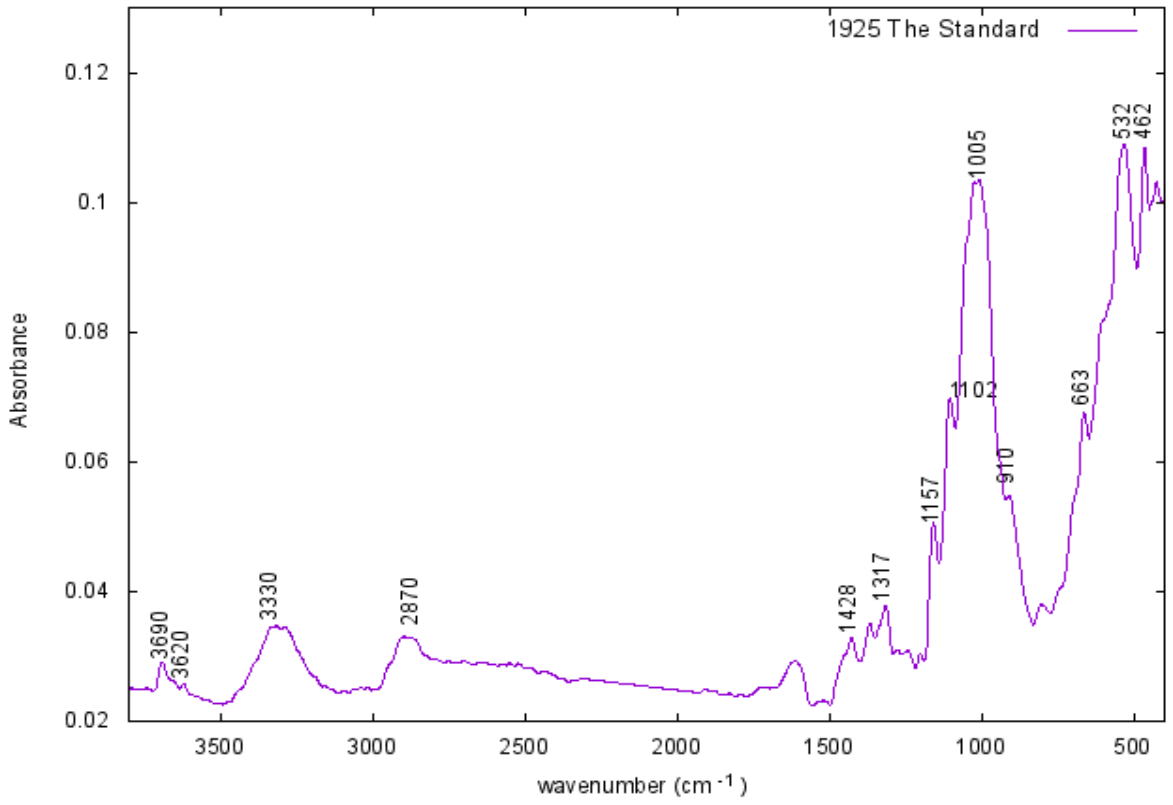

Figure A10: FTIR spectrum of *The Standard* sample with relevant wave numbers.

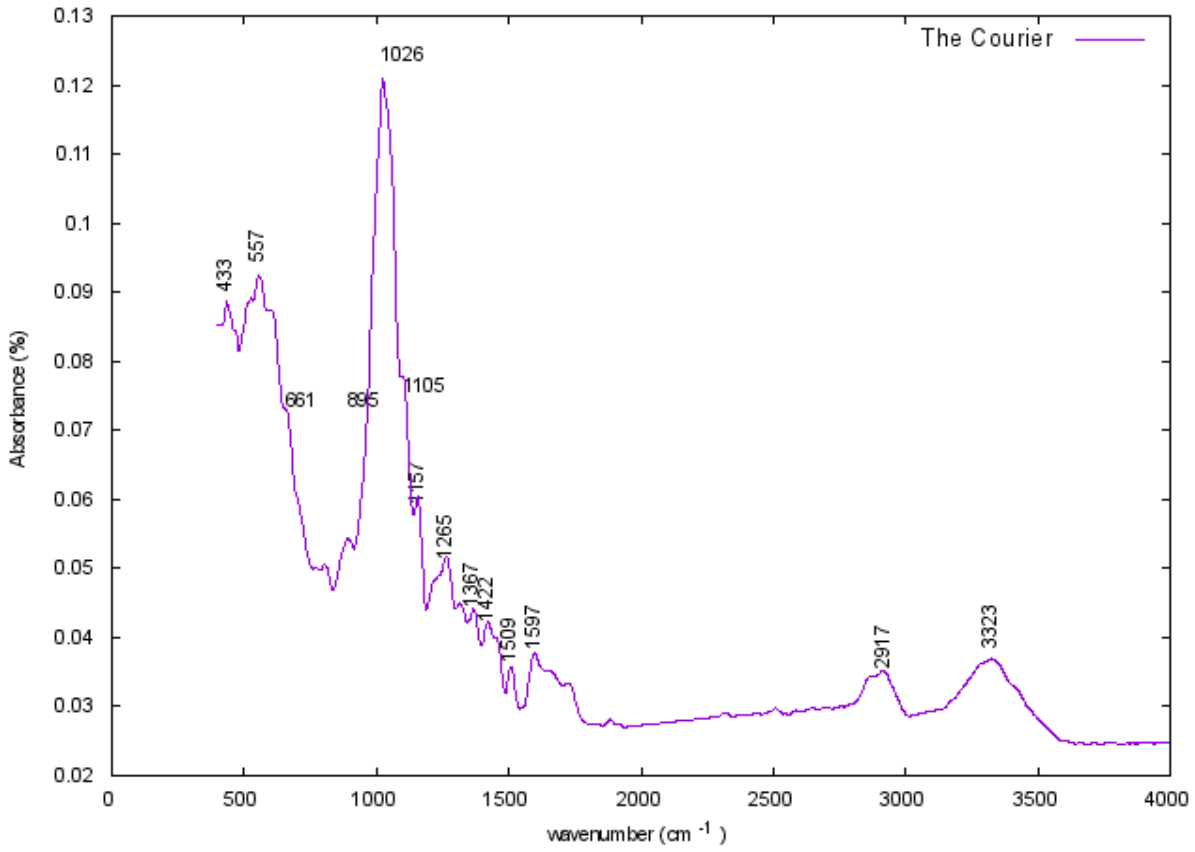

Figure A11: FTIR spectrum of *The Courier* sample with relevant wave numbers.

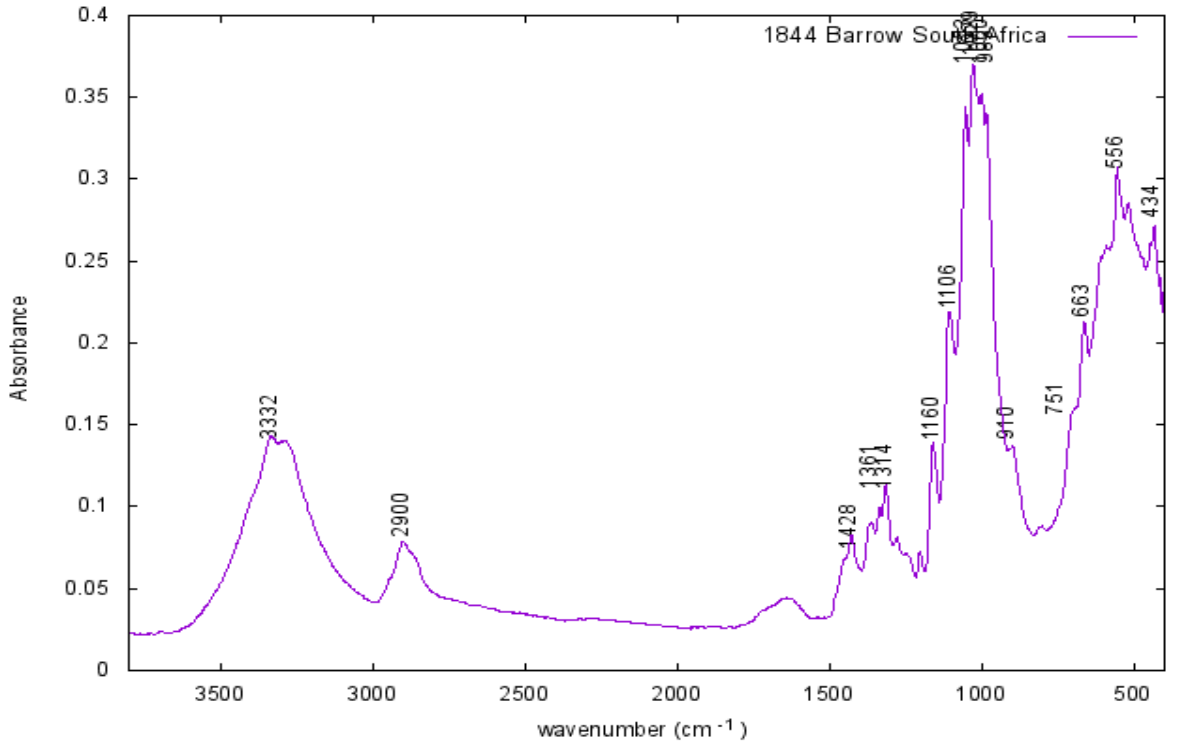

Figure A12: FTIR spectrum of *the Wild Sport of Africa* sample with relevant wave numbers.

Appendix B : Publications from the thesis

Appendix C : PLM micrographs of samples studied.

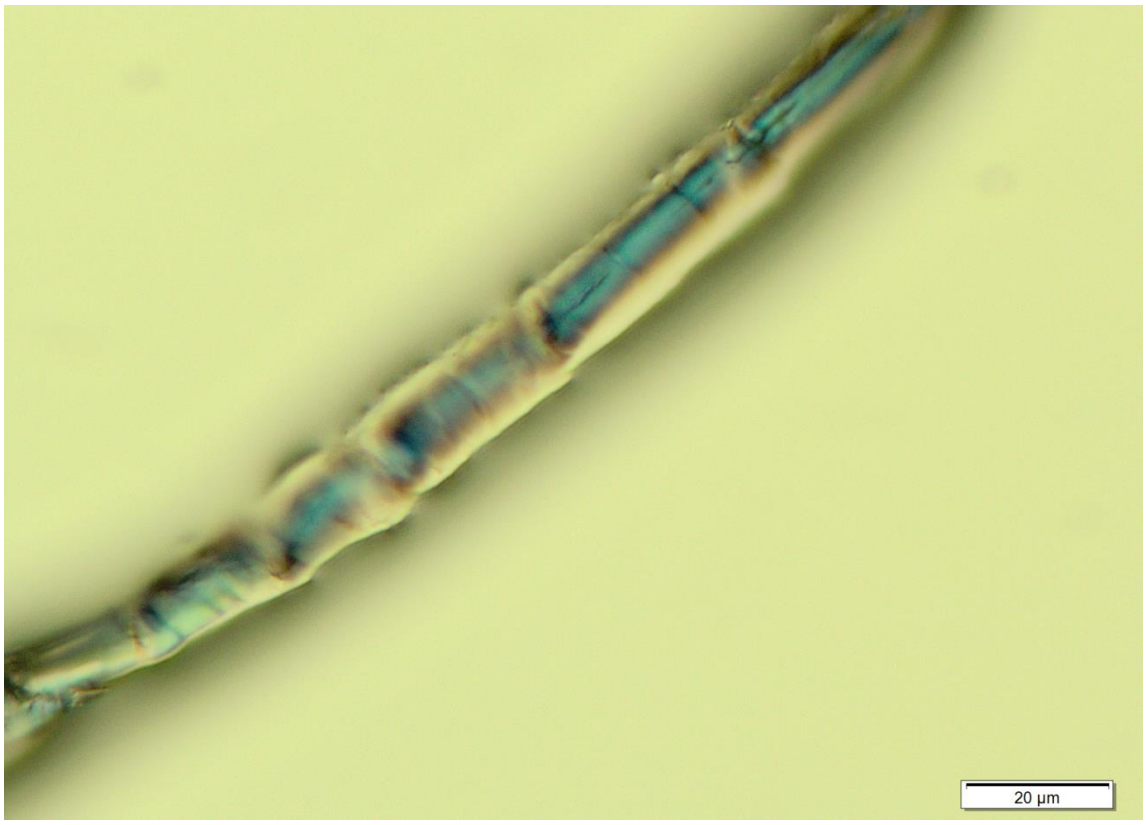

Figure C1: Micrograph of Hemp

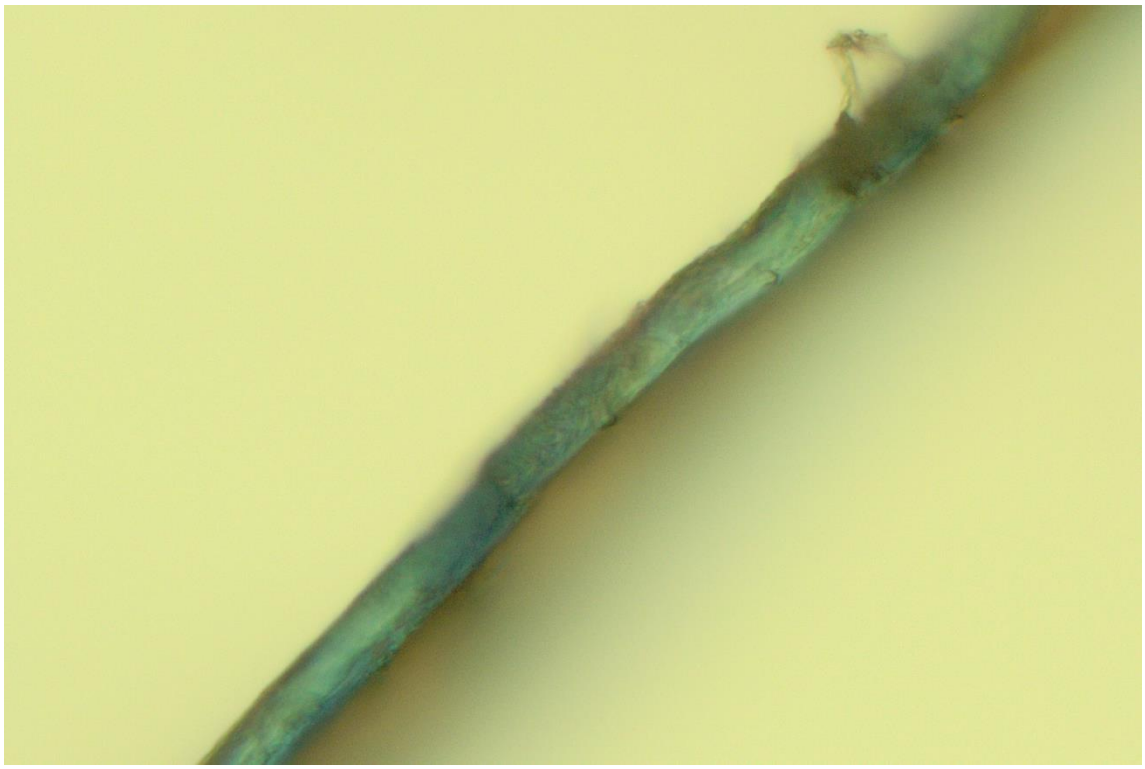

Figure C2: Micrograph of *The Standard* sample

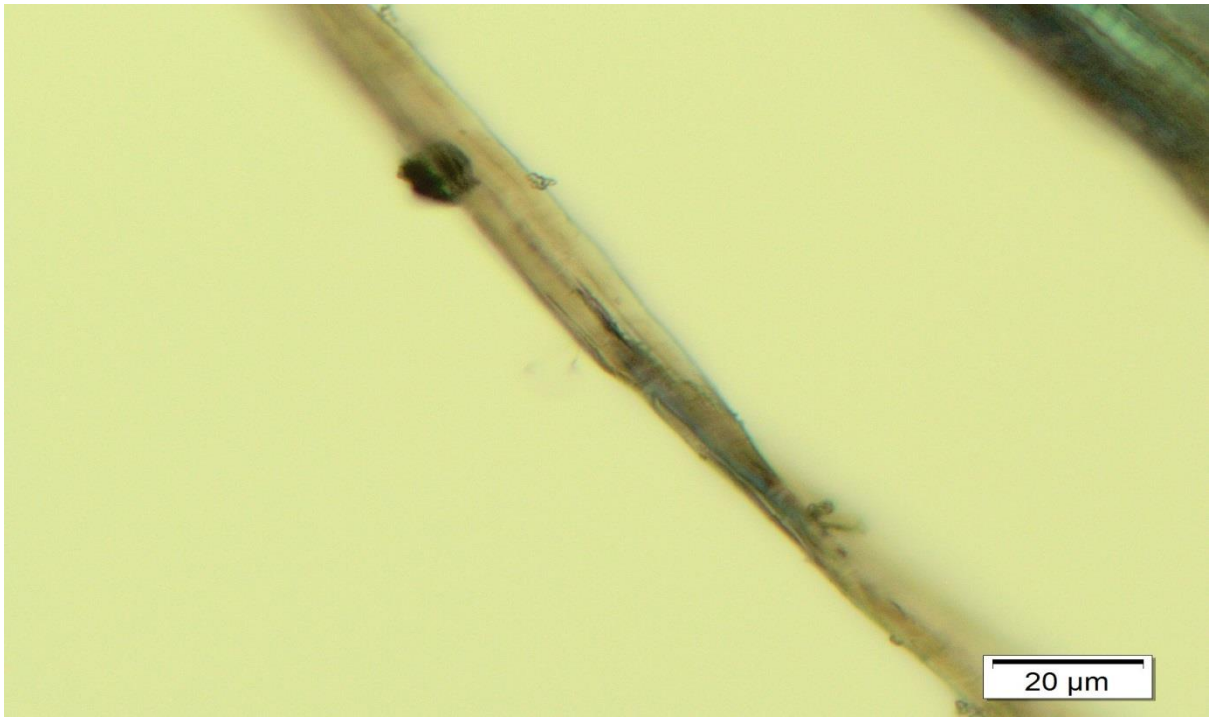

Figure C3: Micrograph of linters reference fibre

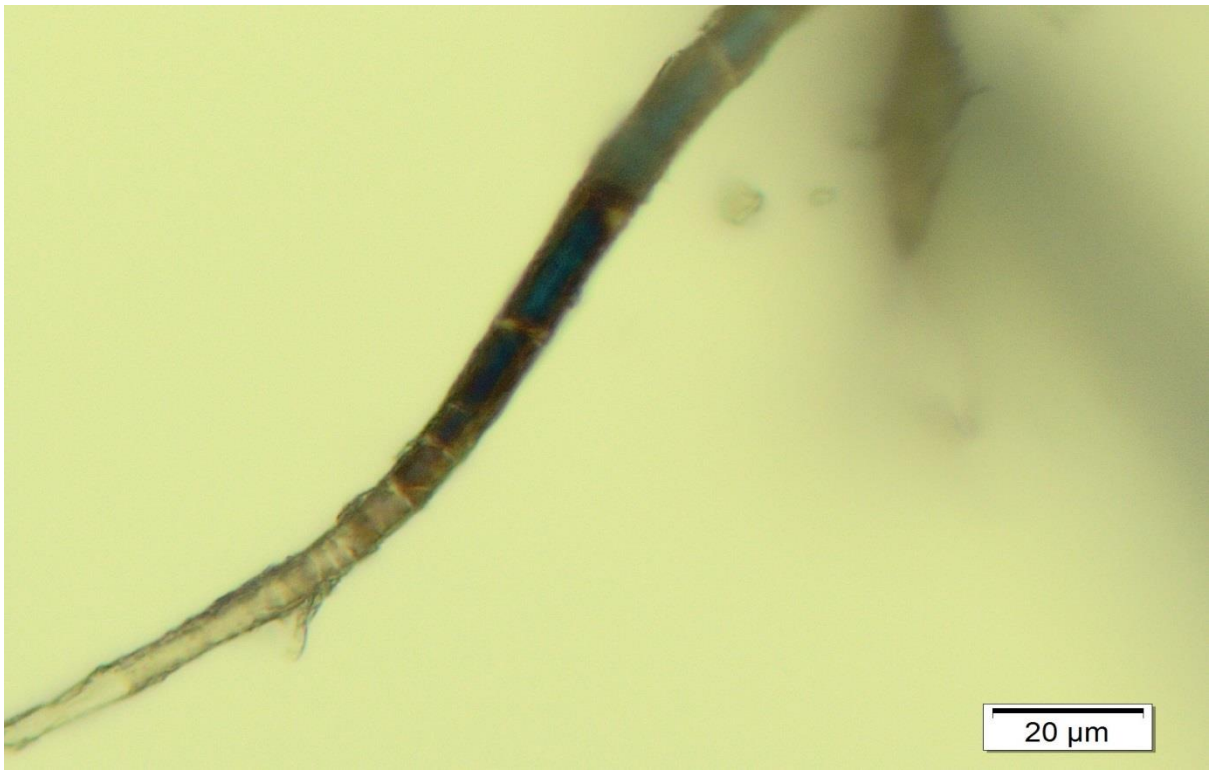

Figure C4: Micrograph of the *Natal Almanac* sample

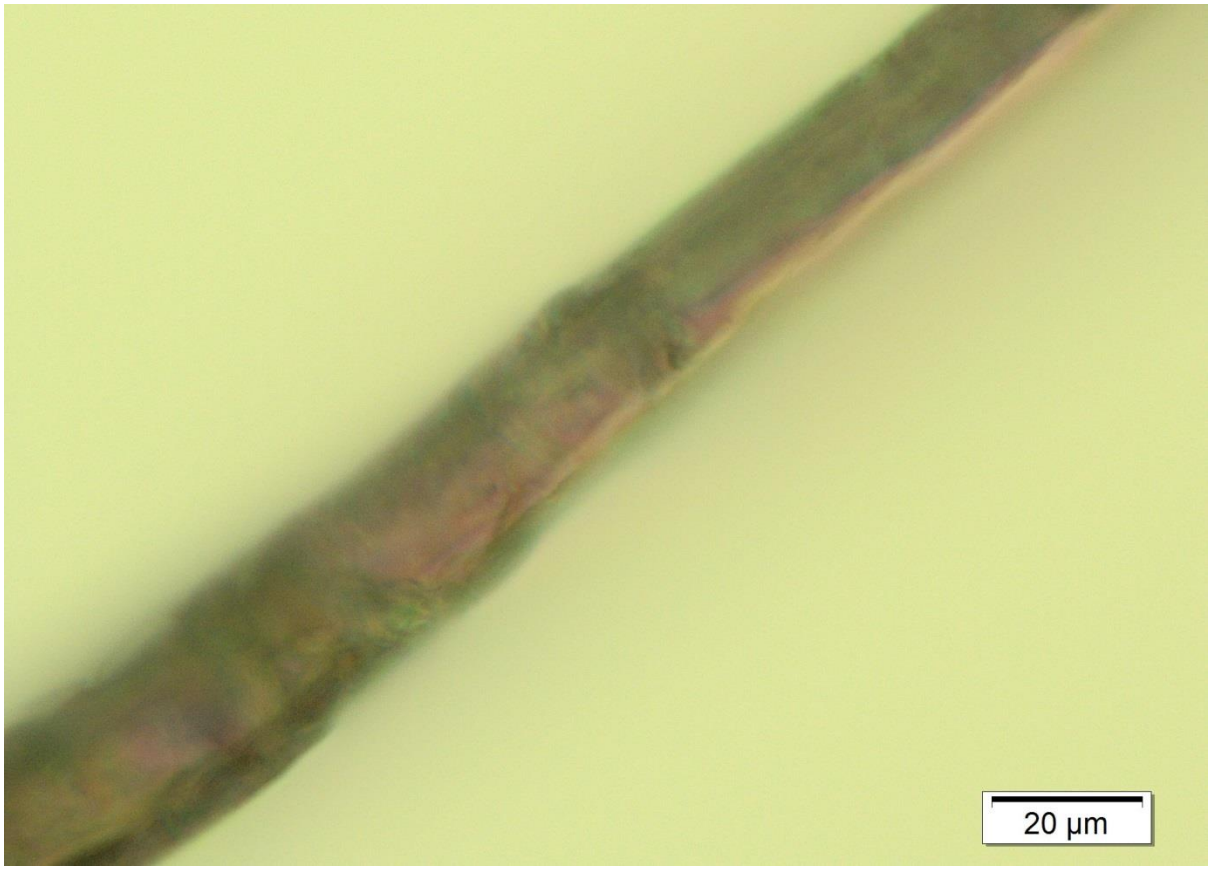

Figure C5: Micrograph of the *rammie reference* fibre

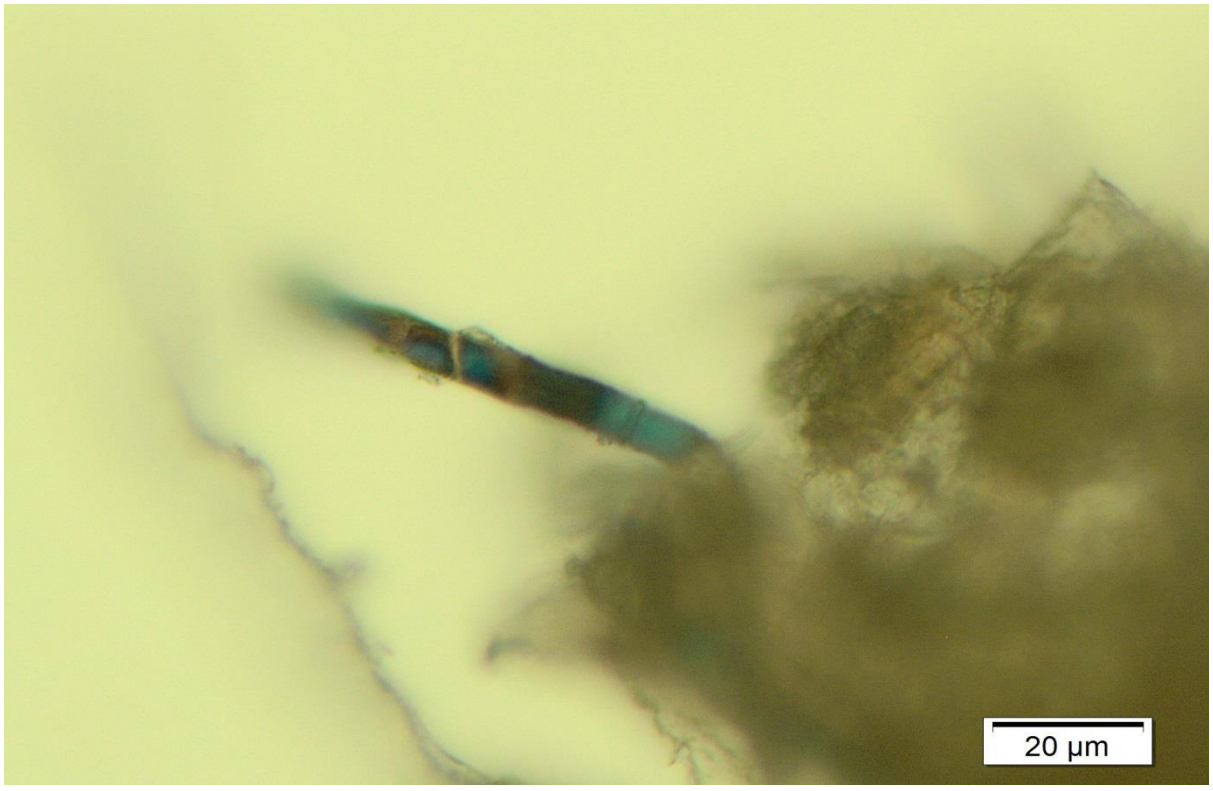

Figure C6: Micrograph of the *Regulatien* sample

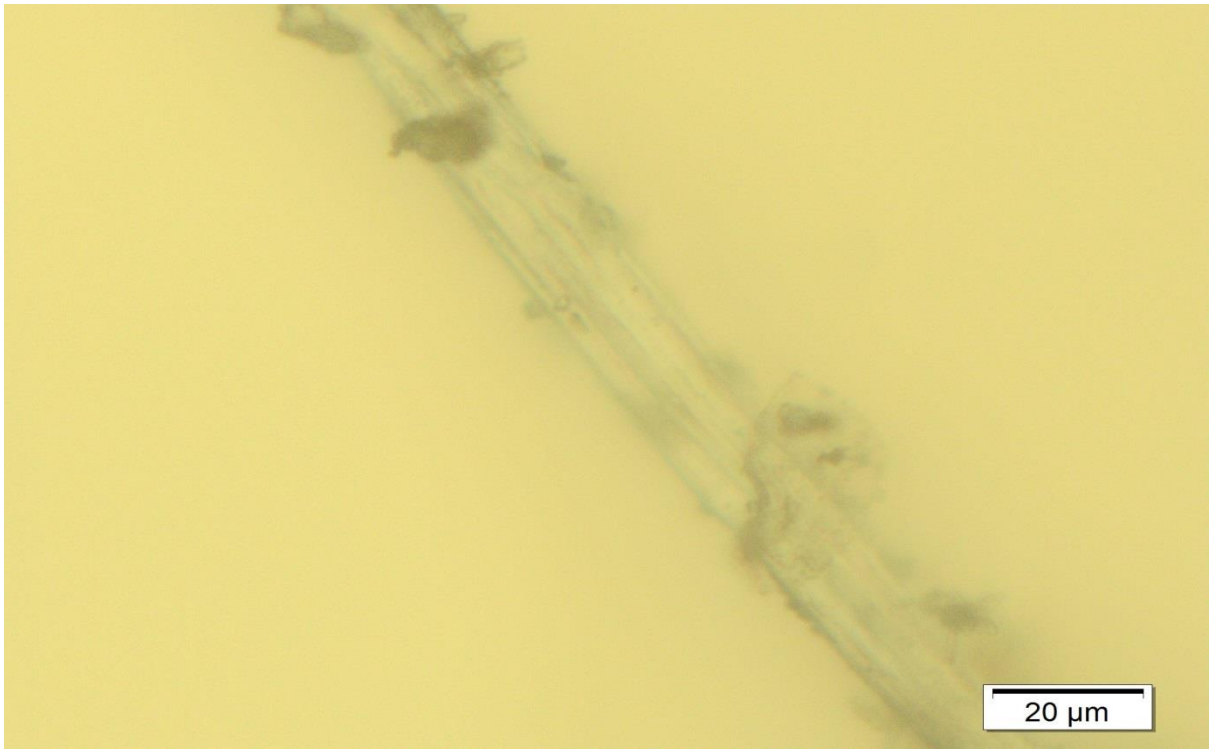

Figure C7: Micrograph of *The Press* sample.

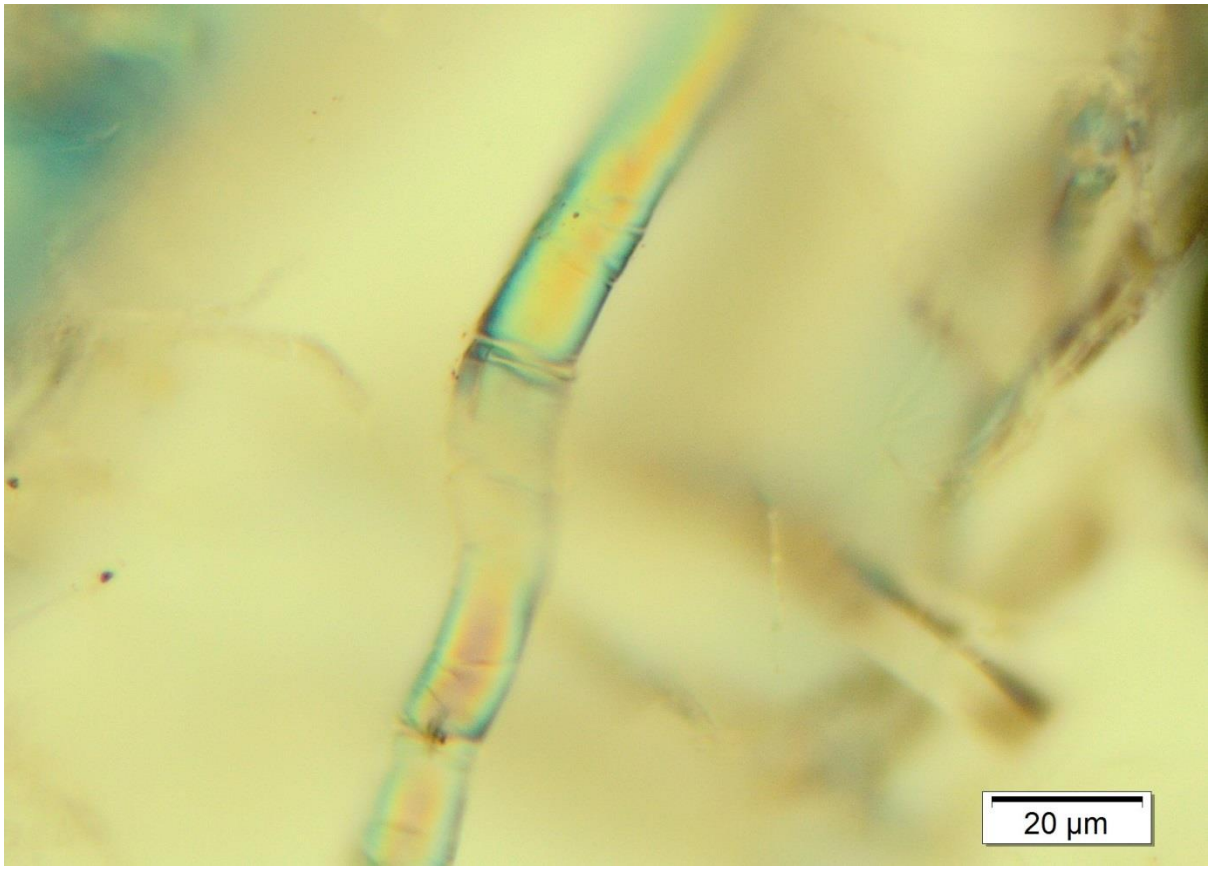

Figure C8: Micrograph of the *Timbuktu manuscript* sample

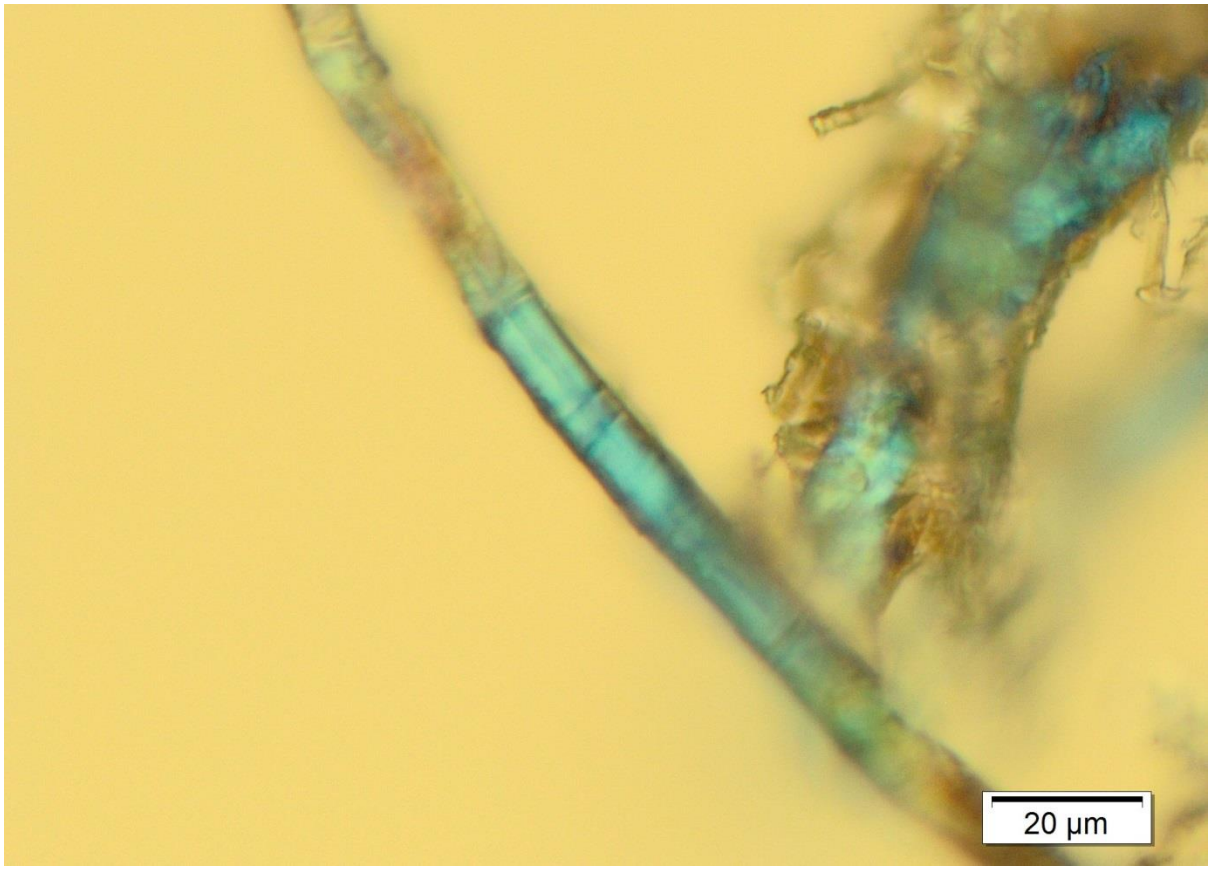

Figure C9: Micrograph of the *Wild Sport* sample

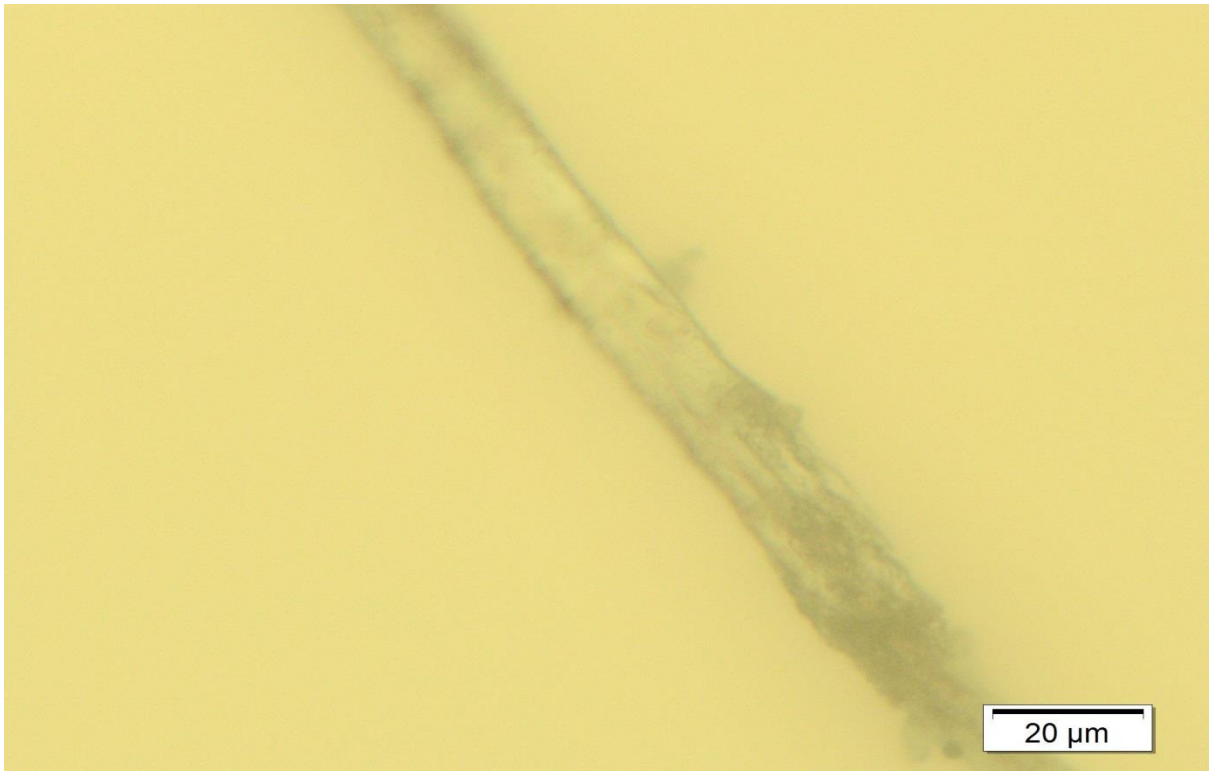

Figure C10: Micrograph of the *Die Husegnoot* sample

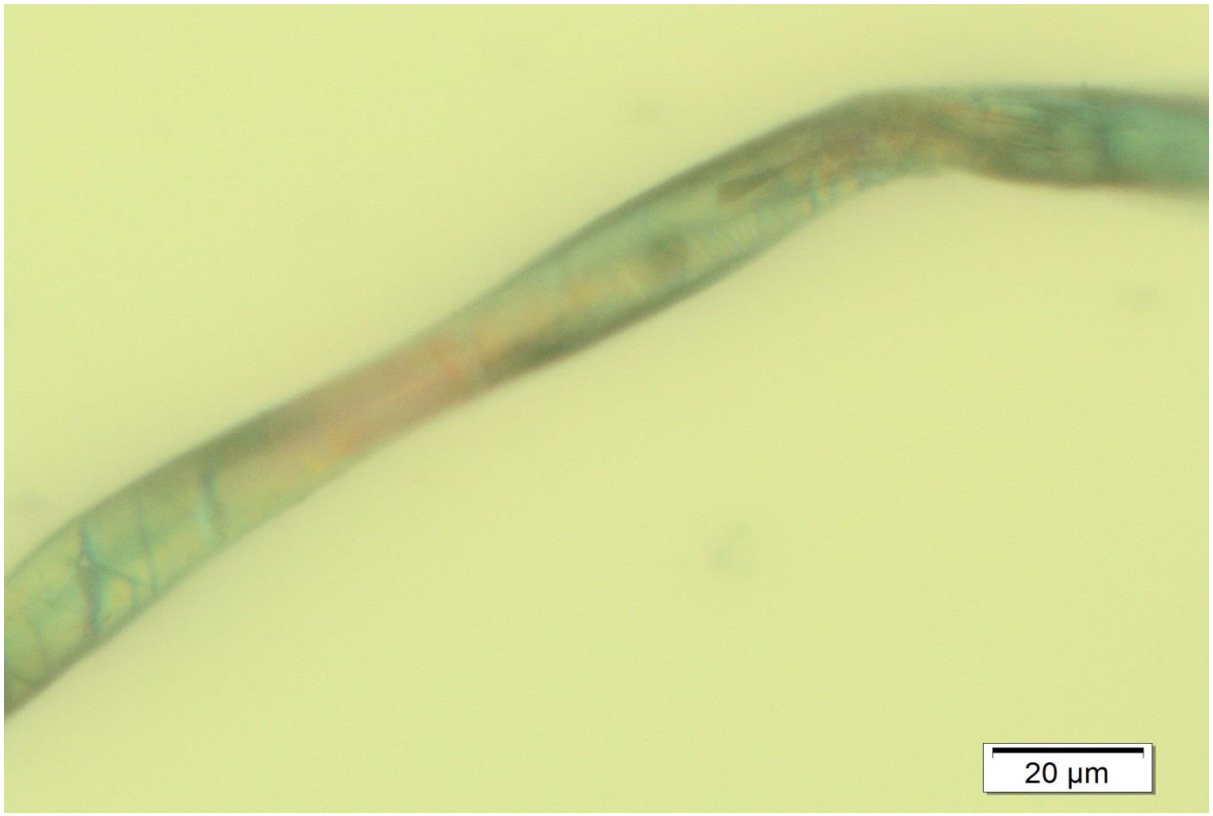

Figure C11: Micrograph of the *Barrow South Africa* sample

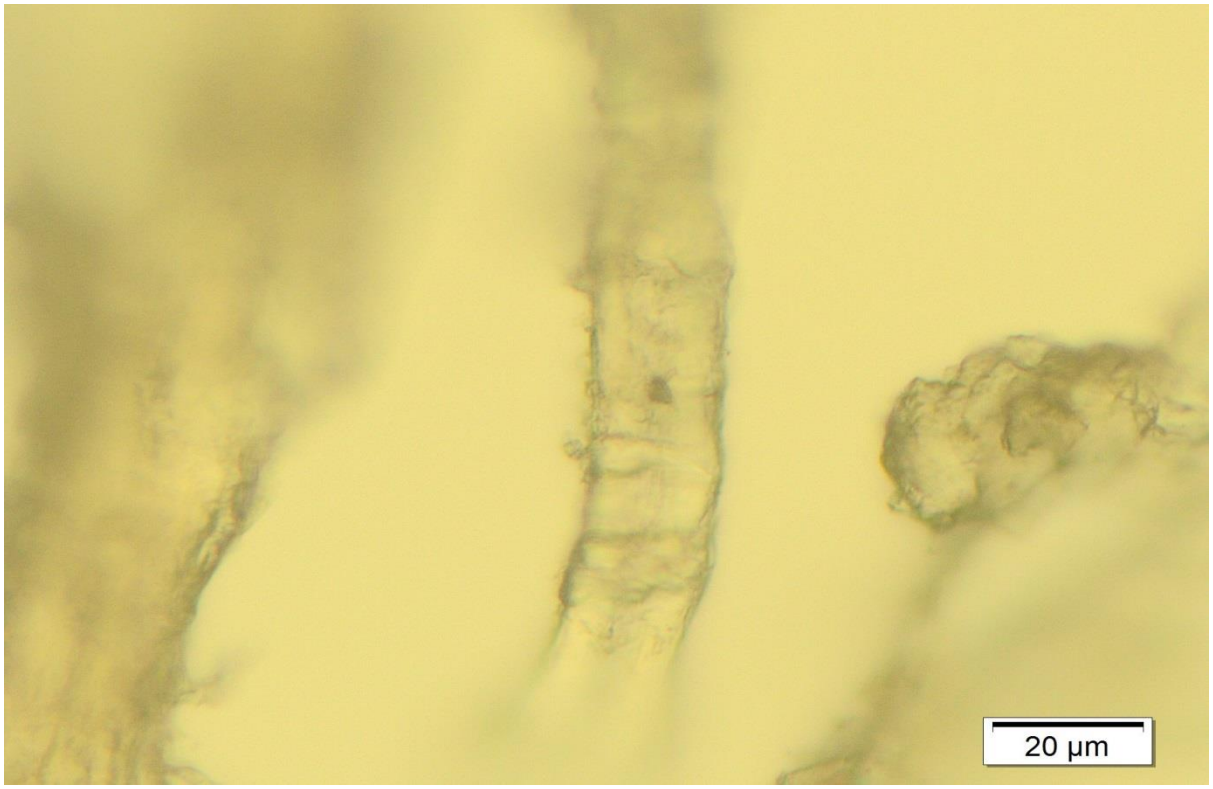

Figure C12: Micrograph of the *Alweer* sample

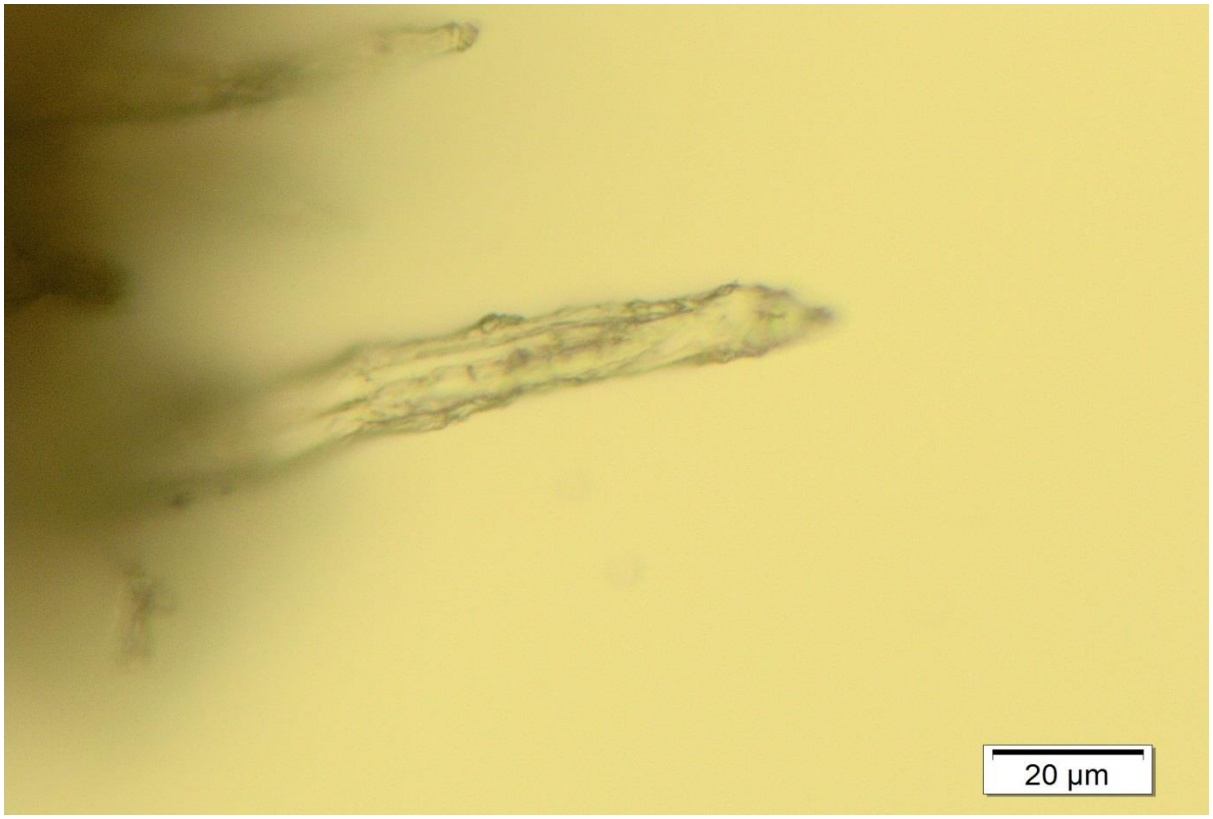

Figure C13: Micrograph of the *19th Century vol. 39* sample

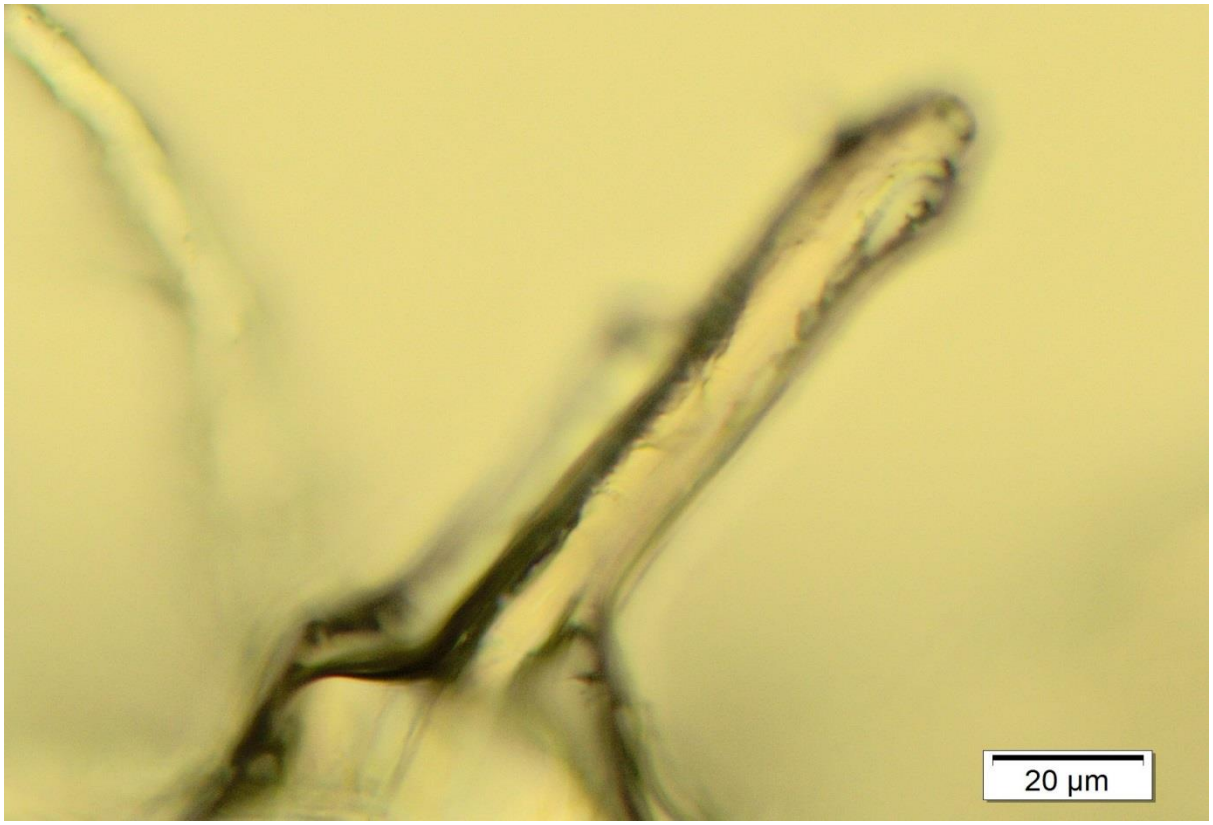

Figure C14: Micrograph of the *19th Century vol. 33* sample

References

[1] J. Lojewska, P. Miśkowiec, T. Lojewski, L.M, Cellulose oxidative and hydrolytic degradation: In situ FTIR approach, *Polymer Degradation and Stability 88* (2005) 512-520.

[2] M. Ali, A.M. Emsley, H. Herman, R.J. Heywood, Spectroscopic studies of the ageing of cellulosic paper *Polymer 42* (2001) 2893-2900

[3] M. Polovka, J. Polovkovà, K. Vizàrovà, S. Kirscnerovà, L. Bielikovà, M. Vrskà, Application of FTIR spectroscopy on characterisation of paper samples modified by Bookkeeper process, *Vib. Spectrosc 41*(2006) 112

[4] V.S. Šelih, M. Strlič, J. Kolar, B. Pihlar, The role of transition metals in oxidative degradation of cellulose, Polymer *Degradation and Stability 92* (2007) 1476

[5] T. Trafela, M. Strlic, J. Kolar, D.A. Lichtblau, M. Anders, D.P. Mencigar, B. Pihlar, Nondestructive analysis and dating of historical paper based on IR spectroscopy and chemometric data evaluation, *Anal. Chem 79* (2007) 6319

[6] M. Manso, M.L. Carvalho, Application of spectroscopic techniques for the study of paper documents: A survey, *Spectrochimica Acta Part B 64* (2009) 482

[7] S. Pessana, M. Manso, M.L. Carvahlo, Application of spectroscopic techniques to the study of illuminated manuscripts: A survey, *Spectrochimica Acta Part B* 71-72 (2012) 54.

[8] J. Kolar, A. Stolfa. M. Strlič, et al. 2006. Historical iron gall ink containing documents: properties affecting their condition. *Analytica Chimica Acta* 555: 167–174.

[9] J. Malesic, J. Kolar, and M. Strlič. 2002. Effect of pH and carbonyls on the degradation of alkaline paper: factors affecting ageing of alkaline paper. *Restaurator* 23: 145–153

[10] M. Strlič, J. Kolar. 2005. Review of practices for aqueous paper deacidification. In *ICOM Committee for Conservation, 14th Triennial Meeting, The Hague, 12–15 September. Preprints*, 231–237.

[11] P. Calvini, and A. Gorassini. 2002. FTIR-deconvolution spectra of paper documents. *Restaurator* 22: 48–66.

[12] N. Ferrer, and M. C. Sistach. 2005. Characterization by FTIR spectroscopy of ink components in ancient manuscripts. *Restaurator* 26: 105–117.

[13] J. Lojewska, A. Lubanska, T. Lujewski, P. Miskowiec, and L. M. Proniewcz, Kinetic approach to degradation of paper: In-situ FTIR transmission studies on hydrolysis and oxidation. *e-preservationscience.org* 2 (2005) 1–12.

[14] G. Spoto, A. Torrisi, A. Contino Probing archaeological and artistic solid materials by spatially resolved analytical techniques, *Chem. Soc. Rev 29* (2000) 429-439.

[15] K. Dziedzic-Kocurek, A. Banas, W.M. Kwiatek, J. Stanek, X-ray Absorption Near Edge Structure and Mössbauer Spectroscopy in Study of Iron Valence States in Tissues, *Acta Physica Polonica A 109* (3) (2006) 341-345.

[16] B. Wagner, E. Bulska, B. Stahl, M. Heck, M.H. Ortner, Analysis of Fe valence states in iron-gall inks from the XVIth century manuscripts by ^{57}Fe Mössbauer spectroscopy, *Analytica Chimica Acta 527* (2004) 195-201.

[17] I. Arcon, J. Kolar, A. Kodre, D. Hanzel, M. Strlic, XANES analysis of Fe valence in iron gall inks, *X-Ray Spectrom 36* (2007) 199–205

[18] A. Jamrozik, M. Mazurkiewicz, A. Małolepszy, L. Stobin´ski, K. Matlak, J. Korecki, K. J. Kurzydłowski, K. Burda, Mössbauer spectroscopy analysis of iron compounds in carboxylated multiwall carbon nanotubes and their ammonium salt, *Phys. Status Solidi A* 208 (8) (2011), 1783-1786

[19] B. Fultz, "Mössbauer Spectrometry", in Characterization of Materials, *John Wiley*, New York, 2011.

[20] M. Strlič; J. Kolar, In Ageing and stabilization of paper; Strlič, M., Kolar, J.; Eds.; *National and University Library,* Ljubljana, 2005; pp 199-203.

[21] R.H.Marchessault, and P. R. Sundararajan, (1983) In Cellulose, in the Polysaccharides. New York: *Academic Press*, p. 11.

[22] E. Sjöström, Wood Chemistry. Fundamentals and Applications, 2nd ed., *Academic Press*, Boston, 1993.

[23] I. Simon, H. A. Scheraga and R.J. Manley, Structure of cellulose. 1. Low-energy conformations of single chains. *Macromolecules 21*(1988), 983-990.

[24] J. Sugiyama, J. Persson. and H. Chanzy,. Combined IR and electron diffraction study of the polymorphism of native cellulose. *Macromolecules 24* (1991), 2461-2466.

[25] R. H. Atalla and D.L. Vanderhart (1989) Studies on the structure of cellulose using Raman spectroscopy and solid state 13C NMR. In Cellulose and Wood: Chemistry and Technology, *Proceedings of the tenth Cellulose Conference (C. Schuerch, ed.*). New York: John Wiley and Sons, 169-187.

[26] M. A Hubbe, Paper's response to wetting, *BioResources 2* (1), 2006, 106-145

[27] K. Garlick: A brief review of the history of sizing and resizing practice,. *AIC Book and Paper Group Annual 4* (1986): 94-107.

[28] H. Voorn, “A Brief History of the Sizing of Paper,” *The Papermaker 30* (1) (1961): 47–53

[29] W.J.Barrow, Research Laboratory. *Physical and Chemical Properties of Book Paper, 1507-1949.* (Permanence/Durability of the Book--VII) Richmond, Virginia: *Barrow Research Laboratory*, 1974.

[30] I. Bruckle, The role of Alum in Historical Papermaking, *IPC Conference*, Manchester, England 1992

[31] J. de Lalande, *The Art of Papermaking* (1761), transl. by R. Atkinson. County Clare, Ireland: Ashling Press, 1976.

[32] S. Green, An outline history of sizing methods with special reference to practices at Hayle Mill. Conference papers manchester (1992) *Third International Institute of Paper Conservation Conference*, Manchester. 197-200.

[33] G.A Smook, (1982). Handbook for pulp & paper technologists. Joint Textbook Committee of the Paper Industry.

[34] T.R Arnson, The chemistry of Aluminium salts in papermaking. *Tappi 65* (1982):125-130.

[35] J.M Gess, Rosin Sizing of Papermaking Fibers, *Tappi Journal 72(7)* (1989) 77-80.

[36] T. D. Barrett, Early European papers/contemporary conservation papers: A report on research undertaken from fall 1984 through fall 1987, *Paper Cons.13 (*1989) 1-108

[37] D. Erhardt, M.F. Mecklenburg, In *Materials issues in art and archeology IV,* Cancun, Materials Research Society Symposium Proceedings 352 (1995) May 16-21; pp 247-270.

[38] H.Z Ding, and Z.D Wang, On the degradation evolution equations of cellulose, *Cellulose 15* (2008) 205-224.

[39] Emsley AM, Heywood RJ, Ali M, Eley CM (1997) On the kinetics of degradation of cellulose. *Cellulose 4*(1997) 1–5

[40] P. Calvini, A. Gorassini On the rate of paper degradation: lessons from the past. *Restaurator 27*(4) (2006) 275–290

[41] S. Zervos, “Natural and accelerated ageing of cellulose and paper: A literature review*",* In: Lejeune, A and Deprez, T. (eds)"*Cellulose: Structure and Properties, Derivatives and Industrial Uses*". New York. 2010. Nova Science Publishers

[42] A. Barański, J. M. Łagan, T. Łojewski, In *Ageing and stabilization of paper*; Strlič, M., Kolar, J.; Eds.; *National and University Library*: Ljubljana, 2005; pp 93-109.

[43] D. Klemm, B. Philipp, T. Heinze, U. Heinze, W. Wagenknecht, Comprehensive Cellulose Chemistry*, WILEY-VCH, Weinheim*, 2001, vol. 1.

[44] V. Ivanov, I.; Lenshina, N. Y.; Ivanova, V. S. *J. Polym. Sci. (*1961) **53**, 93-97.

[45] C. Stephens, H.; Whitmore, P. M.; Morris, H. R.; Bier, M. E. *Biomacromolecules 9 (*2008) 1093-1099.

[46] D. Chamberlain. Anion-mediation of aluminium-catalysed degradation of paper, *Polymer Degradation and Stability 92* (2007) 1417-1420.

[47] A. Barański, Łagan, J. M.; Łojewski, T. In Ageing and stabilization of paper; Strlič, M., Kolar, J.; Eds.; *National and University Library*: Ljubljana, 2005; pp 93-109.

[48] C. Shahani, S. B. Lee, F.H Hengemihle, G. Harrison, P. Song, M.L. Sierra, C.C Ryan, N. Weberg, Report on: Accelerated aging of paper: I. Chemical analysis of degradation products. II. Application of Arrhenius relationship. III. Proposal for a new accelerated aging test: ASTM research program into the effect of aging on printing and writing papers; *Library of Congress: 2001.*

[49] A.L. Dupont, C. Egasse, A. Morin, F. Vasseur, F. *Carbohydr. Polym.68 (*2007), 1–16.

[50] D. Erhardt, M.F Mecklenburg, In *Materials issues in art and archeology IV,* Cancun, May 16-21, 1994; Vandiver, P. B., Druzik, J. R., Madrid, J. L. G., Freestone, I. C., Wheeler, G. S.; Eds.; Materials Research Society Symposium Proceedings 352; *Materials Research Society*: 1995; pp 247-270.

[51] C.H. Stephens, P.M Whitmore, H.R Morris, M.E. Bier, .B*iomacromolecules 9 (*2008) 1093-9.

[52] A. Lattuati-Derieux, S. Bonnassies-Termes, B.J Lavédrine, Characterisation of compounds emitted during natural and artificial ageing of a book. Use of headspace-solid-phase microextraction/gas chromatography/mass spectrometry *Cult. Heritage 7 (*2006) 123–133.

[53] D. Kočar, M. Strlič, J. Kolar, J. Rychlý, B. Pihlar, L. Rychlá, Chemiluminescence From Paper III. The Effect of Superoxide Anion and Water, *Polym. Degrad. Stab 88* (2005) 407-414.

[54] L.F. McBurney, Degradation of cellulose, 1. Kinetics of Degradation Reactions, in: E. Ott, H.M. Spurlin, M.W. Grafflin (Eds.), *Cellulose and Cellulose Derivatives*, **I**, Interscience, New York, 1954, 99-130.

[55] X. Zou, T. Uesaka, N. Gurnagul, Prediction of paper permanence by accelerated aging. Part I: Kinetic analysis of the aging process, *Cellulose 3* (1996) 243-267.

[56] T.P. Nevell, S.H. Zeronian, Cellulose Chemistry and Its Applications, *Ellis Horwood*, Chichester, 1985.

[57] J. Kolar, Mechanism of Autoxidative Degradation of Cellulose, *Restaurator 18* (1997) 163-176.

[58] J. Kolar, M. Strlič, G. Novak, B. Pihlar, Aging and Stabilization of Alkaline Paper, *J. Pulp Pap. Sci.24* (1998) 89-94.

[59] C.J. Knill, J.F. Kennedy, Degradation of cellulose under alkaline conditions, *Carbohydr. Polym.51* (2003) 281-300.

[60] D.T. Sawyer, Oxygen Chemistry, *Oxford Press*, Oxford, 1991.

[61] B.H.J. Bielski, D.E. Cabelli, R.L. Arudi, Reactivity of HO2/O2– radicals in aqueous solution, *J. Phys. Chem. Ref. Data 14* (1985) 1041-1100

[62] P.J. Thornalley, A. Stern, The production of free radicals during the autoxidation of monosaccharides by buffer ions, *Carbohydr. Res. 134* (1984) 191-204.

[63] S.J.H.F. Arts, E.J.M. Mombarg, H. van Bekkum, R.A. Sheldon, Hydrogen Peroxide and Oxygen in Catalytic Oxidation of Carbohydrates and Related Compounds, *Synthesis 6* (1997) 597-613.

[64] M. Strlič, D. Kočar, J. Kolar, J. Rychlý, B. Pihlar, Degradation of pullulans of narrow molecular weight distribution - the role of aldehydes in the oxidation of polysaccharides*, Carbohydr. Polym.54* (2003) 221-228.

[65] J. Malešič, J. Kolar, M. Strlič, Effect of pH and carbonyls on the degradation of alkaline paper: factors affecting ageing of alkaline paper, *Restaurator 23* (2002) 145-153.

[66] L.M. Marraccini, T.N. Kleinert, Spectrophotometric Estimation of Peroxide in Cellulosic Materials, *Svensk Papperstidn 65* (1962) 78-80.

[67] C.J. Shahani, F.H. Hengemihle, The Influence of Copper and Iron on the Permanence of Paper, Historic Textile and Paper Materials, *American Chemical Society* (1986), 387-410.

[68] J. Kolar, M. Strlič, Stabilisation of ink corrosion, Postprints of the Iron Gall Ink Meeting, *The University of Northumbria*, Newcastle, UK, 2001, 135-140.

[69] M. Strlič, J. Kolar, B. Pihlar, Some preventive cellulose antioxidants studied by an aromatic hydroxylation assay, *Polym. Degrad. Stab.73* (2001) 535-539.

[70] M. Strlič, J. Kolar, V.-S. Šelih, D. Kočar, B. Pihlar, A Comparative Study of Several Transition Metals in Fenton-Like Reaction Systems at Circum-Neutral pH, *Acta Chim. Slov.50* (2003) 619-632.

[71] R. Blattner, R.J. Ferrier, Effects of Iron, Copper, and Chromate Ions on the Oxidative Degradation of Cellulose Model Compounds, *Carbohydr. Res.138* (1985) 73-82.

[72] J.C. Tongren, *Paper Trade J. 107 (8)* (1938):76.

[73] D.H. Page, A theory for the tensile strength of paper, *Tappi 52 (4)* (1969) 674

[74] E. Back, Thermal Auto-crosslinking in Cellulose Material,*Pulp and Paper Mag. of Canada 68* (1967) 165-171.

[75] P.Luner, Paper permanence, *Tappi 52 (5)* (1969) 796.

[76] E.L. Graminski, The stress-strain behaviour of accelerated and naturally aged papers, *Tappi 53* (3) (1979) 406-410.

[77] C.H. Krekel, The chemistry of historical iron gall inks; understanding the chemistry of writing inks used to prepare historical documents. *Int. J. Forensic Document Examiners 5* (1999) 54–58.

[78] B. Reigland, Ink corrosion: Aqueous and non-aqueous treatments of paper objects –state of the art. *Resteurator* 20 (1999) 167–180.

[79] R.L. Feller, Artists' Pigments: A Handbook of Their History and Characteristics. vol. 1.New York: *Oxford University Press*, 1999.

[80] A. Roy, Artists' Pigments: A Handbook of their History and Characteristics. vol. 2.New York: *Oxford University Press*, 1983.

[81] E. West Fitzhugh, Artists' Pigments: A Handbook of their History and Characteristics.vol. 3. *Washington: National Gallery of Art*, 1997.

[82] K. Nesměrák I. Němcová. Dating of Historical Manuscripts Using Spectrometric Methods: A Mini-Review, *Analytical Letters, 45:4* (2012) 330-344.

[83] K. Nakamoto, Infrared and Raman Spectra of Inorganic And Coordination Compounds, Parts A and B, *John Wiley & Sons*, New York, 1997.

[84] D.A. Prystupa, A.M. Donald, Infrared study of gelatin conformations in the gel and sol states *Polym. Gels Netw. 4* (1996) 87–110.

[85] J.H. Muyonga, C.G.B. Cole, K.G. Duodu, Fourier transform infrared (FTIR) spectroscopic study of acid soluble collagen and gelatin from skins and bones of young and adult Nile perch (Lates niloticus), *Food Chem. 86* (2004) 325–332.

[86] P. Calvini, A. Gorassini, FTIR–Deconvolution Spectra of Paper Documents, *Restaurator 23* (2002), 48–66.

[87] V. Rouchon, E. Pellizzi, K. Janssens. FTIR techniques applied to the detection of gelatine in paper artefacts: from macroscopic to microscopic approach, *Applied Physics A 100* (2010) 663-669.

[88] P. Garside, P. Wyeth. Identification of Cellulosic Fibres by FTIR spectroscopy: Thread and Single Fibre Analysis by Attenuated Total Reflectance, *Studies in Conservation, Vol. 48*, No. 4 (2003), 269-275.

[89] H.G.M. Edwards, D.W. Farwell, D. Webster, FT-Raman microscopy of untreated natural plant fibres, *Spectro Chimica Acta – Part A 53* (1997) 2383-2392.

[90] B. Schrader, Infrared and Raman Spectroscopy; Schrader, B. ed., *VCH Publishers Inc*.: New York, 1995; Chapter 4.

[91] K. Castro, S. Pessanha, N. Proietti, E. Princi, D. Capitani, M.L. Carvalho, J.M. Madariaga, Noninvasive and nondestructive NMR, Raman and XRF analysis of a blaeu coloured map from the seventeenth century, *Anal. Bioanal. Chem. 391* (2008) 433–441.

[92] M. Bicchieri, A. Sodo, G. Piantanida, C. Coluzza, Analysis of degraded papers by non-destructive spectroscopic techniques, *J. Raman Spectrosc. 37* (2006) 1186–1192.

[93] J. Lojewska, M. Missori, A. Lubanska, P. Grimaldi, K. Zieba, L.M. Proniewicz, A. Congiu Castellano, Carbonyl groups development on degraded cellulose. Correlation between spectroscopic and chemical results, *Appl. Phys. A* 89 (2007) 883–887.

[94] K. Castro, M. Perez-Alonso, M.D. Rodriguez-Laso, L.A. Fernandez, J.M. Madariga, On-line FT-Raman and dispersive Raman spectra database of artists' materials (e-VISART database) *Anal. Bioanal. Chem. 382* (2005) 248-258.

[95] G. Bitossi, R. Giorgi, M. Mauro, B. Salvadori, L. Dei, Spectroscopic techniques in cultural heritage conservation: A survey, *Appl. Spectrosc. Rev. 40* (2005) 187–228.

[96] B. Wagner, E. Bulska, A. Hulanicki, M. Heck, H.M. Ortner, Topochemical investigation of ancient manuscripts, Fresenius' *J. Anal. Chem. 369* (2001) 674–679.

[97] G. Spoto, A. Torrisi, A. Contino, Probing archaeological and artistic solid materials by spatially resolved analytical techniques, *Chem. Soc. Rev. 29* (2000) 429–439.

[98] M. Manso, M. Costa, M. Carvalho, From papyrus to paper: elemental characterization by X-ray fluorescence spectrometry, *Nucl. Instrum. Methods A 580* (2007) 732–734.

[99] M. Manso, M. Costa, M.L. Carvalho, Comparison of elemental content on modern and ancient papers by EDXRF, *Appl. Phys., A Matter. 90* (2008) 43–48.

[100] M. Rozic, M.R. Macefat, V. Orescanin, Elemental analysis of ashes of office papers by EDXRF spectrometry, *Nucl. Instrum. Methods B* 229 (2005) 117–122.

[101] M. Manso, M.L. Carvalho, Elemental identification of document paper by X-ray fluorescence spectrometry, *J. Anal. At. Spectrom. 22* (2007) 164–170.

[102] M. Manso, M. Costa, M. Carvalho, X-ray fluorescence spectrometry on paper characterization: a case study on XVIII and XIX century documents, *Spectrochim. Acta Part B 63* (2008) 1320–1323.

[103] E. A. Wood, Crystals and Light: An Introduction to Optical Crystallography. 2e, *Dover Publications Inc*., New York, 1977.

[104] R. E. Stoiber and S. A. Morse, Crystal Identification with the Polarizing Microscope. *Chapman & Hall*, New York, 1994,

[105] P. C. Robinson and S. Bradbury, Qualitative Polarized-Light Microscopy. *Oxford Science Publications*, New York, 1992.

[106] J.G. Delly, Essentials of Polarised Light Microscopy, *Hooke College of Applied Sciences*, Illinois, 2011

[107] Brent Fultz, “Mössbauer Spectrometry”, in Characterization of Materials. *John Wiley*, New York, 2011.

[108] R.L. Mössbauer, Recoilless Nuclear Resonance Absorption*Ann. Rev. Nuclear Sci. 12* (1962) 123

[109] H. Frauenfelder, The Mössbauer Effect, *W.A. Benjamin Inc*, New York, 1962

[110] G.K. Wertheim, Mössbauer Effect, Principles and Applications, *Academic Press*, New York, 1964.

[111] P. Gutlich, R. Link, A. Trautwein, Mössbauer Spectroscopy and Transition Metal Chemistry*,.Springer*, Heidelberg, 1978.

[112] E. Fluck, W. Kerler, W. Neuwirth, *Angew. Chem. 75* (1963) 461

[113] I. Arcon, J. Kolar, A. Kodre, D. Hanzel, M. Strlic, XANES analysis of Fe valence iniron gall inks, *X-Ray Spectrom 36* (2007) 199–205

.[114] A. Jamrozik, M. Mazurkiewicz, A. Małolepszy, L. Stobin'ski, K. Matlak, J. Korecki,et al., Mössbauer spectroscopy analysis of iron compounds in carboxylated mul-tiwall carbon nanotubes and their ammonium salt, *Phys. Status Solidi A 208* (8)(2011) 1783–1786.

[115] Introduction to Mössbauer Spectroscopy." Royal Society of Chemistry. 2008. 23 June 2008 http://www.rsc.org/Membership/Networking/Interest Groups/MössbauerSpect, accessed on 23 January 2015.

[116] www.vscht.cz/anl/vibspec/FTIR%20Reflection%20Techniques.pdf , accessed on 20 February 2015.

[117] C.E. Cain, and V. F. Kalasinsky, Characterization of eighteenth- and nineteenth-century paper using Fourier transform infrared spectroscopy and thin-layer chromatography. In Application of Science in Examination of Works of Art: Proceedings of the Seminar, September 7-9, 1 983, ed. P. A. England and L. van Zelst, 55-58 . Boston: Research Laboratory, Museum of Fine Arts.

[118] G. Banik, W.K. Sobotka, Paper Preservation, Current Issues and Recent Developments, Ed P. Luner, *Tappi Press*, Atlanta, 1988.

[119] W. Wachter, J. Liers, E. Becker, ICP Conference Papers London 1997, Ed. J. Eagan, *The Institute of Paper Conservation*, Leigh(UK), 1998, 224

[120] W. Feindt, H.V. Rudolph, S. Schiewe, B. Werthmann, *Restauro*, 1998, *124*, p120

[121] J.J. Kozak, R.E. Spartz, Deacidification of Paper by the Bookkeeper Process, in Paper Conservation, Current Issues and Recent Developments, Ed. P. Luner, *Tappi Press*, Atlanta, 1988.

[122] H.J. Porck, 'Mass Deacidification – an Update of possibilities and Limitations', European Commission on Preservation and Access(ECPA), Amsterdam, and Commission on Preservation and Access (CPA), Washington 1996.

[123] A. Bluher, B. Vogelsanger, Mass Deacidification of Paper, Art and Chemical Sciences, *Chimica 55* (2001)981-989

[124] C.J. Shahani, F.H. Hengemihle, *Advances in Chemistry Series 212* (1984) 387

[125] J. Kolar, M. Strlic, M. Budnar, J. Malesic, V.S. Selih, J. Simcic, *Acta Chim. Slov.50* (2003) 763

[126] G. Kolbe, *Restaurator 25(1*) (2004) 26

[127] M. Bicchieri, S. Ronchoni, F.P. Romano, L. Pappalardo, M. Corsi, G. Cristoforetti, S.Legnaioli, V. Palleschi, A. Salvetti, E. Tognoni, *Spectro chimica Acta Part B 57 (2002):* 1235.

[128] K. Dzinavatonga, K. Baruth-Ram, T.R. Medupe, Mössbauer spectroscopy analysis of valence state of iron in historical documents obtained from the National Library of South Africa, *Journal of Cultural Heritage 16* (2015) 377-380

[129] M.Strlic, J. Kolar, V.S. Selih, D. Kocar, B. Pihlar, *Acta Chim. Slov 50* (2003) 619

[130] http://www.mccroneatlas.com/index.asp, accessed on 10 March 2015.

[131] Environment test kit manual, Minnesota Historical Society, Minnesota, 2005, pp. 14.

[132] K. Nesmerak, I. Nemcova, Analytical letters 45:4 (2012***)*** 330